Vol. 14 No. 1 MARCH 2020

FOR THE MIM, CIM AND SINTER-BASED AM INDUSTRIES

POWDER INJECTION MOULDING INTERNATIONAL

MIM in China

Sinter-based AM: A beginner's guide

Lowering the cost of MIM IN713C

Published by Inovar Communications Ltd

www.pim-international.com

www.ryerinc.com

CataMIM®

- A direct replacement for all current commercially available catalytic debind feedstocks
- Improved flow
- Stronger green and brown parts
- More materials available and better surface finish
- Custom scale-up factors available
- Faster cycle times
- 65°C / 150°F mold temperature

AquaMIM®

- Water Debind
- Custom scale-up factors available
- Large selection of available materials

SolvMIM®

- Solvent, Super Critical Fluid Extraction (SFE) or Thermal Debind methods
- Hundreds of materials available
- Custom scale-up factors available

MIM/PIM FEEDSTOCKS

- At RYER, all our feedstocks are manufactured to the highest level of quality, with excellent batch-to-batch repeatability.
- RYER is the ONLY commercially available feedstock manufacturer to offer all five debind methods.
- RYER offers the largest material selections of any commercially available feedstock manufacturer.
- RYER offers technical support for feedstock selection, injection molding, debinding and sintering.

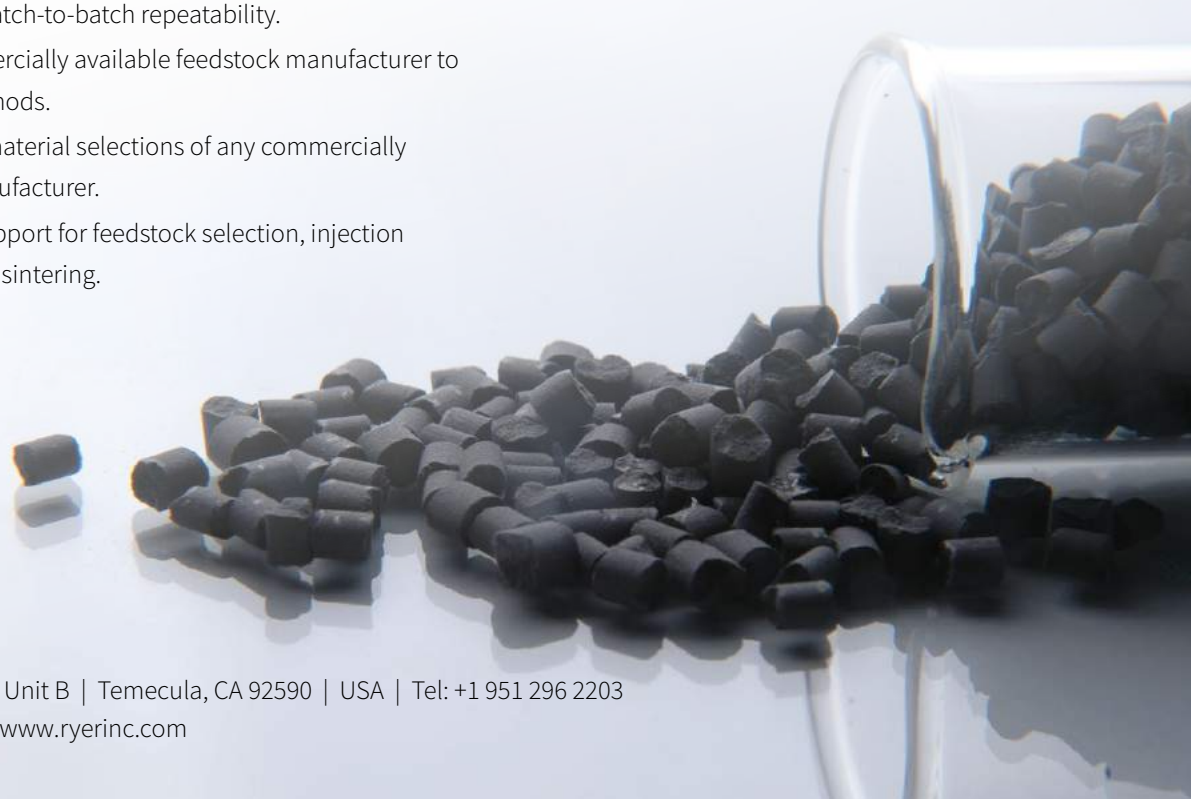

RYER, Inc. | 42625 Rio Nedo Unit B | Temecula, CA 92590 | USA | Tel: +1 951 296 2203
Email: dave@ryerinc.com | www.ryerinc.com

Publisher & Editorial Offices
Inovar Communications Ltd
11 Park Plaza
Battlefield Enterprise Park
Shrewsbury SY1 3AF
United Kingdom

Tel: +44 (0)1743 211991
Fax: +44 (0)1743 469909
www.metal-am.com

Managing Director & Editor
Nick Williams
nick@inovar-communications.com

Publishing Director
Paul Whittaker
paul@inovar-communications.com

Deputy Editor
Emily-Jo Hopson-VandenBos
emily-jo@inovar-communications.com

Assistant Editor
Kim Hayes
kim@inovar-communications.com

Consulting Editors
Prof Randall M German
Former Professor of Mechanical Engineering,
San Diego State University, USA

Dr Yoshiyuki Kato
Kato Professional Engineer Office, Yokohama, Japan

Professor Dr Frank Petzoldt
Deputy Director, Fraunhofer IFAM, Bremen,
Germany

Dr David Whittaker
DWA Consulting, Wolverhampton, UK

Bernard Williams
Consultant, Shrewsbury, UK

Production Manager
Hugo Ribeiro
hugo@inovar-communications.com

Advertising
Jon Craxford, Advertising Sales Director
Tel: +44 (0)207 1939 749
Fax: +44 (0)1743 469909
jon@inovar-communications.com

Subscriptions
Powder Injection Moulding International is published on a quarterly basis as either a free digital publication or via a paid print subscription. The annual print subscription charge for four issues is £145.00 including shipping.

Printed by
Cambrian Printers, Aberystwyth, United Kingdom

ISSN 1753-1497 (print)
ISSN 2055-6667 (online)

Vol. 14 No. 1 March 2020

INOVAR COMMUNICATIONS

POWDER INJECTION MOULDING INTERNATIONAL

For the MIM, CIM and sinter-based AM industries

China's MIM industry looks to growth through innovation

China's MIM industry has come a very long way in a relatively short space of time and today accounts for 40% of MIM part sales worldwide. Whilst the growth of the smartphone, and the consumer electronics sector as a whole, has been the biggest driver behind this achievement, within the 3C sector there is an ongoing shift in dynamics.

No longer do international smartphone brands dominate the market. The rapid growth of Chinese smartphone producers has put more control of product development and the direction of innovation in China's hands. This, of course, is a reflection of the broader picture of manufacturing in China, in which the economy is transitioning to an innovation-driven model.

The end result is a rich source of opportunities for China's MIM producers, not only in the 3C sector but also in the automotive industry, the rapidly growing medical device sector and beyond. Supporting this is a strong commitment to R&D, demonstrated through partnerships between MIM manufacturers, research centres and academia with the goal of exploring new application areas, developing new material systems and overcoming the technical barriers that currently limit the further exploitation of MIM's advantages.

As Prof Yimin Li acknowledges in this issue's lead article, there is also an ongoing awareness in the industry of the need to further improve process control in MIM production in order to further raise the quality bar of MIM parts. This recognition, which exists on an international level, will help the industry to maintain the impressive levels of growth that it has achieved over the past decade.

Nick Williams,
Managing Director & Editor

Cover image
A representative selection of MIM smartphone parts (Parts courtesy of Shenzhen Shindy Tech. Co., Ltd)

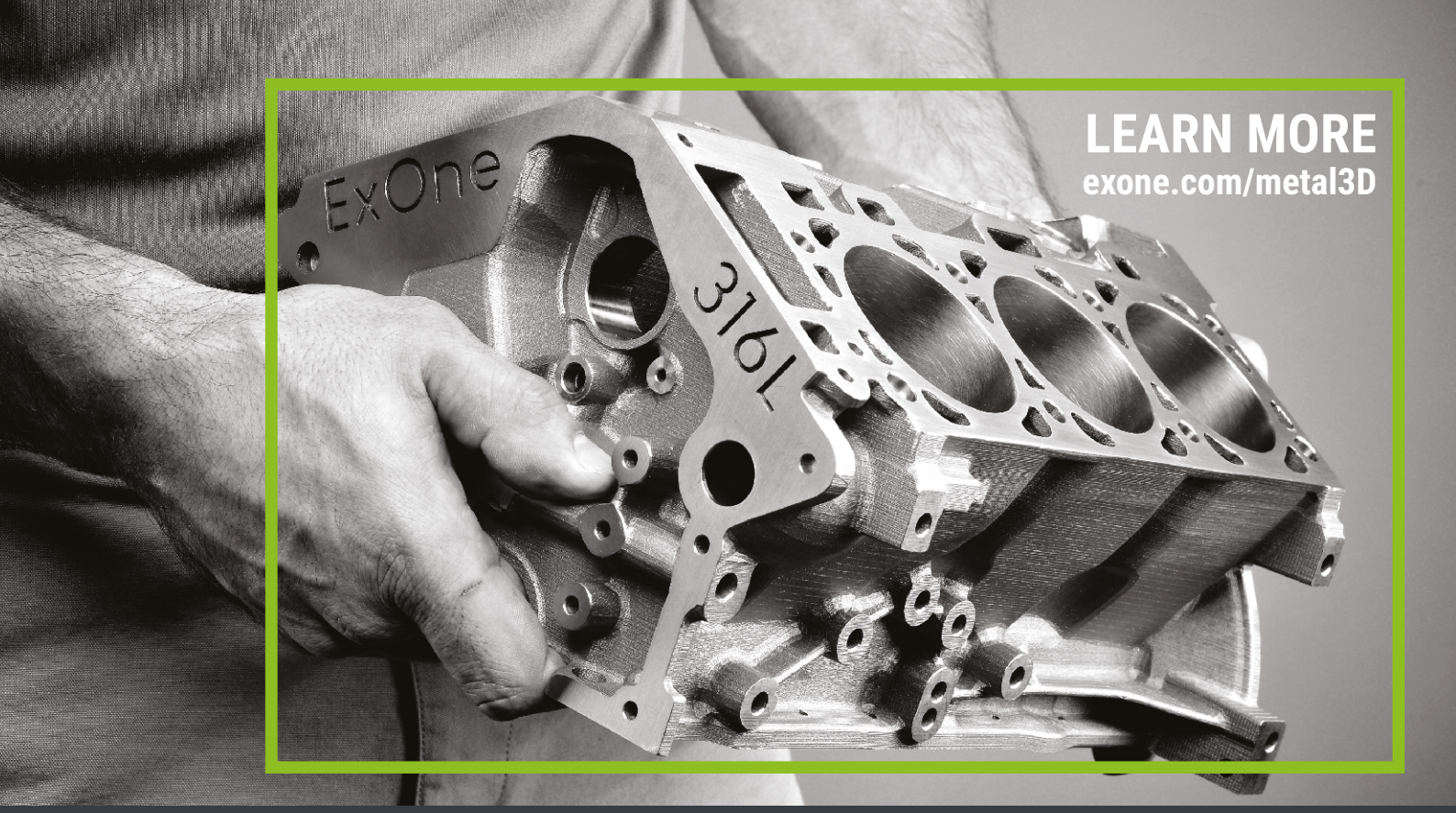

LEARN MORE
exone.com/metal3D

The X1 160Pro
BIG METAL PRODUCTION

- Advanced 3D printing of ultra-fine MIM metal powders
- Largest metal binder jetting system available today
- 3D prints more than 20 metals, ceramics and composites
- Exclusive technology for industry-leading density, repeatability
- Quality 3D printing with fast speeds topping 10,000 cm^3/hour

NEW
ExOne's 10th metal 3D printer

WATCH THE VIDEO
YouTube

ExOne™

March 2020

Powder Injection Moulding International



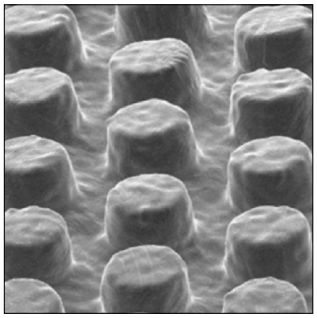

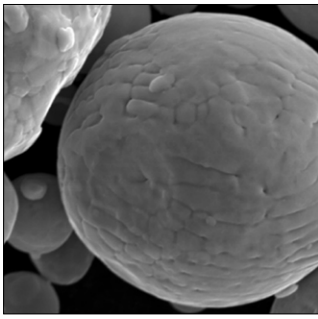

27 28 53 59 82

In this issue

Regular features

ELNIK SYSTEMS

Leaders in MIM/AM Debind + Sinter.
Yesterday. Today. Tomorrow.

Elnik's innovations and experiences in all areas of temperature and atmosphere management have led us to become the benchmark for the Batch-based Debind and Sinter equipment industry. We have applied these core competencies across a wide variety of industries through our 50 year history and look forward to the emergence of new technologies that will continue to drive demand for new innovative products. Elnik is your partner for the future.

Innovation drives our manufacturing and design solutions
Quality takes precedence in all areas of our business
Experience motivates our team to always do what's right
Excellence is the benchmark for all customer relationships

From First Stage Debind Equipment (Catalytic, Solvent, Water) and Second Stage Debind & Sinter Furnaces (All Metal or Graphite) to support with ancillary utility equipment, Elnik's experienced team is driven to be the only partner you need for all your MIM and Metal AM equipment needs.

Innovation. Quality. Experience. Excellence.

107 Commerce Road | Cedar Grove, NJ 07009 USA | +1 973.239.6066 | elnik.com

Industry News

Beijing-based researchers recognised for their work on development and application of PIM

Professor Xuanhui Qu and his team from the University of Science and Technology Beijing have received China's prestigious National Technological Invention Award of the People's Republic of China for their work on 'Near-net Shape Manufacturing Technology and Applications of High-performance Special Powder Materials'.

The award was presented at the National Science and Technology Award Conference, which took place in Beijing, January 10, 2020. A presentation event was held in the Great Hall of the People, Beijing, with President Jinping Xi, Premier Keqiang Li and other leaders in attendance to present prizes to the winning delegates.

According to Professor Qu, high-performance materials play a critical role in the development of cutting-edge technologies, but some of these materials cannot be manufactured using conventional processes such as machining. This greatly limits their effective utilisation and is an obstacle in the development of high-tech applications.

With the increasing demand for lightweighting and miniaturisation, component sizes are getting smaller, while the geometry of components is becoming ever more complex. A further challenge is that conventional machining processes are often financially unviable for the scale-up of micro-sized parts.

Professor Qu and his team have reportedly spent over a decade establishing Powder Injection Moulding processes for a variety of materials including refractory metals, high-performance iron-based alloys and special ceramics. Significant advances were also made by the team in processing technologies such as feedstock fabrication, binder design, sintering and microstructural control.

Thanks to cooperation with leading Chinese MIM firms such as Shanghai Future High-tech Co., Ltd., Shanghai, China, and Jiangsu Gian Tech. Co., Ltd., Changzhou, the team has also been able to establish an industry-university-research innovation platform, overcoming challenges in the further industrialisation of PIM and delivering volume production with a high level of process stability, precision and efficiency. As a result, common applications for MIM now include smartphones, fibre-optic communications, laptops, medical devices, electric tools and automotive systems.

Professor Qu and his team have published more than 200 academic papers, authorised over sixty patents, and educated more than 300 post graduate students.

www.ustb.edu.cn
www.future-sh.com
www.jsgian.com

Osaka Titanium Technologies receives AS9100 certification for spherical Ti alloy powder

Osaka Titanium Technologies Co., Ltd., Amagasaki, Hyogo Prefecture, Japan, has been awarded JIS Q 9100 (AS9100) certification for its TILOP (Pre-Alloy) spherical titanium alloy powder. AS9100 is a widely adopted and standardised quality management system for the aerospace industry and defence sector.

TILOP (Titanium Low Oxygen Powder) is the brand name given by Osaka Titanium Technologies to its method of producing titanium powder by gas atomisation for Additive Manufacturing and Metal Injection Moulding. OTC produces several titanium powders under the TILOP brand name, including commercial pure (CP) titanium powder, Ti-6Al-4V pre-alloyed powder, both with ranges of powder particle size distribution tailored to the customer's specific applications.

The product's AS9100 certification recognises it as meeting the requirements imposed by the standard for the manufacturing and sale of high-performance materials. Certification was awarded by the Japan Quality Assurance Organization (JQA).

www.osaka-ti.co.jp

MIM engineering and prototyping specialist Neota completes move to its new facility

Neota Product Solutions LLC, a provider of Metal Injection Moulding solutions, has moved into its new facility in Loveland, Colorado, USA. The move is expected to support the continued growth of the Neota team as it offers engineering and prototyping services for MIM, as well as both low- and high-volume MIM production.

The company can provide prototype MIM parts in four weeks or less and, using the 'Neota Approach', the company's services are designed around three distinct phases of part production, with specific resources dedicated to each.

In phase one, Design for Manufacturability (DFM), the Neota team assists customers in considering their part's design, material, quality systems, prototyping approach, validation plans, cost analysis and project planning in order to get their product to market as quickly as possible. Phase two comprises the design validation and prototyping stage of a part's development, involving functional testing of actual MIM parts.

In parallel with design validation and prototyping, Neota's tool room can produce a multi-cavity production tool, so that once the design is fully validated, tooling can be completed and made ready for full-scale production without any downtime.

In phase three, the production phase, Neota has the resources to support full-scale series production. The company is, however, also able to facilitate the transition of full-scale production to a customer's preferred MIM vendor where necessary.

In addition to its MIM capabilities, Neota offers plastic injection moulding and Additive Manufacturing services.

www.neotagroup.com

Neota's new facility in Loveland, Colorado, USA (Courtesy Neota Product Solutions LLC)

ATMIX

EPSON ATMIX CORPORATION

Finer Powder Production

Cleaner Powder Production

Shape Control of Powders

- Low Alloy Steel
- High Alloy Steel
- Stainless Steel
- Magnetic Materials
- Granulated Powder

PACIFIC SOWA

JAPAN
Mr. Ryo Numasawa
Numasawa.Ryo@exc.epson.co.jp

ASIA and OCEANIA
Ms. Jenny Wong
jenny-w@pacificsowa.co.jp

CHINA
Mr. Hideki Kobayashi
kobayashi-h@pacificsowa.co.jp

U.S.A and SOUTH AMERICA
Mr. Tom Pelletiers
tpelletiers@scmmetals.com

EU
Dr. Dieter Pyraseh
Dieter.Pyrasch@thyssenkrupp.com

KOREA
Mr. John Yun
dkico@hanafos.com

MIM specialist Gevorkyan announces plans for Austrian R&D centre

Gevorkyan s.r.o., based in Vlkanová, Slovakia, reports that it will establish a new R&D centre in Austria. The announcement follows a successful 2019 for the company, which saw increasing turnover of €42 million and EBIDTA of €12 million.

Dipl. Ing. Artur Gevorkyan, the company's main shareholder, explained, "We want to be closer to our customers, who mainly come from Western Europe, and at the same time to simplify the logistics and organisation of meetings concerning new projects between customers and our R&D."

"This idea came after several organised meetings with customers near the Vienna airport," he added. "Thanks to modern technologies, it is basically the same for an R&D engineer wherever they are situated during the development phase of a project. Moreover, engineers will have the additional benefit of a few weeks out of a main office with its routine problems and daily disturbances."

The company produces and supplies metal parts made by PM, MIM and HIP technologies to customers in more than thirty countries worldwide. Its end-user sectors include the automotive, lock and security systems, garden and hand tool, oil, medical, cosmetic and fashion industries. In 2018, it announced plans to install the technology for metal Additive Manufacturing at its main facility through 2019.

Its team develops over a hundred new parts each year and manufactures two thousand different types of component annually. A large part of its component portfolio is made up of PM and MIM components transferred from conventional technologies, such as casting or machining. To further automate production, the company added a further fourteen robots to its manufacturing lines in 2019.

www.gevorkyan.sk/en

Gevorkyan develops over a hundred new parts each year and manufactures two thousand different types of component annually (Courtesy Gevorkyan)

M. Holland adds BASF metal filament to its offering

M. Holland Company, Northbrook, Illinois, USA, a distributor of thermoplastic resins, has announced an expanded distribution agreement with BASF 3D Printing Solutions, Heidelberg, Germany. Adding to its portfolio of AM products and services, M. Holland is now distributing Ultrafuse® 316L, BASF's stainless steel composite filament. This filament can be processed using standard Fused Filament Fabrication (FFF) machines and debinding and sintering processes.

"We are excited to broaden our existing relationship with BASF and are fortunate to be among the select organisations authorised to distribute Ultrafuse® 316L," stated Haleyanne Freedman, Market Manager, 3D Printing at M. Holland. "This metal polymer composite filament is a groundbreaking and industry-changing product that is also cost-effective. Our clients can leverage this distinct material to complement existing plastic injection moulding opportunities and a wide array of other applications."

"By expanding our distribution partnership with M. Holland to now include our Ultrafuse® 316L metal filament for Additive Manufacturing, we are able to make the printing of metal parts more accessible and affordable to manufacturers," added Firat Hizal, Head of Metal Systems, BASF 3D Printing Solutions. "As we expand our presence in North America, customers can quickly and reliably create stainless steel parts, utilising their existing printers and an established debinding and sintering network."

This distribution arrangement follows a prior agreement with BASF, and enhances a growing portfolio of AM materials from suppliers Henkel, Owens Corning and 3DXTech. This highlights M. Holland's commitment to strategic growth in the AM market. The company is also focused on how ancillary materials can complement its already extensive portfolio of materials and services, including consulting support, prototyping and equipment selection.

www.mholland.com

GAIN A MATERIAL ADVANTAGE WITH AMP'S MIM AND PIM FEEDSTOCK

Our metal injection molding feedstocks – available in POM-based (**Advacat**®) or wax-based (**Advamet**®) binder systems – will allow you to produce world-class precision parts for the aerospace/defense, automotive, firearms, industrial, and medical/implantable markets.

- Tight dimensional control
- Higher yield
- Enhanced cracking resistance
- Excellent green strength
- Superior homogeneity
- Lot-to-lot consistency
- Alloys never made obsolete

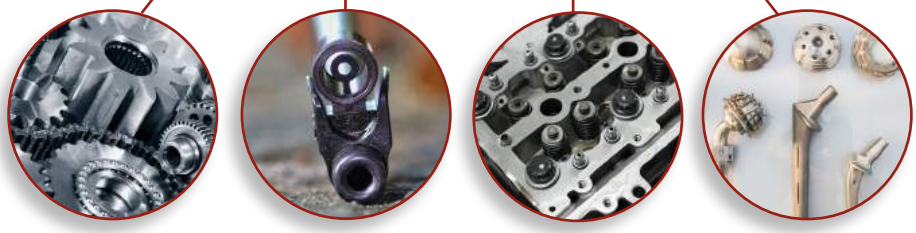

Automotive | Firearms | Industrial | Medical/Implantables

NOW offering...

Toll Processing and Material Rejuvenation Services

WorldPM2020 / MonTreaL

See AMP at Booth 322-324

June 27 – July 1, 2020
Montreal, Canada

For more information visit **www.ampmim.com** or contact **Chris@ampmim.com** or **724-396-3663**

AMP advanced metalworking practices

MEMBER MPIF

ISO 9001:2015 CERTIFIED SMITHERS

www.ampmim.com

PIM binder specialist eMBe rebranded Krahn Ceramics, targets filament-based AM

Krahn Ceramics sees its role as a project partner for those looking to process ceramic and metal powders both by Powder Injection Moulding and filament-based Additive Manufacturing (Courtesy Krahn Ceramics)

eMBe Products & Service GmbH, Thierhaupten, Germany, has been rebranded as Krahn Ceramics GmbH following the company's acquisition by Krahn Chemie GmbH in May 2019. The company's headquarters have also been relocated from Thierhaupten to Hamburg and its machines and equipment integrated into a new technical centre in Dinslaken, Germany.

Krahn Ceramics states that it sees its role as a project partner for those looking to process ceramic and metal powders both by Powder Injection Moulding and filament-based Additive Manufacturing (AM). The company reported that it can support its customers through all stages of the production process, from raw materials supply to the finished component.

Services offered to Krahn Ceramics' customers range from consulting to laboratory services, tailor-made product development and small series production. Dr Stefan Stolz, the company's Managing Director, stated, "The feedback we received at the Formnext trade fair confirmed that the market has a great interest in such a broad-based technology partner and source of inspiration. We are very much looking forward to realising the numerous product ideas of our customers together."

"In addition to the European market, we also have an eye on the USA and Asia," he added. "There, we can draw on established structures and networks of the Otto Krahn Group, among other things. This means that we have internal access to a lot of market-relevant information in order to be able to develop business."

www.krahn-ceramics.com

Exentis Group demonstrates industrialisation of its 3D screen printing Additive Manufacturing technology

A copper sample part (left), a metallic forcep for medical applications (centre) and a casting filter for low-pressure casting of aluminium rims (right) (Courtesy Exentis Group AG)

Exentis Group AG, located in Stetten, Switzerland, demonstrated its 3D Mass Customization® technology during the recent opening of its new 1,200 m^2 customer innovation centre. The company's industrialised Additive Manufacturing technology offers rapid series production of millions of components, in either metal or ceramic based materials, using a screen printing process followed by a final sintering stage.

Exentis' technology can be used to additively manufacture components for a wide range of applications and industrial sectors. The eco-friendly cold printing process is said to generate ultra-fine structures without reworking, with wall thicknesses and cavities down to 70 µm being possible. The process allows for complex designs with undercuts and closed cavities, without any supporting structures. Porosity can be adjusted to between 0 and 40% and surface roughnesses of Ra ≤ 2 µm can be achieved.

According to the group, productivity is comparable to that of injection moulding (metal or polymer), with a major advantage being the rapid setup time thanks to the lack of need for expensive tooling which takes many weeks to produce. Exentis can provide screens within just a few days.

Customers have the option to purchase the Additive Manufacturing systems for in-house production, with guidance on the appropriate materials, development and supply of specific paste systems, screens, process technology and training provided by Exentis. Alternatively, the company can manufacture components for customers at its operations in Switzerland or Germany.

Exentis reports that it has already installed three inline 3D production units at customer sites, each with the capacity to produce several millions of parts.

www.exentis-group.com

Precision medical components manufacturer MICRO celebrates 75th anniversary

MICRO, a manufacturer specialising in precision medical components, sub-assemblies and complete devices for laparoscopic surgical procedures, headquartered in Somerset, New Jersey, USA, celebrates its 75th anniversary this year. The company is a full-service contract manufacturer of medical devices using technologies that include MIM and CIM.

Originally called Micro Stamping Corporation, MICRO was founded in 1945 in Maplewood, New Jersey, with a focus on manufacturing high-precision metal stampings. It is now a leading global provider of medical device contract manufacturing services, and its operations have expanded from 2,600 m^2 to nearly 16,700 m^2, increasing manufacturing capacity to meet market needs.

The company employs over 450 people and has annual sales revenue of over $100 million. MICRO also recently opened an expanded research and development centre to showcase its product development capabilities.

MICRO's medical device division began developing ligation clips for use in surgical procedures and currently produces over a million endoscopic instruments annually in its environmentally controlled Class 8 cleanroom. The company states that its Design for Manufacturability expertise allows MICRO to help customers design products optimised for production, keeping costs manageable and maximising return on investment.

"We are incredibly proud to celebrate seventy-five years providing engineering and technical expertise, fulfilling our vision to help our customers save lives," stated Brian Semcer, President, MICRO. "As a trusted and valued product development partner to our clients, innovation has always been the hallmark of our business and we continually seek ways to improve and reinvest in technology, equipment, state-of-the-art facilities and training to create new and better solutions for customers and their patients."

Frank J Semcer Jr, Director of Human Resources, MICRO, explained, "At the heart of our company's growth and success are our employees, who we consider family. We're deeply committed to their development, which reflects our core values."

He continued, "We routinely invest in our employees through competitive compensation, benefits and on-the-job training, while our culture allows us to attract and retain top talent. With continued success, MICRO provides opportunities and career growth to graduates of top engineering programmes as well as high school graduates who elect not to pursue a college degree but want to learn a trade."

www.micro-co.com

Metal injection moulded parts produced by MICRO (Courtesy MICRO)

CREMER

Thermoprozessanlagen GmbH

Thermal Process Equipment for PIM applications

Continuous Furnaces

Batch Furnaces

HIP/CIP

Whether for MIM or CIM, we design, construct and deliver thermal plants to suit specific thermal applications.

50 Years

Designed, developed and made in Germany

www.cremer-polyfour.de

ExOne qualifies fifteen new materials for use on its Binder Jet AM machines

The ExOne Company, based in North Huntington, Pennsylvania, USA, has qualified fifteen new metal, ceramic and composite materials for Binder Jet Additive Manufacturing on its machines, bringing the company's total supported materials to twenty-one. Among the materials qualified by ExOne to date are ten single-alloy metals, six ceramics and five composite materials. Over twenty-four additional powders are also said to be approved for R&D environments, including aluminium and Inconel 718.

"From the outside, it may look like ExOne's metal printers jumped from six to twenty-one qualified materials overnight. In reality, ExOne's engineering team and our customers have been moving so fast to print new materials since 2013 – the breakthrough year when we began printing dense single-alloy metals – that we haven't slowed down to update the market on our progress," stated John F Hartner, ExOne CEO, in a message following the announcement.

"When we took the time to re-evaluate where we were over the last few months, the numbers surprised even us," he commented. "ExOne customers were printing an astonishing number of materials – fourteen – that had not yet worked all the way through ExOne's rigorous qualification process. That included six single alloys, six ceramics, and two ceramic-metal composites."

"At the same time, we were ready to announce new materials, such as M2 tool steel, had achieved

ExOne has qualified fifteen new materials for use on its AM machines, bringing the total to twenty-one (Courtesy The ExOne Company)

our highest qualified status, and other materials, such as aluminium and titanium, were qualified for controlled R&D printing. So, a major reset was needed," he stated.

Partners that have assisted ExOne in qualifying materials include Global Tungsten & Powders, H.C. Starck Solutions, NASA, Oak Ridge National Laboratory, SGL Carbon, the U.S. Army, the U.S. Department of Energy, the University of Texas at El Paso, and Virginia Tech.

New materials qualification system
As of February 25, 2020, ExOne reported that it has three material qualification levels that recognise different degrees of material readiness for customers with different application needs, namely:

Third-party qualified materials
These materials have passed rigorous ExOne tests over multiple builds, and have verified material property data from an independent third party.

Customer-qualified materials
These materials have been qualified by ExOne customers with their own standards and are being successfully additively manufactured today for their own applications.

R&D-qualified materials
These materials have passed a preliminary qualification phase by ExOne and are deemed suitable for AM, supported by ongoing development.

ExOne's family of machines includes the Innovent+, an entry-level system used for R&D, design and small part production; the X1 25Pro, a mid-sized production AM machine that is large enough for most metal parts manufactured today; and the X1 160Pro, the company's largest metal AM machine, slated for delivery later this year.

www.exone.com

Metal filament producer Virtual Foundry names Sapphire3D as a sintering partner

The Virtual Foundry, LLC, Stoughton, Wisconsin, USA, has announced that Sapphire3D, Inc., a metal and ceramic AM and sintering company based in Chicago, Illinois, USA, will be the first certified sintering partner for its plastic-infused metal filaments, which can be used in Fused Filament Fabrication (FFF) Additive Manufacturing. Sapphire3D states that it has developed expertise in the debinding and sintering of green parts made from The Virtual Foundry's open-architecture plastic-infused metal Filamets™ to produce high-quality, high-purity finished metal parts.

www.thevirtualfoundry.com
www.sapphire3d.com

Randall German to receive MPIF's PM Lifetime Achievement Award

Dr Randall (Rand) German, FAPMI, founder of German Materials Technology, has been selected to receive the Kempton H. Roll Powder Metallurgy Lifetime Achievement Award by the Metal Powder Industries Federation (MPIF). The award will be presented during WorldPM2020, World Congress on Powder Metallurgy & Particulate Materials, in Montreal, Canada, at the Opening General Session on Sunday, June 28.

MPIF stated that German has distinguished himself through his research and teaching of the net shape fabrication of engineering materials via sintering-based processes. He has promoted the growth of Powder Metallurgy technology, in particular Powder Injection Moulding, during his fifty-year career through his involvement in twelve start-up companies, supervising well over a hundred graduate and post-doctoral students, and prolific PM industry publications. German has also been an active member in APMI International, the American Society for Metals, and the American Ceramics Society.

Dr Randall German has been selected for the MPIF's PM Lifetime Achievement Award (Courtesy MPIF)

After completing his bachelor's degree in material science and engineering at San José State University, German began his PM industry career at Battelle Lab, Columbus, Ohio, prior to joining Sandia National Labs (SNL). He obtained his master's degree in metallurgical engineering from The Ohio State University and his PhD in engineering at the University of California—Davis before taking a Director of Research position at Mott Corporation, Farmington, Connecticut.

German's nearly forty-year academic career began in 1980 at Rensselaer Polytechnic Institute (RPI), where he earned the Hunt Chair while teaching and conducting research. In 1991, he accepted a position at The Pennsylvania State University where he became the Brush Chair Professor in Materials and the Director of the Center for Innovative Sintered Products (CISP) before retiring as an emeritus professor.

In 2005, he became the inaugural director for the Center for Advanced Vehicular Systems (CAVS) at Mississippi State University prior to joining San Diego State University in 2008 as Associate Dean for Engineering Research until 2013.

German has published twenty books and has twenty-five patents. He has shared his expertise at the MPIF's Powder Injection Molding tutorials since 1990, and co-chaired over thirty conferences. German received the MPIF Distinguished Service to PM Award in 1993 and was one of the first APMI members to be awarded the prestigious APMI International Fellow Award in 1998. He received an honorary doctorate from Universidad Carlos III de Madrid and fellow awards from two additional technical societies.

The Lifetime Achievement Award, named in honour of Kempton H. Roll, founding Executive Director of MPIF, was established in 2007 in order to recognise individuals with outstanding accomplishments and achievements who have devoted their careers and a lifetime of involvement in the field of PM and related technologies. This will only be the fourth time the award has been given since its inception.

www.mpif.org

HIPER | 恒普

Full Series Debinding and Sintering Furnace

for Metal Injection Molding

This is the Future ! ≤±1.5℃*

* Temperature uniformity

Hiper is the leading MIM furnace manufacturer in the world

- Graphite/Metal hot zone debinding and sintering furnace
- All-in-one walking beam continuous debinding and sintering furnace

E : xiangwei.zou@hiper.cn/W: www.hiper.cn

NO.521,Haitong Road,Cixi City,Zhejiang,China

Arcast begins year installing multiple gas atomisers in USA and Europe

Arcast Inc., Oxford, Maine, USA, has announced it shipped and installed several new gas atomisers in January 2020. The company, a producer of advanced melting and metal powder atomisation systems, has supplied atomisers to the Center for Manufacturing Research of Tennessee Tech, USA; CEIT, San Sebastián, Spain; South Dakota School of Mines and Technology, USA; and North Carolina State University, USA.

"The increase in metal powder research for Powder Metallurgy and AM applications is significant in the USA at the moment," stated Arcast. "We currently have seven inert gas atomisers being supplied within the USA. It is good to see the USA investing in this growing market. This is a big change from just a few years ago when most of the growth in this area was in Europe."

Tennessee Tech has received a VersaMelt multi-mode inert gas atomiser. Due to its wide range of melting and processing options, this atomiser is expected to give the research group the ability to cleanly melt and atomise a large number of diverse materials, including titanium, copper, iron, cobalt, hafnium, tantalum, tungsten and other metal alloys.

An Arc 200 arc melting furnace, with gas atomising option, has been installed at the South Dakota School of Mines and Technology's Materials and Metallurgical Engineering department. The system will enable the research team to work with industrial partners and government agencies to develop new materials and applications.

At North Carolina State University, the Center for Additive Manufacturing and Logistics (CAMAL) will use a VersaMelt gas atomiser for powder production to support its AM hub. The atomiser is expected to allow the centre team, led by Tim Horn, to produce the source material for its AM projects, eliminating long lead times for externally sourced powders.

Outside of the US, a large-scale inert gas atomiser has been shipped to Spain's Centro de Estudios e Investigaciones Técnicas de Gipuzkoa (CEIT), for installation at its new powder development centre in San Sebastián. CEIT's metal powder research includes the atomisation of metal powders for use in AM, magnetic materials and the automotive aeronautic sectors; the development of Powder Metallurgy steels; the manufacture of hard and soft magnetic materials using PM routes; the design of metal powders specifically for AM, and more.

www.arcastinc.com

Tom Pelletiers announced as recipient of APMI International's 2020 Fellow Award

APMI International's most prestigious award recognises APMI members for their significant contributions to the goals, purpose, and mission of the organisation, as well as for a high level of expertise in the technology, practice, or business of the Powder Metallurgy industry. The 2020 Fellow Award recipient will receive elevation to Fellow status at WorldPM2020: World Congress on Powder Metallurgy & Particulate Materials, Montréal, Canada, during the Opening General Session on Sunday, June 28.

The 2020 recipient, Thomas (Tom) Pelletiers II, VP of New Business Development, Kymera International, has dedicated over thirty years to the Powder Metallurgy industry. He is the current APMI International President and has served on many APMI and Metal Powder Industries Federation (MPIF) committees and association boards.

In 2015, Pelletiers received the MPIF Distinguished Service to PM Award. He was a co-chair for PowderMet2011 and several annual MIM conferences. Pelletiers has been a member of the MPIF Technical Board since 2000, chairing the Professional Development Committee. Additionally, he has co-authored various articles for the *International Journal of Powder Metallurgy and ASTM Handbook Volume 7: Powder Metallurgy*. He is a regular speaker at several MPIF seminars and the annual Basic PM Short Course. He co-developed lead-free machinable brass compositions resulting in two US patents and has performed extensive research on aluminium premixes.

Established in 1998, the Fellow Award recognises APMI members for their significant contributions to the society and high level of expertise in the technology of Powder Metallurgy, practice, or business of the PM industry. Fellows are elected through their professional, technical and scientific achievements, continuing professional growth and development, mentoring/outreach, and contributions to APMI International committees.

www.apmiinternational.org
www.mpif.org

Tom Pelletiers II is the recipient of APMI International's 2020 Fellow Award (Courtesy MPIF)

Lithoz supplies ceramic AM parts for ISS BioFabrication facility

Lithoz America LLC, Troy, New York, USA, a division of Lithoz GmbH, headquartered in Vienna, Austria, recently collaborated with engineering company Techshot, Greenville, Indiana, USA, to additively manufacture ceramic components used during a mission to the International Space Station (ISS).

A spacecraft arrived at the ISS on November 2, 2019, with supplies for its 3D BioFabrication Facility (BFF). Along with human cells and bioinks for the BFF, the supplies also included Techshot's tissue conditioning system, manufactured by Lithoz and tested during the mission.

Lithoz partnered with Techshot to develop ceramic fluid manifolds used inside bioreactors, which provide nutrients to living materials additively manufactured in space by the BFF. The ceramic components are expected to replace the prototype polymer manifolds tested in space this summer, and are currently being tested aboard the ISS for their biocompatibility, precision, durability and overall fluid flow properties.

Left to right: Shawn Allan, Nicholas Voellm and Nicole Ross from Lithoz America with the CeraFab 8500 ceramic AM machine

The ceramic manifolds were additively manufactured using Lithoz's lithography-based ceramic manufacturing (LCM) process on a high-resolution CeraFab machine. According to Lithoz, the collaborative work undertaken with Techshot has highlighted an ideal use case for ceramic Additive Manufacturing to enable the production of a special compact device that could not be produced without AM, while enabling a level of bio-compatibility not achievable with polymer AM. Techshot engineers were reportedly able to interface the larger bio-structures with the additively manufactured ceramic manifolds.

"It's been an absolute pleasure working with Lithoz," stated Dr Carlos Chang, Techshot's Senior Scientist. "Their expertise in ceramic processing really made these parts happen."

Shawn Allan, Vice President of Lithoz, commented, "The success of ceramic Additive Manufacturing depends on working together with design, materials, and printing. Design for Ceramic Additive Manufacturing principles were used along with print parameter control to achieve Techshot's complex fluid-handling design with the confidence needed to use the components on ISS."

www.lithoz.com

www.techshot.com

Metallic3D's new sinter-based Additive Manufacturing machine uses metal paste as feedstock

Metallic3D, based in Stuart, Florida, USA, has added a new metal Additive Manufacturing machine, the M3D300. Utilising the company's bound metal paste deposition technology, the M3D300 is reported to offer a safe, easy to use system capable of manufacturing components in a wide range of metals.

The bound metal paste process is said to be suitable for any office or workshop environment, with no fumes or odours created in the M3D300 machine. Due to the use of a solvent-based binder in the feedstock, the company states that most of the binder evaporates during the build. Any residual binder is then removed during the sintering stage, rather than an additional debinding stage, which Metallic3D says makes its AM process faster from initial design to fully finished part.

"Additive Manufacturing has now for some time been the solution of choice when producing highly diverse parts," states owner of the company, Dan Defelici. "3D printing enables the emergence of radical product innovation through function-oriented design properties. Paired with the outstanding material properties of high-performance ceramics and advanced metal powders, industries and research teams can now explore entirely new areas of applications."

By building the complete system in-house Metallic3D states it can significantly lower the barrier of entry into Additive Manufacturing. "Our new desktop printer is up to 10x less expensive than alternative metal Additive Manufacturing technologies and up to 100x less than traditional fabrication technologies like machining or casting. This gives the owner of a Metallic3D printer a higher ROI, less time making parts and fewer worries over quality," added Defelici.

Metallic3D's new M3D300 AM system (Courtesy Metallic3D)

www.metallic3d.com

COMPLEX TO IMAGINE. EASY TO CREATE.

BINDER-JET 3D PRINTING IS YOUR SOLUTION!

Indo-MIM brings you the cutting-edge new technology in association with **Desktop Metal Inc. USA.** We can now produce complex parts which cannot be produced through Metal Injection Molding, using a revolutionary new technology that enables you to 3D print complex components, 100X faster than Laser 3D printing.

Consider Binder-Jet 3D Printing for:

- Part geometry is medium to extremely complex. • Proto samples in 10 days.
- Part weight between 5 grams ~ 250 grams. • Volume 10 ~ 50,000 parts/yr.

(Will be ready to tackle volumes in 50,000 ~500,000 by 2021)

WE ACCEPT PROTO-SAMPLE ORDERS STARTING JANUARY 2020. MATERIALS OFFERED CURRENTLY ARE STAINLESS STEELS 17-4PH & SS 316. MORE MATERIAL OPTIONS BY SUMMER, 2020.

INDO-MIM®
COMPLEXITY SIMPLIFIED

CONTACT FOR MORE DETAILS

North America: Email: InfoUS@indo-mim.com Ph: +1 734-834-1565
Europe: Email: InfoEU@indo-mim.com Ph: +49 1732656067
Asia: InfoHQ@indo-mim.com Ph: +91 98459 47783 / +91 98450 75320

ISO 9001: 2015 / IATF 16949:2016 / AS 9100 : Rev D / ISO 13485:2016 / ISO 14001:2015

Dutch Aerospace Centre to install Xerion Fusion Factory Compact

The Dutch Aerospace Centre (NLR), based in Marknesse, the Netherlands, in cooperation with the Dutch Ministry of Defence, will install a Fusion Factory Compact debinding and sintering unit for use in its development of sinter-based AM. This jointly undertaken research reportedly focuses on defence applications such as battle damage repair.

The Fusion Factory Compact debinding and sintering unit, which began serial production at the beginning of 2020, is built by Xerion Berlin Laboratories GmbH, Berlin, Germany. With a footprint of just 1.2 m², the unit is designed to debind and sinter parts additively manufactured with BASF Ultrafuse 316L® filament, enabling the processing of parts within twenty-four hours. In accordance with the BASF Catamold® principle, debinding is carried out by catalytic process, while the sintering furnace can reach temperatures of up to 1,450°C under protective gas conditions. Sintering under a 100% hydrogen atmosphere is also possible.

With no powder bed used in the Fused Filament Fabrication (FFF) process, and 100% of the metal powder contained within the filament, this developers state that this manufacturing technology can be used in particularly rough or hazardous conditions, such as those found on marine vessels. The overall size of the unit, with external dimensions of 1,200 x 1,000 x 2,000 mm, further supports these applications.

www.xerion.de
www.nlr.org

Xerion's ultra-compact Fusion Factory debinding and sintering unit (Courtesy Xerion Berlin Laboratories GmbH)

Ametek to sell its Reading Alloys business to Kymera

Titanium is widely used in medical applications (Courtesy Reading Alloys)

Kymera International, a speciality materials company headquartered in Raleigh, North Carolina, USA, has entered into a definitive agreement with Ametek, Inc., Berwyn, Pennsylvania, USA, to acquire its Reading Alloys business, a provider of highly engineered materials for mission-critical applications in numerous markets. Founded in 1953, and acquired by Ametek in 2008, Reading Alloys designs, develops and produces master alloys, thermal barrier coatings and titanium powders. The business is a preferred supplier for producers of high-quality titanium and superalloy mill products that are used in aerospace and aircraft applications.

Kymera has been owned by affiliates of Palladium Equity Partners, LLC, New York, USA, a middle-market private equity firm with approximately $3 billion in assets under management, since 2018. The transaction is expected to close in the first quarter of 2020. The terms were not disclosed.

"Reading Alloys is an outstanding company with highly skilled people and an excellent product and endmarket portfolio that we believe fits in perfectly with our existing business," stated Barton White, CEO of Kymera International. "For Kymera, we believe this is a transformative acquisition that will give our combined company strong technical and commercial resources to help fuel our growth in the aerospace, defence, medical and industrial markets."

Adam Shebitz, Managing Director of Palladium, commented, "The acquisition of Reading Alloys, Kymera's second to date, is right on strategy as the Kymera management team continues to build the company into a leading speciality materials producer. Kymera represents another great example of Palladium's value creation framework, which pulls on both organic and M&A driven levers. We are excited about this opportunity to enhance the Kymera platform with Reading's value-added products, growing end-markets and its talented employees."

www.kymerainternational.com
www.readingalloys.com
www.ametek.com

CIM specialist Formatec adds ceramic AM to its production offering

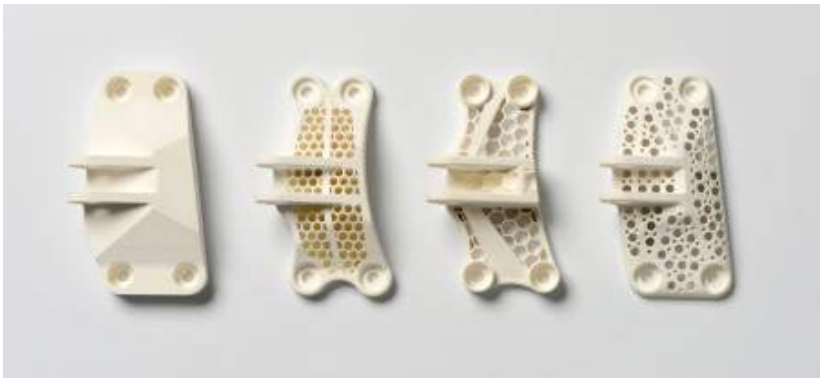

Geometrically complex parts produced using ceramic AM (Courtesy Formatec Ceramics)

Formatec Ceramics, Goirle, the Netherlands, has added ceramic Additive Manufacturing (AM) to its production services. The company has for twenty years offered Ceramic Injection Moulding services, from consulting and engineering across the full process chain of tooling development, injection moulding, debinding and sintering, finishing and quality control.

The company specialises in the production of CIM parts for the chemical, medical and aesthetic industries, where the need for excellent product properties and finish quality is inherent. The addition of ceramic AM is expected to enable the company to achieve similar material properties as with CIM, while reducing production time, labour and costs and adding value through the ability to produce more geometrically complex parts.

René Bult, General Manager of Formatec, commented, "With our team we can offer our customers added value through our extensive knowledge and experience with ceramics as a CIM pioneer. This combined with the almost endless possibilities that 3D printing offers we are excited for the opportunities that lie ahead."

Formatec now offers five different ceramic production methods, making it possible to identify and pursue the best fit for each of its customers depending on quantity, investment and lead time. One company which recently opted to use Formatec's ceramic AM capabilities is Thermo Fisher Scientific. Peter Glajc, a Mechanical Engineer at Thermo Fisher Scientific, explained, "We've chosen 3D printing because we wanted to compare this quite new and interesting technique with 'standard' ceramics manufacturing. 3D printing was cheaper and faster."

www.hightechceramics.com

Ceramic Injection Moulding enables production of bluetooth-connected jewellery

Nolato AB, Torekov, Sweden, is enabling the production of bluetooth-connected and and sensor-containing jewellery through the Ceramic Injection Moulding of zirconia. The items produced by the company include the Miragii smart pendant, a collection of bluetooth-connected rings and pendants for technology design studio Vinaya, and a family of wearable sensors for digital health company Cloudtag.

According to Nolato, the use of zirconia has previously been restricted by a very complicated production process. Together with materials suppliers and researchers at Chinese universities, the company states that it has now developed materials that make production easier and allow zirconia to be used in high-volume manufacturing.

Among the items produced using Nolato's zirconia CIM process, Vinaya's necklace connects to the wearer's smartphone and vibrates when a call or message is received. This allows the wearer to keep their phone out of sight without missing important communications.

Cloudtag's wearable sensors continually measure a range of health indicators in users and transfer them wirelessly to a smartphone. The material's properties mean the sensors can be worn on the body at all times without harm to the skin or health.

Nolato executes a full prototyping process flow with its customers. This allows the company to work with its customers in the early project phase, anticipate technical and process parameters for mass production, and quantify and eliminate quality risks.

www.nolato.com

A bluetooth-connected ring with elements produced with CIM zirconia (Courtesy Nolato AB)

ASL commissions new 400 kg gas atomiser specifically for AM and MIM powders

Atomising Systems Ltd. (ASL), Sheffield, UK, has expanded its capacity through the installation of a new 400 kg gas atomiser aimed specifically at the Additive Manufacturing and Metal Injection Moulding powder markets.

An additional melter is now being installed for greater flexibility and capacity. The in-house-designed atomiser, equipped with ASL's proprietary anti-satellite and hot gas system, produces high yields of MIM and/or AM powders, enabling ASL to continue to serve its expanding AM and MIM customer base.

Paul Rose, Commercial Director, stated, "The addition of another atomiser, along with the associated sieving and classification equipment, means that we are able to keep pace with the growth of our existing client base and the requirements of new clients, especially in the AM and MIM sectors."

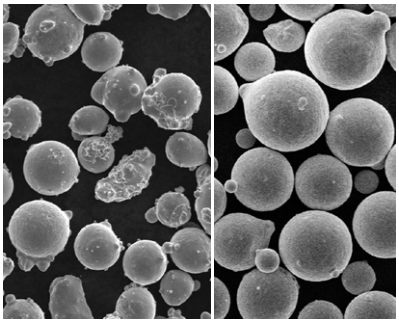

Powder from a conventional gas atomiser (left) vs powder from ASL's atomiser with anti-satellite system (right) (Courtesy Atomising Systems Ltd.)

Rose added, "In these sectors, the benefits of ASL's Anti-Satellite technology are clearly recognised through the excellent powder shape and flow properties."

www.atomising.co.uk

PM China 2020 announces new dates

The 13th International Exhibition for Powder Metallurgy, Cemented Carbides and Advanced Ceramics (PM China 2020), organised by Uniris Exhibition Shanghai Co., Ltd, has been moved to August 12–14, 2020, following the coronavirus (Covid-19) outbreak.

Originally set to take place at the Shanghai World Expo & Convention Center from March 24–26, 2020, over 500 organisations were reported to have reserved booths at the event. "We once again apologise for any inconveniences caused to you by the postponement and are sincerely grateful for your kind understanding and continual support. We look forward to seeing you on August 12–14, 2020, at Shanghai World Expo Exhibition Center!," stated the event organisers.

http://en.pmexchina.com

富驰高科
Future High-tech

COMPLEX COMPONENTS SOLUTIONS

Shanghai Future High-tech Co., Ltd. was founded in 1999. With over 20 years' MIM development and manufacturing experiences, we have become one of the leading MIM manufacturers in the world. We have three production bases, two in Shanghai and another in Shenzhen, to provide best-in-class products at a competitive cost to our customers.

We're providing new products from design, prototype, small batch to volume production to our customers with one-stop technical support. Our main product applications covering automobile, medical, consumer electronics, tools, locks, etc…

- 95% + feedstock self-developed
- 95+ MIM patents
- In-house tooling workshop (design & fabrication)
- Early involvement in customer design stage
- 47+ materials application
- Molding machine : 350+ sets
- In-house equipment design & modify
- Dedicated automation department

http://www.future-sh.com
+86-021-56445177
marketa@future-sh.com.cn

Injection moulding machine specialist Arburg opens new training centre

Arburg GmbH & Co KG officially opened its new Training Centre at the company's headquarters in Lossburg, Germany, on March 6. Covering 13,700 m^2, the new building has increased the total usable space at the Arburg's headquarters by just under 5%, taking it to approximately 180,000 m^2. The training area alone spans two floors, while the remaining three floors house open-plan administrative offices and a new health centre. Through this development, the company aims to set new standards in customer education, with a focus on cutting-edge digital training.

Amongst the 170 guests in attendance at the opening were Dr Klaus Michael Rueckert, Administrator of Freudenstadt district where Lossburg is situated; Lossburg Mayor Christoph Enderle; plus representatives of the companies and institutions involved in the building's construction.

"Arburg is known for the premium range of services it offers and its focus on customers. We're always thinking ahead and we set new standards time and time again. Whether we're developing products and processes or working on construction projects, we create a blend of outstanding functions and aesthetic appeal – and we combine high-tech, innovative ideas with sustainability and a prudent attitude to resources," stated Michael Hehl, who is responsible for Plant Development in his role as Managing Partner at Arburg.

"The fact that we have invested a double-digit million euro sum in a new Training Centre is testament to just how important our customers and employees are to us," added Hehl. "Not only that, but it also illustrates our strong belief in Germany as a location in which to do business – and specifically how much we value Lossburg itself."

He continued, "This is a building of the future, where customers and other stakeholders can take advantage of the industry's latest training resources. Over these 2,200 m^2, we can now offer interactive, networked learning opportunities focusing on both theory and practice – right here in Lossburg."

The ground-floor machine hall is the heart of the training area, spanning some 1,160 m^2 and housing fifteen electric, hybrid, hydraulic and vertical all rounder injection moulding machines of various sizes, including a multi-component version. The machines chosen for the hall represent a cross-section of all the sizes and drive versions available in Arburg's product range. Each injection moulding machine is equipped with a robotic system plus an IoT gateway, and is linked to the Arburg ALS host computer system. There is also a Freeformer available for training in Additive Manufacturing.

While the training rooms themselves have a dedicated area on the first floor, theoretical concepts and their practical applications will be knitted more closely together in future. To achieve this, each of the eleven training rooms is equipped with a state-of-the-art smart board and every course participant will work on their own touch screen PC with a simulated control system. The PCs will also be networked with one another, enabling interaction, screen sharing and application sharing – making it possible to transfer the on-screen content from one computer to another and work collaboratively on the same document.

Arburg states that digitalisation will take things even further, allowing data to be transferred from the training room's smart board to a smaller board on each machine. This will enable participants to work together in real time, wherever they are and no matter what device they are working on.

The new Arburg Training Center in Lossburg (Courtesy Arburg GmbH & Co KG)

Since Arburg first launched its training courses in 1969, more than 120,000 participants in Germany alone have taken advantage of the extensive range of learning opportunities in order to tap fully into the potential of machinery, application technology and service. Today, the thirty-strong training team organises 650 to 700 courses for more than 3,500 customers every year.

www.arburg.com

Dates announced for 20th Plansee Seminar

Plansee Group, headquartered in Reutte, Austria, has announced the dates for its 20th Plansee Seminar, the International Conference on Refractory Metals and Hard Materials, which will take place at its Reutte headquarters, June 7–11, 2021.

Originally established by Professor Paul Schwarzkopf in 1952 as a four-yearly event, the seminar is a global forum for the technical and scientific Powder Metallurgy community to exchange ideas and keep up to date with the latest innovations and market trends in the fields of refractory metals and hard materials.

Plansee Group states that the aim of the conference is to provide insights into all aspects of these materials – from materials science to the latest achievements in extractive metallurgy, manufacturing technology, industrial applications and recycling.

Presentations are expected to cover all market segments where refractory metals and hard materials are playing an important role, or where they may provide promising alternatives to present material solutions. The following fields of application, in particular, will be addressed:

Refractory metals and composites for application in:

- Transportation
- Electronics
- Thermal management
- Lighting technology
- Medical technology
- Energy generation and distribution
- Power engineering
- Chemical engineering
- Coating technology
- Joining technology
- Metal, glass, plastic, and ceramics production
- High-temperature furnaces and devices
- New areas

PM hard materials for application in:

- Wear parts
- Machining of metals, composites, graphitic materials, wood and stone
- Precision tooling
- Chipless forming
- Mining and constructions
- Joining technology

www.plansee-seminar.com

Arburg appoints Guido Frohnhaus as Managing Director of Technology & Engineering

Arburg GmbH + Co KG, headquartered in Lossburg, Germany, has appointed Guido Frohnhaus as its new Managing Director of Technology & Engineering. Its Technology & Engineering management division had recently been led on an interim basis by Managing Partner Juliane Hehl, however the senior management team is now complete with the appointment of Frohnhaus.

Fronhaus was formerly Managing Director of Werner Turck GmbH & Co. KG, Halver, Germany, a leader in industrial automation solutions, where he was responsible for the development and production departments. Prior to this, he was Vice President of Technology at the Turck national subsidiary in the USA as well as several years working in management roles at an automotive supplier. He started his career by completing an apprenticeship as a toolmaker and went on to study mechanical engineering, specialising in manufacturing engineering, at the University of Wuppertal, Germany. During his time working in the USA, he also completed an MBA from Capella University, Minneapolis, Minnesota, USA.

www.arburg.com

OOCII | MATRIX

Partners for custom made components

MIM & CIM Process

Metal and Ceramic Injection Molding

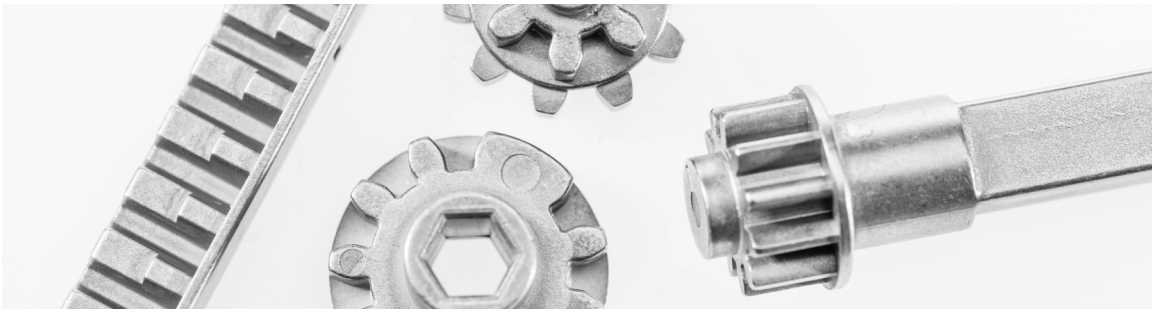

Canadian FabLab installs Rapidia metal Additive Manufacturing system

The Rapidia system builds parts using water-based metal paste technology (Courtesy Rapidia)

The Kootenay Association for Science and Technology (KAST) based in Trail, British Columbia, Canada, has installed a Rapidia metal Additive Manufacturing system, at its MIDAS Lab. The Metallurgical Industrial Development Acceleration and Studies – or MIDAS – Lab is reported to be the first rurally located FabLab (fabrication laboratory) in Canada to install a metal AM system.

The MIDAS Lab provides access to the equipment needed for digital fabrication and rapid prototyping, as well as project work areas, a research and development lab, a metal shop, a woodshop, a computer lab and a training centre.

"Metal printing is a game-changer for fabricating parts and prototypes," stated Cam Whitehead, Executive Director of KAST. "Lower costs and increased speed to produce prototypes means faster innovation and more competitiveness. This all means more jobs and wealth for the region. Our services are available to commercial members, unlike most universities – these machines are so new and expensive that previous focus has been on research and not necessarily business needs."

"MIDAS Lab is unique in Canada and has been since it opened its doors in 2016," added Whitehead. "We're thrilled that it's received countrywide recognition and we're using some of the lessons learned to help other start-up fabrication labs and innovation centres across BC."

The Rapidia system uses a water-based metal paste which eliminates the debinding step, enabling the two-stage Rapidia process to produce most parts in under twenty-four hours. The system is also believed to cut Additive Manufacturing time further by avoiding the need to produce a metal base plate or most metal supports. It is capable of building a range of materials including stainless steel, Inconel, tool steel, ceramics and titanium.

"While there are printers that can do what the Rapidia can do, we chose this one because of its safe operation, the speed at which you can operate and create the designs and parts that our industry partners and Selkirk College needs," explained Jason Taylor, Instructor & Applied Researcher at Selkirk College.

KAST partner, Selkirk College plans to launch Digital Fabrication & Design, a two-year diploma programme that trains graduates for advanced manufacturing, in September 2020. Daryl Jolly, School of the Arts chair, stated that the Rapidia system will be an exciting new educational tool students will be able to utilise. "As we launch this new programme, it's exciting to again see that Selkirk College students will be trained on and have access to world-class equipment. We expect our graduates will be well-positioned to support continued economic growth in our region, bringing value to industry and innovation," he commented.

www.kast.com
www.midaslab.ca
www.rapidia.com

KAST's MIDAS Lab has installed a Rapidia metal AM system (Courtesy KAST/ MIDAS Lab)

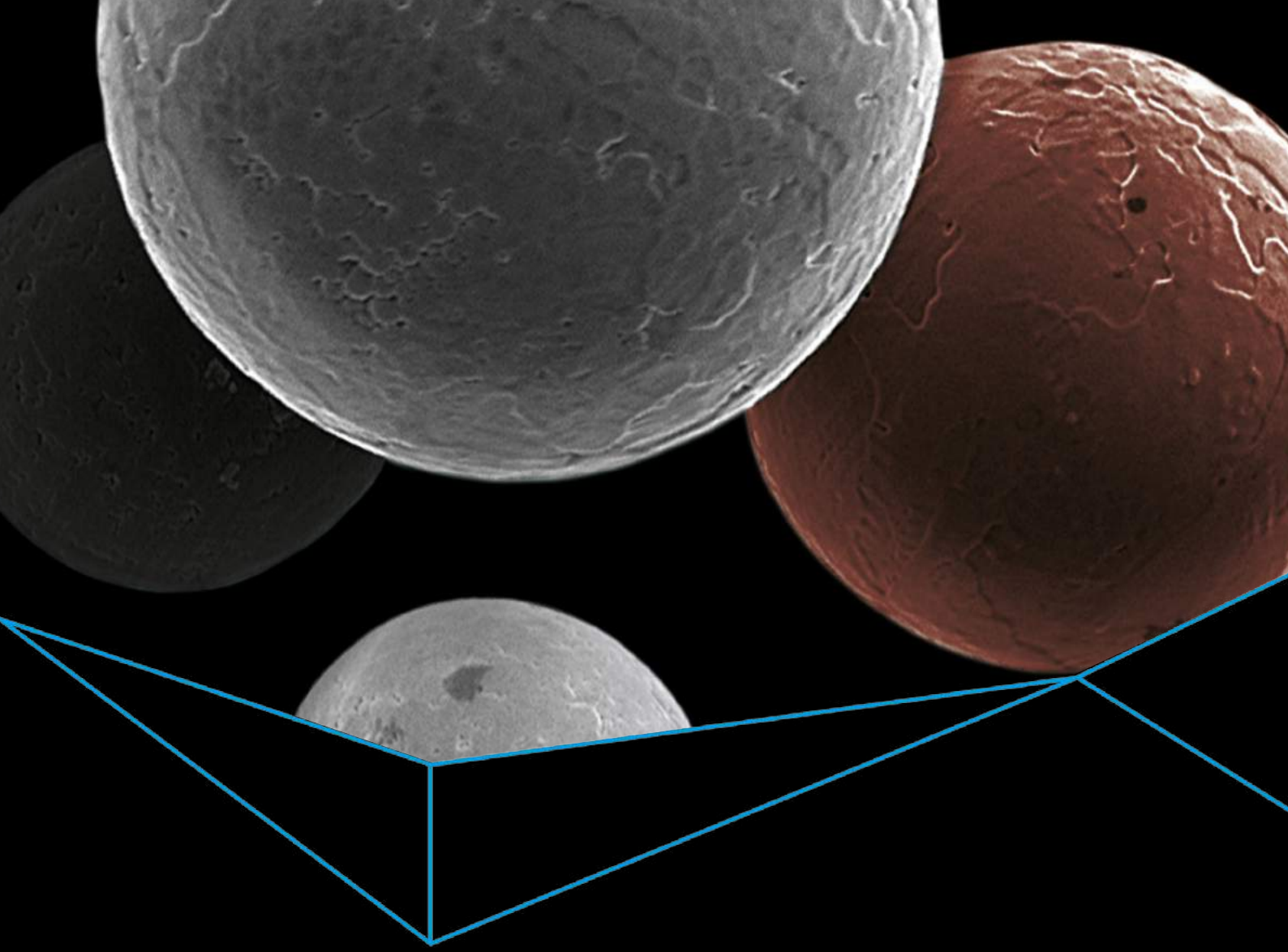

POWDER BY SANDVIK
IT DOESN'T GET FINER THAN THIS

In Metal Injection Moulding, the finest detail gives the best outcome. Place our gas atomized Osprey® metal powder under a microscope and see the uniform consistency made for MIM. The spherical shape of our metal powders makes for excellent flow and high packing density. Essential qualities in the aerospace, automotive, electronics and dental industries. In general engineering too.

Our powders are available in a wide range of particle sizes – from under 5 µm and up to 38 µm. And, in an extensive range of alloys, like stainless steels, maraging steels, nickel-based superalloys, tool steels, cobalt alloys, low alloy steels, aluminium alloys, plus copper and bronze alloys.

Need more information or something tailor-made as a small batch?
Contact us today.

Visit us at | TCT Asia 2020 | Booth E6-M16 | July 8-10 | Shanghai
Visit us at PM China 2020 | August 12-14 | Shanghai

E-MAIL: POWDER.OSPREY@SANDVIK.COM | PHONE +44 (0) 1639 634 121
METALPOWDER.SANDVIK

SANDVIK

European Powder Metallurgy Association to establish new secretariat in France, closing UK base

The European Powder Metallurgy Association (EPMA) has announced that it will close its UK-based head office on April 30, 2020, and will establish a new secretariat team located in Chantilly, France. The EPMA was founded in Brussels in 1989, and has had its secretariat based in Shrewsbury, UK, since 1990. A second office, established as a base for the EPMA's technical team, was opened in Chantilly, France, in 2018.

According to the EPMA, the decision was made in order to improve overall efficiency, as well as enabling a better platform for cost optimisation. As of May 1, the French office will become the association's main administrative base and home to a new secretariat team. The EPMA's registered headquarters will remain in Brussels. To ensure a level of continuity in the run-up to the Euro PM2020 Congress & Exhibition, taking place in Lisbon, Portugal, in October, key UK-based staff members will continue to work from home, with employment extended until the event.

www.epma.com

MPIF announces Edwin Pope as keynote speaker for WorldPM2020 Montreal

The Metal Powder Industries Federation (MPIF) has announced that Edwin Pope, Principal Analyst at IHS Markit, has been selected as keynote speaker for the co-located conferences, WorldPM2020, AMPM2020 and Tungsten2020, which will take place in Montréal, Canada, from June 27–July 1, 2020.

WorldPM is held every two years and in 2018 took place in Beijing, China. The conference is held in North America once every six years, and this will be the second time that it has been co-located with Tungsten2020 and AMPM2020.

During the Opening General Session on June 28, 2020, Pope is expected to discuss outlooks and trends for the global automotive market, propulsion system design, transmission design, electrification, and metal Additive Manufacturing within the automotive sector.

Further information and registration details are available via the event website.

www.mpif.org/Events/WorldPM2020

EWIE Group launches Additive Manufacturing brand Azoth 3D

The EWIE Group of Companies (EGC), a family of manufacturing brands headquartered in Ann Abor, Michigan, USA, recently launched a new brand focused on the provision of Additive Manufacturing services to its group companies and customers. Azoth 3D offers both metal and polymer Additive Manufacturing, as well as associated services such as design and prototyping, and 3D scanning and reverse engineering.

East West Industrial Engineering Company, the founding brand of EGC, was founded in the 1980s and has since focused on using technology to reduce its customers' operating costs and improve production efficiencies. The group's companies now service 300+ facilities in twelve countries.

Explaining the decision to enter the Additive Manufacturing market, EGC stated that, understanding the shifting landscape of manufacturing as part of Industry 4.0, the need to diversify became clear. One of the largest subcategories of items that its brands are often asked to source are machine spare parts, with most production facilities stocking rooms full of brackets, gripper fingers, fixtures, motors, and automation components in order to minimise the impact of machine downtime.

In many cases, when a machine part fails, it is too old to locate an original manufacturer to source a replacement. This is further complicated when submitting a one-off emergency order to a local machine shop, where lead times are long and prices are high. This, EGC saw, offered the perfect opportunity to take advantage of Additive Manufacturing's unique capabilities.

"The EGC's success, and consistent growth, can be attributed to three things," explained Joey Mullick, Vice President, Azoth 3D. "First, identifying the best technology for a plant operation. Second, consolidating the vendor base by identifying manufacturers who provide world-class products and global support. Lastly, benchmarking best practices and replicating them throughout a customer's manufacturing facilities. Azoth is leveraging these same principles in the world of additive."

Azoth 3D's Center of Excellence, also located in Ann Arbor, is said to have grown from an empty warehouse into an impressive lab of the industry's highest-performing technology in less than two years. The team stated that it envisions being able to support the bulk of orders from this HQ, focusing primarily on Binder Jetting for its metal AM offering.

To support its metal AM capabilities, the company has so far built partnerships with Digital Metal and its parent company Höganäs, Höganäs, Sweden; Desktop Metal, Burlington, Massachusetts; and Elnik Systems, LLC, and its sister company DSH Technologies, Cedar Grove, New Jersey, USA. "Just as a traditional manufacturing facility could not procure all its tools from one toolmaker; Azoth is diverse in its partnerships and holistic in its services," stated Mullick. "The team has built up a network that includes shops that offer technologies they do not, machine distributors, and partners with deep additive expertise. They are also providing reverse engineering and DFA services."

ECG reports that its vision for Azoth is to transform the physical inventory of a plant into a digital one, thereby reducing the costs of its customers. To this end, the company has coined a new phrase: 'Take One Make One' or 'TOMO'. "The problem Azoth seeks to solve was ever-present in EGC's existing customer base, and early adoption of their business model has been significant," explained Mullick.

"Since the issues surrounding spare parts are common to all manufacturing facilities, Azoth has been able to grow beyond the group's common customer architype," he continued. "New customers choose Azoth because of their ability to manufacture precision parts to blueprints, their vast knowledge of the additive tools available in the market, and the ability to implement digital inventory on demand. Customers that choose to work with Azoth get more than a 3D printed part. They get a team focused on generating solutions, with access to the latest technology in AM, and EGC's manufacturing history."

www.azoth3d.com
www.ewie.com

Cody Cochran, Azoth 3D's Key Account Manager, with an installed furnace from Elnik Systems, LLC (Courtesy Azoth 3D)

Predicting the future for Metal Injection Moulding

In a Special Interest Seminar titled 'The Future of MIM', at the Euro PM2019 Congress, organised by the European Powder Metallurgy Association (EPMA) and held in Maastricht, the Netherlands, October 13-16, 2019, an analysis of the current status of Metal Injection Moulding technology and predictions for its future development were provided in a presentation from Benedikt Blitz, Managing Director, SMR Premium GmbH, Germany.

SMR Premium is a member company of the SMR Group and specialises in the provision of market intelligence for High Value Materials. Powder Metallurgy production is one focus of the company's materials portfolio. This report focuses on Blitz's assessment of MIM, in keeping with the presentation's title, although other powder-based processes, such as HIP and Additive Manufacturing, were also considered during the presentation.

Blitz began with a short overview of the global steel industry, which identified that the total annual tonnage of all PM processes (~1.3 million tonnes) equates to less than 0.1% of total steel product tonnage (~1,800 million tonnes). The presentation emphasised that 94% by volume of metal powders are consumed by conventional 'press and sinter' Powder Metallurgy, but, for the remaining 6% (including MIM powders), the tenet is to concentrate on value rather than volume and target the high end of the market (Fig. 1).

In describing the current status of MIM, data were provided (Fig. 2) on the breakdown of products by material type and customer sector. In relation to powder type, stainless steels account for 53% by volume, other steel types 25%, superalloys 11% and a variety of other metals 11%.

The global breakdown by industry sector revealed a broad range of applications. The application breakdown by geographical region shows significant differences; in Europe, automotive applications are relatively dominant; in North America, medical and consumer goods; and, in Asia, information technology (Fig. 3).

An analysis of MIM products by weight and size emphasised that they are currently predominantly small parts. Data were also provided

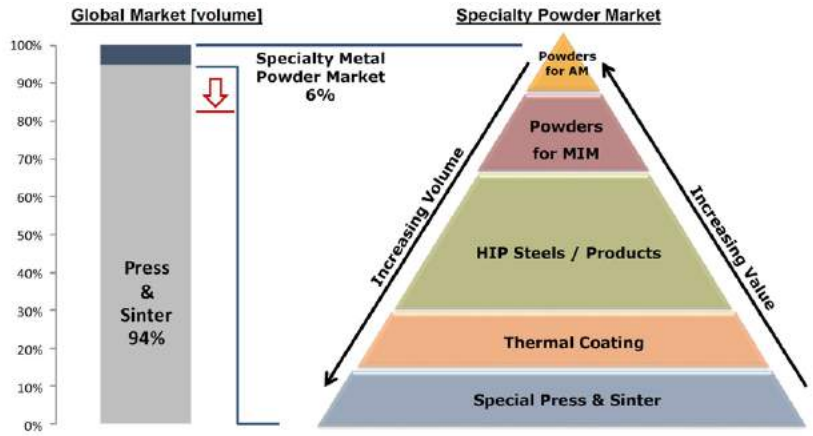

Fig. 1 Focus on value rather than volume in metal powder developments (Courtesy Benedikt Blitz / As presented at Euro PM2019)

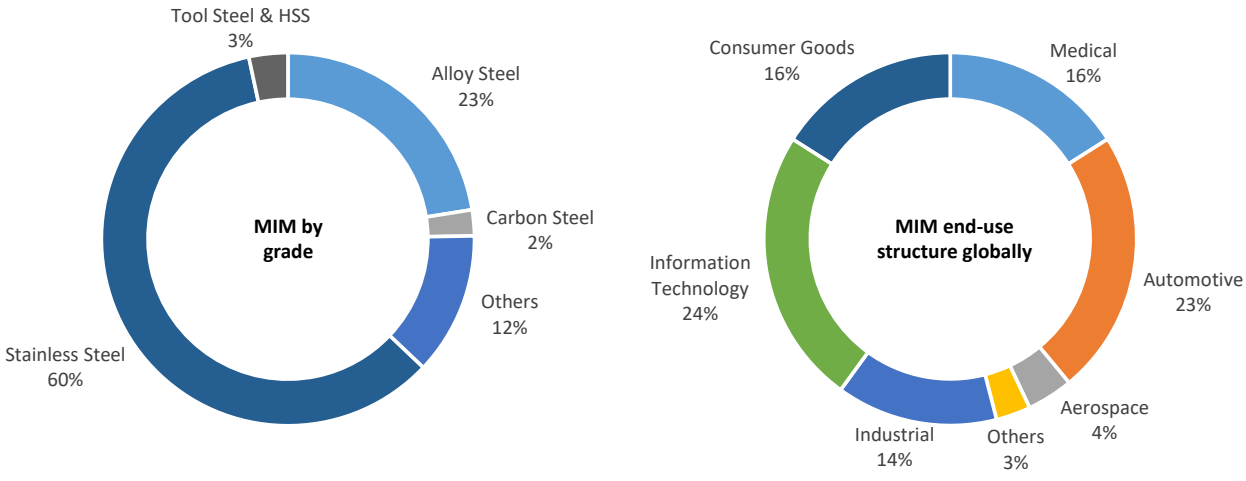

Fig. 2 Current global MIM applications by material type and end-use sector (Courtesy Benedikt Blitz / As presented at Euro PM2019)

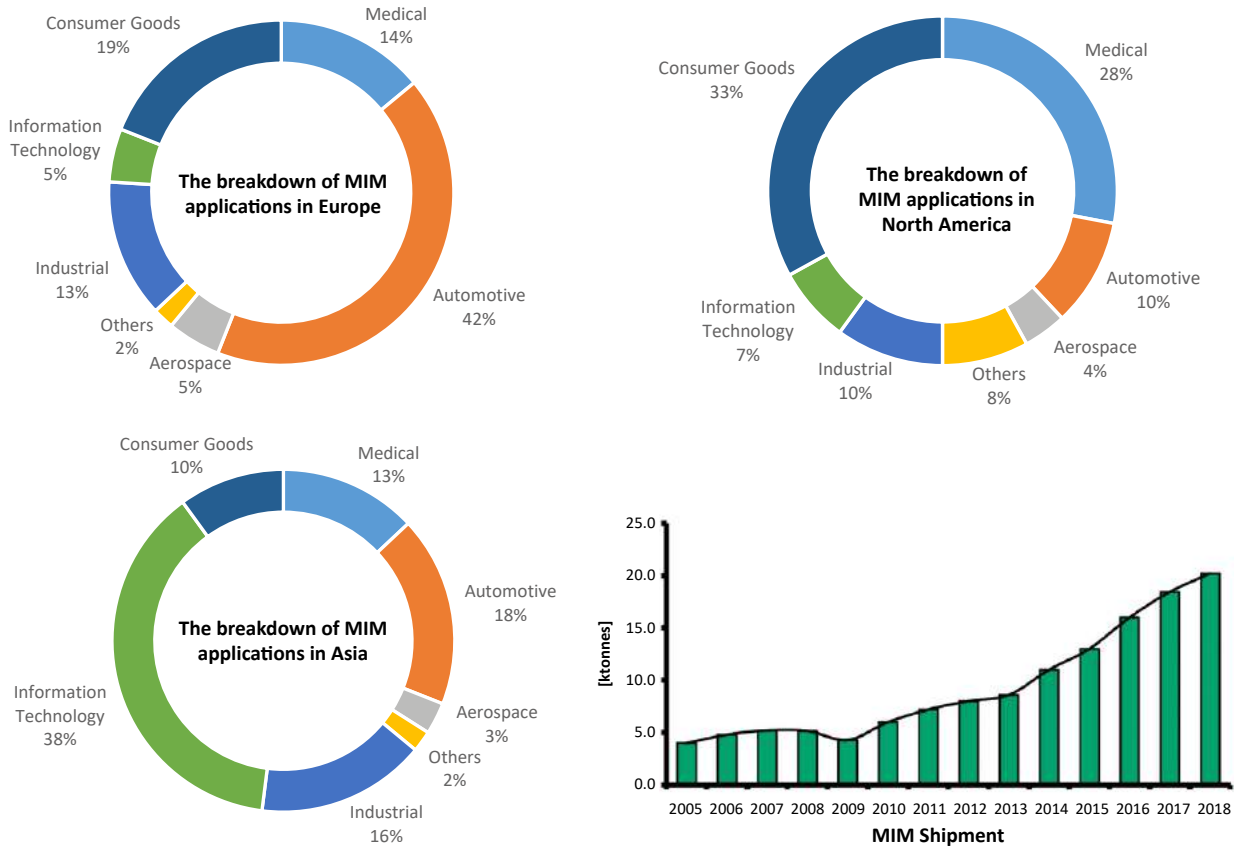

Fig. 3 Breakdown of MIM applications by geographical region (Courtesy Benedikt Blitz / As presented at Euro PM2019)

to divide the global totals for sales turnover (~€2,300 million) and active parts producers (630) by geographical region, emphasising the significant role of China.

It was then emphasised that the widespread markets for MIM products mean that these applications are encountered in every aspect of daily life, particularly in transportation, aerospace, the 3C industry and a broad range of consumer products. In relation to the future market developments, it was predicted that the significant rise already observed in production levels for Boeing and Airbus will continue more strongly over the next eight-to-ten years (Fig. 4).

Finally, an overall summary of SMR's predictions for PM global market evolution by manufacturing technology type up to 2025 was shown. MIM is predicted to show a compounded annual growth rate (CAGR) of around 11% over the period. This was second only to the predicted growth rate for AM (25%), although, of course, AM is starting from a much lower base level. These figures can be compared with the predicted CAGR for Press & Sinter PM, the traditional bedrock of the PM sector, of only around 3%.

In terms of MIM market development by end-use sector and geographical region, the predicted growing significance of automotive applications and demand in China was also emphasised.

www.smr-premium.com

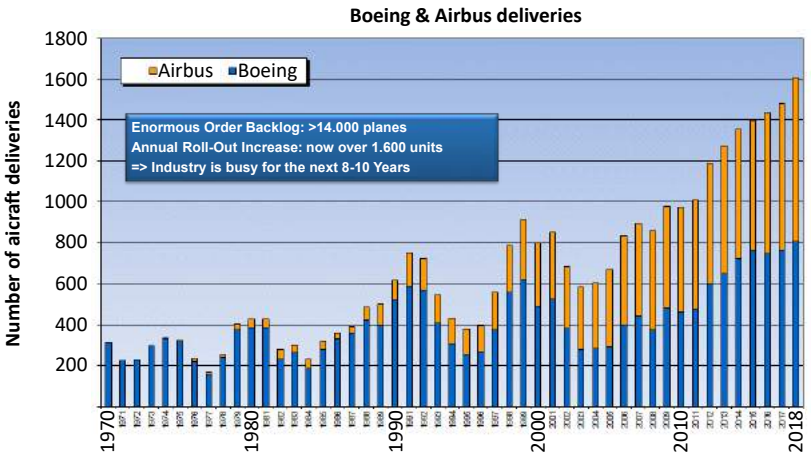

Fig. 4 Predicted growth in aerospace demand (Courtesy Benedikt Blitz / As presented at Euro PM2019)

Ricoh's new resin-coated powders and cross-linking ink to expand range of metals for Binder Jetting

Ricoh, based in Kanagawa, Japan, has developed a new resin-coated metal powder and cross-linking 'ink' for use in the Binder Jetting process. Said to increase the diversity of metals available for Binder Jetting and improve the quality of components, the new range is aimed at those adopting Binder Jetting as a manufacturing process.

The metal powders are coated with a uniform layer of binder resin around 100 nm in thickness, in a process developed from coating technology acquired through electrophotography. A cross-linking material in the ink is said to work with the resin to form the green part.

According to Ricoh, a key advantage of the new material is to remove the risk of dust explosions associated with fine powder particles and potentially explosive powders, such as aluminium and titanium. Fine powders tend to offer improved sinterability and can lead to higher achievable density and low surface roughness. However, fine powders can be more explosive than coarse powders.

The new powders are coated with resin selected to improve both the minimum ignition energy and explosible concentration, important parameters in avoiding dust explosion. The resin-coating is said to prevent the propagation of fire between particles. This allows the use of fine powders and results in improved surface finish, reducing the need for additional post processing steps.

A further advantage of Ricoh's new process is the ability to control the permeability of the ink toward the powder bed. If permeation is less than expected, for example, it can cause increased porosity in the green part and if the ink permeates too far, it affects the dimensional accuracy of the parts produced.

The control of ink permeability is a key factor for the achievement of the correct density and accuracy for a part. Using its new materials, Ricoh stated that it has achieved the adjustment of the contact angle between the ink and powder surface, and a level of control over permeability through a selected combination of surfactant and coating resin.

www.ricoh.com

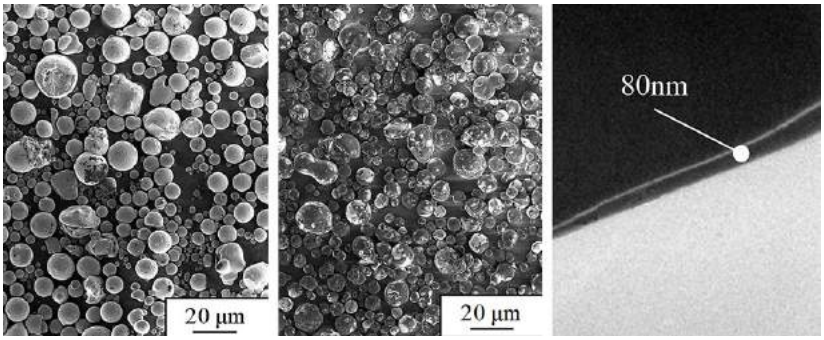

SEM images of left) uncoated powder, centre) coated powder, right) cross-section of coated powder of stainless steel 316L (Courtesy The Ricoh Company)

Isostatic Toll Services opens new HIP facility in Spain

Isostatic Toll Services Bilbao SL, opened its new Hot Isostatic Pressing facility on January, 29, 2020, in Abanto Zierbena, Biscay, Spain. With a total investment of €14 million ($15.5 million), the new plant reportedly offers the largest available HIP systems in southern Europe.

Already installed and operational at the Bilbao facility is an AIP52 HIP unit, with a second identical system due to be installed in December 2020. With a hot zone diameter of 1100 and depth of 2500 mm at 103 MPa, the AIP52 is capable of processing large components, such as engine blades, vanes and integral rings used in the aviation industry. In addition to supporting the high-tech aerospace sector, the facility is expected to serve the region's growing medical implant manufacturing industry.

The new facility has been granted EN 9100 approval by Bureau Veritas and has been successfully audited and approved by Rolls-Royce and Pratt & Whitney. Safran approval is currently underway, with Nadcap approval planned for mid-2020.

In addition to providing toll services, staff at ITS Bilbao will support a new AIP European Competence Centre, established to serve the EMEA region with installation, commissioning, maintenance, inspection and repair of AIP's range of presses and systems.

www.isostatictollservices.com
www.aiphip.com

The new ITS facility in Bilbao, Spain (Courtesy ITS Bilbao)

TEKNA

METAL POWDER MANUFACTURER

Ti64

Ni ALLOYS

- Plasma Quality Powder
- Low Oxygen Content
- High Packing Density
- Traceability
- Capacity
- AS9100:D and ISO 9001:2015

Contact us for
more information

+1 819 820 2204

TEKNA.COM

Soft magnetic properties of Fe-35%Co alloy produced by Metal Injection Moulding

Soft magnetic materials are those which are easily magnetised and demagnetised, and are widely used for household appliances, computer-related equipment, energy converters, generators, solenoid valves in fuel injection devices, solenoid cores, injector cores, and various sensors and torque sensor cores. Iron-cobalt alloys are an important soft magnetic material because they have a high Curie point and corrosion resistance, allowing them to be used at relatively high temperatures and in harsh environments. Additionally, Fe-Co alloys have the highest saturation induction (B_s) among all soft magnetic materials, which makes them ideal for applications such as solenoid valves. However, Fe-Co alloys are also extremely hard, which makes them difficult to machine.

Powder Metallurgy and Metal Injection Moulding offer a cost-effective alternative route to producing net shape soft magnets, and both PM and MIM are already extensively used for a wide range of soft magnetic applications. However, whilst Fe-Ni, Fe-equiatomic Fe-Co alloys and pure Fe have all reportedly been produced by PM and MIM, little data has been reported on the production of Fe-35%Co alloys using MIM. Researchers at the Southern University of Technology, Shenzhen, China, in collaboration with metal powder producer Sandvik Osprey Ltd, Neath, UK, have, therefore, been investigating a soft magnetic Fe-35%Co alloy made using MIM technology, and published a paper on the results of their research in the *Journal of Magnetism and Magnetic Materials*, Vol. 497, 2020, p. 7. In particular, their research focused on the development of a mathematical model which can be used to predict the magnetic properties of the sintered Fe-35%Co alloy from its microstructure.

The authors used a pre-alloyed Fe-35%Co powder, having particle size D90 = 16 µm, which was mixed with a polyformaldehyde (POM)-based binder system to produce the MIM feedstock. Powder loading in the feedstock was fixed at 63 vol.%. The MIM feedstock was injection moulded at 190°C to produce green annular samples, as shown in Fig. 1(a). The green parts were debound in a catalytic debinding furnace to remove the POM binder followed by a thermal debinding process conducted in a vacuum

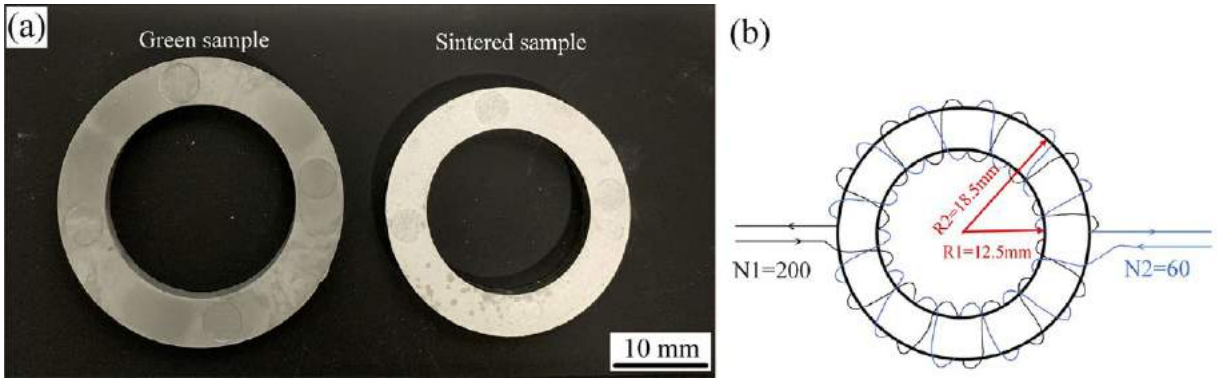

Fig. 1 (a) Samples produced by MIM (after injection moulding and sintering, respectively); (b) the geometric configuration of the samples produced by MIM used for the magnetic property tests. (From paper: 'Microstructures and magnetic properties of Fe-35%Co alloy fabricated by Metal Injection Molding', by Y Zhang, et al, Journal of Magnetism and Magnetic Materials, Vol. 497, 2020. Available online October 2019)

furnace to remove the remaining binders. The samples were subsequently sintered in the same furnace at different temperatures (1275, 1300, 1325, 1350 and 1375°C) for 3 h under a reducing atmosphere (flowing argon with 2% hydrogen). After sintering, the samples were cooled slowly in the furnace, resulting in a low level of internal stress.

The authors stated that the Fe-35%Co powder samples sintered at different temperatures all exhibited a single α-FeCo solid solution phase, and the interstitial impurity contents in the sintered samples were very low. Both sintered density and grain size were found to increase with increasing sintering temperatures. These features are said to make it an ideal model material for studying the relationship between magnetic properties and microstructures of the sintered MIM Fe-35%Co alloy.

The method used for measuring magnetic properties is illustrated in Fig. 1(b), where coils made from 0.35 mm diameter copper wire were used. The number of turns for the measuring coil and the magnetisation coil are 60 and 200, respectively. The saturation field intensity was maintained at 15,000 A/m in the study.

The authors reported that the saturation induction (B_s) of the sintered material increases with density. Therefore, the samples sintered at 1375°C exhibited the highest sintered density (7.67 g/cm^3) and saturation induction (2.152 T). The coercivity (*Hc*) of the sintered samples was found to increase linearly with the grain size, while the initial permeability (μ_i) is inversely proportional to the square root of the coercivity (H_c). Samples sintered at 1375°C therefore exhibited the lowest coercivity (171.7 A/m) and the highest initial permeability (1730 mH/m). Table 1 provides a summary of the magnetic properties of MIM Fe-35%Co alloy as related to different sintering temperatures, and the densities and grain sizes obtained.

Based on this established relationship, the authors stated that a mathematic model has been developed which can predict the coercivity (H_c) and initial permeability (μ_i) of the sintered Fe-35%Co alloy from its grain size. The model could also serve as a guide for producing Fe-Co alloys with the desired magnetic properties.

www.sustech.edu.cn/en/

www.journals.elsevier.com/journal-of-magnetism-and-magnetic-materials

Sintering temperature (°C)	*Bs* (T)	*Hc* (A/m)	*μi* (mH/m)	Grain size (μm)	Density (g/cm^3)	Impurity (wt.%)		
						C	O	N
1275	2.065	293.7	423	19.62	7.523	0.028	–	–
1300	2.092	260.2	435	21.86	7.546	0.024		
1325	2.106	258.3	445	23.85	7.574	0.030		
1350	2.124	225.5	449	27.71	7.584	0.024		
1375	2.152	171.7	545	34.10	7.670	0.020		

Table 1 Summary of sintered densities, grain sizes, interstitial impurity contents and magnetic properties of Fe-35%Co samples sintered at different temperatures. (From paper: 'Microstructures and magnetic properties of Fe-35%Co alloy fabricated by Metal Injection Molding', by Y Zhang, et al, Journal of Magnetism and Magnetic Materials, Vol. 497, 2020. Available online October 2019)

Sinter bonded AISI 4340 steel and WC-Co composites produced by inserted Powder Injection Moulding

Components are often required for applications which require high toughness properties on the inner part and high abrasion resistance on the outer part. Cutting tools are one example of this type of component, and a range of research has been undertaken on the bonding of, for example, WC-Co hardmetal and steel by methods such as diffusion welding or diffusion bonding, soldering, etc. However, the different physical and chemical properties of steel and hardmetal can significantly influence the desired shear strength of the bonded region. For example, metals and ceramics can have different thermal expansion coefficients, which can cause residual stresses in the components during cooling and may result in cracking or separation in the intermediate bonding zone.

A research project undertaken at Gazi University, Ankara, Turkey, has been studying the use of Inserted Powder Injection Moulding (IPIM) to produce functional components where the inner tough material is a solid AISI 4340 steel and the outer part is a wear resistant WC-9%Co hardmetal. A paper by Harun Kocak, Mehmet Subasi, and Cetin Karatas, published in *Ceramics International* (Vol. 45, July 2019, 22331–22335), describes the use of nickel as a bonding interlayer between the steel and injected moulded WC-Co, with the researchers having investigated the shear strength of the Ni bond achieved between the two materials during sintering.

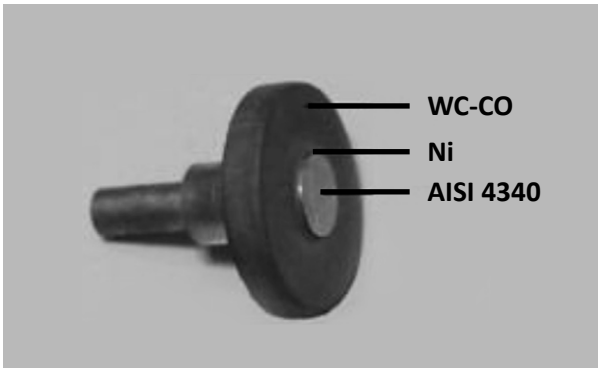

Fig. 1 Composite AISI 4340 steel-WC-Co part produced by the IPIM method (after sintering at 1250°C). (From paper: 'Sinter bonding of AISI 4340 and WC-Co using Ni interlayer by inserted Powder Injection Molding', by H Kocak, M Subasi and C Karatas. Ceramics International, Vol. 45, 2019, 22331–22336)

The authors stated that prior to injection moulding of the WC-Co feedstock, the cylindrical AISI 4340 inserts were electrolytically coated with Ni to coating thicknesses of 25, 50 and 100 µm. The Ni-coated inserts were then placed into the moulds, and WC-Co feedstock was injection moulded onto them. The WC-9%Co feedstock comprised powder having D50 particle size of 0.28 µm. The IPIM components underwent debinding in ethanol at 60°C for 48 h, followed by drying in a furnace at 60°C and sintering at 1250°C under controlled $95N_2$-$5H_2$ atmosphere. Sintering times were varied from 120 to 360 min in order to determine the diffusion bonding effect during sintering on the shear strength values of the Ni-bonded AISI 4340-WC-Co composite. Fig. 1 shows the composite IPIM part after sintering at 1250°C.

The authors found that increasing the Ni interlayer thickness to 100 µm also increased the shear strength of the bond, with the highest shear strength value being 266 MPa. Increasing interlayer thickness was also found to decrease the defects in the intermediate bonding zone, and it was found that shear strength increased as the sintering time increased to 240 min. It was further found

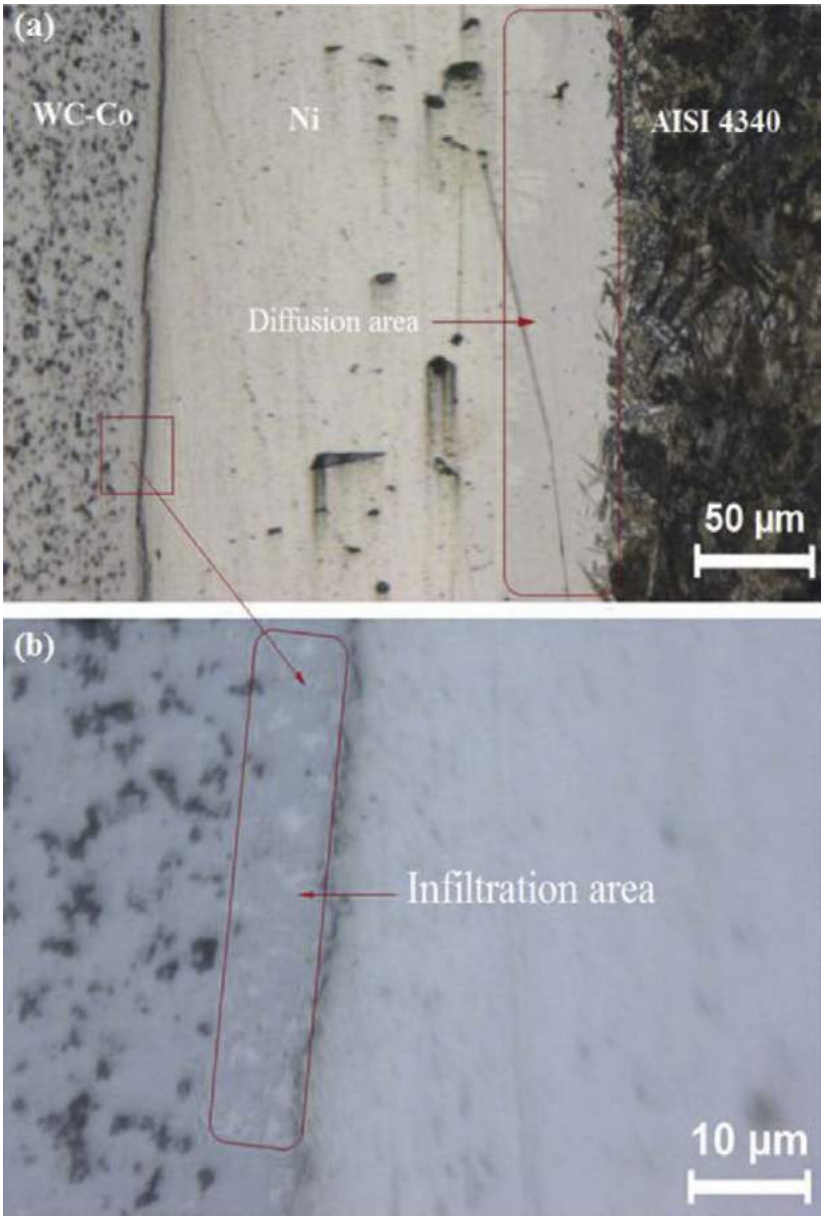

Fig. 2 Microstructures of 100 µm Ni interface in AISI 4340-WC-Co IPIM component sintered at 1250C for 240 min. (From paper: 'Sinter bonding of AISI 4340 and WC-Co using Ni interlayer by inserted Powder Injection Molding', by H Kocak, M Subasi and C Karatas. Ceramics International, Vol. 45, 2019, 22331–22336)

that the Ni interlayer diffused towards the steel side and infiltrated towards the WC-Co side, as can be seen in Fig. 2. EDS analysis showed a diffusion of 13.7% W, 4.41% Co to 4340 insert and 1.22% Fe, 1.7% Ni to WC-Co side.

Hardness studies showed that, whilst W and Co (which diffused more to the insert) increased the hardness of insert at the points close to intermediate zone, Fe and Ni (which diffused to the WC-Co side) caused a slight decrease in the hardness of WC-Co in this zone. However, only 0.8 mm from the intermediate bonding zone, hardness was found to be around 1400 HV. The authors concluded that IPIM can be used in all applications where toughness of the inner part and abrasion resistance of the outer part are desired, as for example in the production of cutting tools.

http://gazi.edu.tr/
www.journals.elsevier.com/ceramics-international

Low-Pressure Powder Injection Moulding used to produce NiO-YSZ anode-supported SOFC fuel cell/stacks

Solid oxide fuel cells (SOFCs) are modular, scalable, and highly efficient energy conversion devices that can convert a wide variety of gaseous, liquid and even solid fuels into electricity with almost zero pollution emissions. A typical fuel cell is made up of layers only a few millimetres thick which can be connected in series to form a SOFC 'stack'. The most commonly used material is a ceramic made up of a mixture of NiO and yttria stabilised zirconia (YSZ), and because the anode support needs to be porous, powders are used as starting material. Ni plays an electrical conducting role whilst YSZ serves as the ion conductor. For anode-supported SOFCs the shape can be planar, disk, tubular or other more complex shapes, and for large-area planar anode supports, tape casting can be used as the production process. However, tape casting is not suitable for complex-shaped SOFC anode supports, and the process has additional drawbacks in that it uses toxic solvents and other hazardous additives.

Research efforts have, therefore, been underway in recent years to develop a low cost, faster and more environmentally friendly alternative to tape casting for high-volume production, with Powder Injection Moulding offering a potentially economic route to the fabrication of porous Ni-YSZ supports. Most recent research using PIM has been focused on planar, or disk-type SOFCs. However, it is tubular SOFC cells which are said to have higher power output, more reliable stability and easier fuel cell stack design and assembly. Here, the air or fuel passes through the inside of the tubular shape, and the other gas is passed along the outside of the tube

Researchers at the Kunming University of Science and Technology, Kunming, South China University of Technology, Guangzhou, and Jiangxi University of Science and Technology, China, have in recent years reported on the use of Low-Pressure Injection Moulding (LPIM) to produce NiO-YSZ anode-supported tubular shaped SOFC cells/stacks with high production efficiency. The latest results of their research were published in *Ceramics International*, Vol. 45, 2019, 20066–20072. The researchers stated that no reports have been published using LPIM to produce tubular SOCFs, and they therefore paid special attention to the preparation of the ceramic powders used, especially the impact of pre-calcining temperature on the microstructure, porosity, and electrochemical performance of the LPIM NiO-YSZ SOFCs.

The ceramic powders used in the research included NiO and yttria stabilised zirconia (YSZ) at a weight ratio of 1:1. The powders were pre-treated by calcining at 900°C and 1000°C for 2 h respectively, and subsequently ball milled with ethanol to refine particle size. The pre-treated powder mixture was thoroughly dried at 80°C for 3 h and was then mixed with a thermoplastic (paraffin) plus stearic acid binder to produce the LPIM feedstock. The ceramic feedstock was injection moulded at a temperature of 75°C and pressure of 0.8 MPa for 10 sec using an aluminium alloy mould to produce the green tubular anode supports. Debinding was done by placing the green anodes into coarse YSZ powder situated in hollow thermal insulation bricks. The coarse YSZ powder acted as a binder adsorbent and also prevented the anodes from deforming by acting as a support during debinding. The anode supports were ultimately pre-sintered at 1100°C for 2 h. The outside diameters of the two ends of the tubular LPIM anode were 18 and 24 mm, respectively, with a height of 26 mm and a wall thickness of 1 mm.

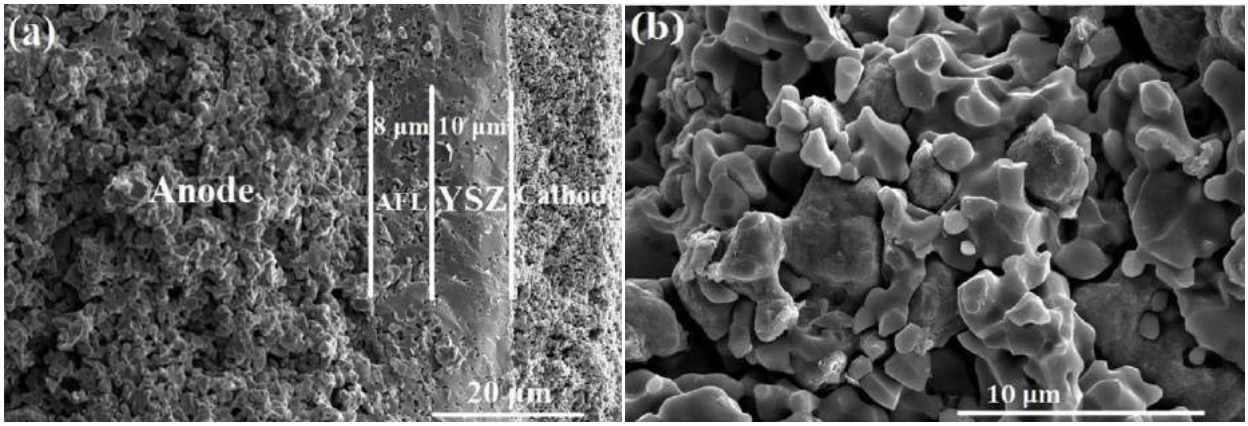

Fig. 1 Cross section SEM image of (a) single SOFC made from powder pre-calcined at 900°C, showing that the four layers are intimately combined, and (b) homogeneous and porous anode supports made by LPIM (From paper: 'Effect of pre-calcined ceramic powders at different temperatures on Ni-YSZ anode-supported SOFC cell/stack by Low Pressure Injection Molding', by Jie Xiao, et al, Ceramics International, Vol. 45, 2019, 20066–20072)

HP Metal Jet. Reinvent Opportunities.

Transform your business with the most advanced metal 3D printing technology for mass production.

Now you can produce complex parts and new applications that were simply not possible before, in cost effective, high-volume runs using HP 3D metal printing technology.

Please visit
hp.com/go/3DMetalJet to learn more
or order a part today.

keep reinventing

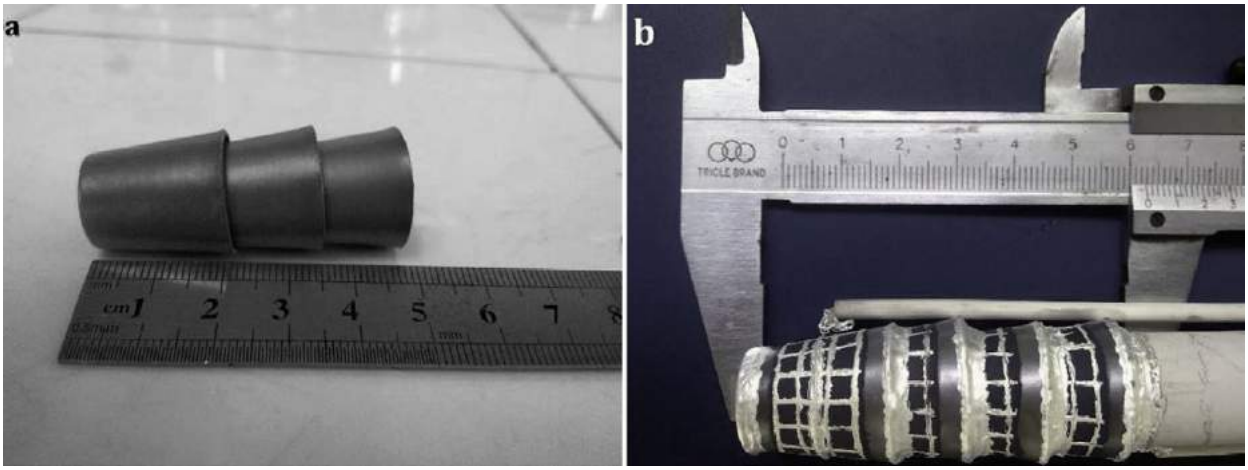

Fig. 2 Images of (a) tubular anode/electrolyte after sintering at 1400°C (b) as-prepared four cell SOFC stack (From paper: 'Effect of pre-calcined ceramic powders at different temperatures on Ni-YSZ anode-supported SOFC cell/stack by Low Pressure Injection Molding', by Jie Xiao, et al, Ceramics International, Vol. 45, 2019, 20066–20072)

A Ni-YSZ anode functional layer and a dense YSZ electrolyte film (10 μm) are then deposited by dip-coating on the pre-sintered anodes followed by sintering the coated anodes at 1400°C in a muffle furnace for 4 h to densify the YSZ film. Finally, a layer of La0.8Sr0.2MnO3-YSZ composite cathode is applied on the anodes by brush painting and sintering at 1100°C for 2 h. Special attention was paid to investigating the impact of the pre-calcining temperature of the ceramic powder on the microstructure, porosity and electrochemical performance of the NiO-YSZ anode cells. Archimedes tests revealed that the porosity of the NiO-YSZ anode support using ceramic powder pre-calcined at 900°C is about 25.9%, which is very close to the optimum value of 26%. The authors reported that a higher degree of homogeneity and porosity was observed in the sintered LPIM tubular anodes made from the NiO-YSZ powder pre-calcined at 900°C than in that pre-calcined at 1000°C, which showed a less porous morphology. The SEM image in Fig. 1(a) shows that homogeneous and porous anode supports could be produced by LPIM which are conducive to the diffusion of the fuel gas and can meet the requirement of SOFC anode microstructures.

It was found that a single cell made with ceramic powder pre-calcined at 900°C, Ni-YSZ/YSZ/LSM-YSZ can give a maximum power density of 671 mW cm^{-2} at 800°C, using humidified hydrogen as fuel and ambient air as the oxidant. This compares with 555 mW cm^{-2} for untreated powder and 648 mW cm^{-2} for cells made from ceramic powder pre-calcined at 1000°C. Fig. 2(a) shows the single cell assembly using silver paste as a current collector for both anode and cathode. The single cell was attached to one end of a corundum ceramic tube using silver paste as sealing and jointing material, and silver wires were applied as voltage and current leads. It was then co-sintered at 800°C for 30 min to fully remove the organic matter in the paste and to ensure the gas tightness of the cell.

The four-cell SOFC assembled stack shown in Fig. 2(b) provides a maximum output power of 4.6 W and an open circuit voltage of 3.2 V fuelled with humidified hydrogen at 800°C.

The authors conclude that further work is underway to improve cell performance using the LPIM technique, such as the effect of different binders, surfactants and pore formers on the microstructure of the tubular NiO-YSZ anodes.

http://english.kmust.edu.cn/

www.journals.elsevier.com/ceramics-international

悦安微特 UNIFINE

Material Technology Innovations Co., Ltd. 纳联材料

岳龙粉末 yuelong powder

SUPERFINE METAL POWDER SPECIALIST AND GLOBAL LEADING SUPPLIER

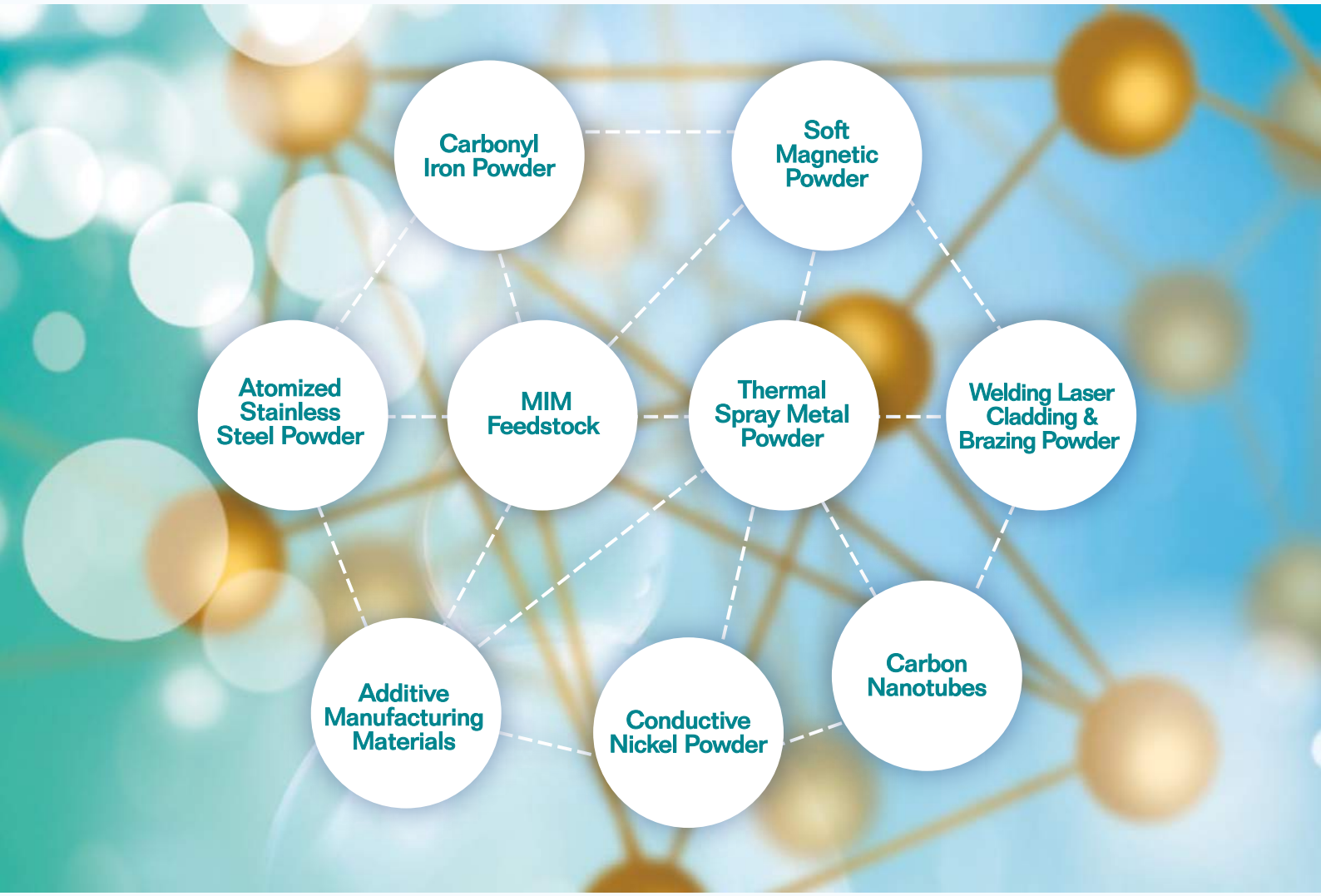

FOR MORE INFORMATION, CONTACT

Manufacturer:

JIANGXI YUEAN ADVANCED MATERIALS CO.,LTD
f.tong@yueanmetal.com
Tel: +86 797 8772 566 www.yueanmetal.com

US location:

2115 Little Gap Road Palmerton, PA 18071
rhonda.kasler@usmetalpowders.com
+1 (610) 826-7020 x262

German location:

Gwinnerstraße 7 – 9,D-60388 Frankfurt
Daojun.ni@yuelongpowder.com
+49 (0) 176 62193407

New process for producing micro-textured surfaces on stainless steel MIM parts

Stainless steels such as precipitation hardened 17-4 PH and austenitic 316L have wide ranging properties (good strength, hardness, corrosion resistance, etc) which enable them to meet the requirements of an equally wide range of applications in the aerospace, automotive, marine, medical and consumer industries. These stainless steels are well known for their ease of manufacturing, making them ideal candidates for research into applications requiring miniaturisation, including micrometre-scale structures and structures with micro-textured surfaces.

The methods used to produce such functional miniaturised stainless steel structures in small batch production include machining or micromilling, and electrical discharge machining (EDM). Laser surface micro-texturing of stainless steel is also used to create micro-scale surface textures, but the technology is said to produce relatively rough surfaces, and the method has shape limitations as well as being relatively slow. Metal Injection Moulding techniques have also been developed recently to create various surface textures and complex geometries using simple replication by combining the LIGA (Lithographie Graphik Abformung) process with MIM. However, this process is considered to be complex and time consuming.

To overcome some of these restrictions, researchers at Joensuu Campus at the University of Eastern Finland, and Karella University of Applied Sciences, also in Finland, have developed what they state is a new, cost-effective method to allow mass production of microtextures on planar or curved surfaces of 316L and 17-4PH stainless steel components. Lena Ammosova, Kari Mönkkönen and Mika Suvanto reported in a paper published in *Precision Engineering* (Vol. 62, 2020, pp 89–94), that the technology developed by their research group initially focused on surface modifications of aluminium and nickel injection mould inserts using a robotically controlled technique to achieve various surface geometry designs. For example, nickel micro-textured mould inserts have been used in plastic injection moulding for replicating the complex topographies on plastic surfaces. The researchers extended the use of their simple and low-cost method to the production of MIM stainless steels with micro-textures.

The key to the process shown in Fig. 1 is the use of a computer-controlled microworking robot with high precision control to create micro-structures on the Ni foil, which can then be used as a mould insert for further Powder Injection Moulding processes. The nickel foil is just 0.25 mm thick, and round-shaped tungsten carbide working needles with a tip diameter of 100 and 200 µm assembled in the robot arm were used to create the fine micropit or micropillar designs. The authors stated that micro-texturing with a larger needle size, such as 500 µm, does not

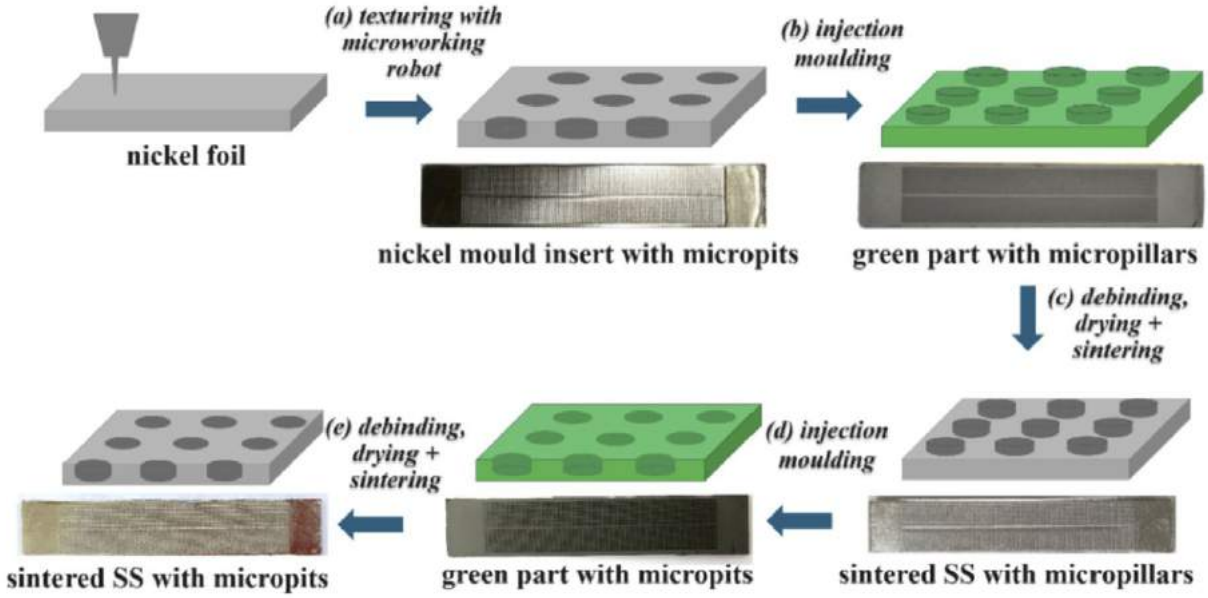

Fig. 1 Schematic of the new process to produce various MIM stainless steel micro-textures such as sintered micropillars and micropits. (From paper: 'Precise fabrication of microtextured stainless steel surfaces using Metal Injection Moulding', by L Ammosova, et al. Precision Engineering, Vol. 62, 2020, pp 89–94)

CHINA'S LEADING SUPPLIER OF MIM POWDERS

ADOPTING ADVANCED GAS AND WATER COMBINED ATOMIZATION TECHNOLOGY

LD METAL POWDERS

Yingtan Longding New Materials & Technology Co., Ltd - Beijing Branch

The company provides various types of structural material powders, magnetic material powders, and other alloy powders in a variety of particle sizes and tap density based on the demands of the customers. The product line includes 316L, 304L, 17-4PH, 4J29, F75, HK30, 420W, 440C, Fe2Ni, 4140, and FeSi. The customers have received the products with high acclaim

Item	T.D(g/cm^3)	S.S.A(m^2/g)	S.D(g/cm^3)
316L	4.8	0.34	7.9
17-4PH	4.7	0.34	7.7
304L	4.8	0.34	7.8
HK30	4.7	0.34	7.7
4J29	4.9	0.34	7.95
F75	5.0	0.34	8.1

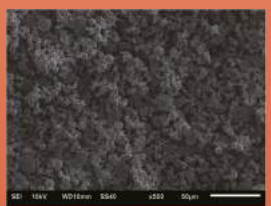
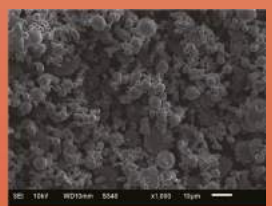
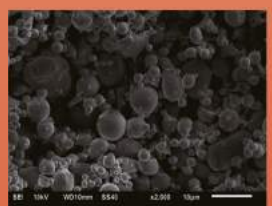
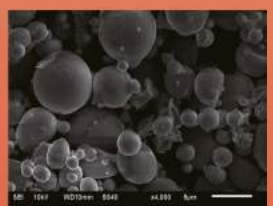

Address: 5 Floor , Block A, Courtyard 88, Caihuying, Fengtai District, Beijing, China.
Fax: +8610-62782757 Tel: +8610-62782757 Contact: Mr. Cheng Dongkai Mobile: 13911018920
Email: chengdongkai@longdingpowder.com Website: www.ldpowder.com

Atect Full-Mould binders

The BINDER for thermal debinding systems, capable of being recycled up to 10 times!

- Just regrind the sprue, runner and unwanted green parts then reuse!
- Use 100% reground material without the need for fresh feedstock!
- No change in the shrinkage ratio or physical properties!
- No change in mouldability!
- No need to modify debinding and sintering setup!

Binder system design

Characteristics required for Binder

- **High flowability at molding temperature**
  Binder design considering the viscosity at around the molding temperature.
- **High expansion property in the mold during injection moulding**
  Wide moulding condition range because of the Barus Effect. (Fig.1 and 2)
- **High thermal decomposition property in the de-binding process**
  There is no effect on the sinter quality, because there is no residue after de-binding. (Fig.3)

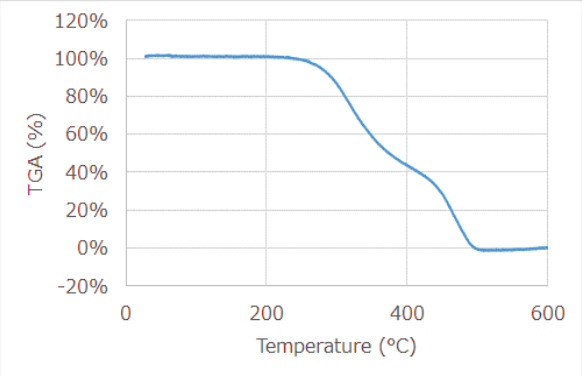

Fig.3 TGA Curve of Binder

※All components are vaporized at around 500℃.

The flow amount F, when the load S is applied to the thermoplastic fluid, is given as following equation.

$$F = aS^n$$

Here, a is the flow characteristic at load=1, n is Barus effect.

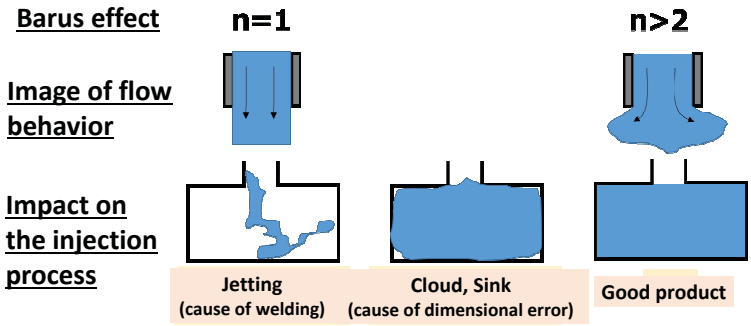

Fig.1 Schematic of the relationship between n value and flow characteristic

※Since larger n value, material expands in the mould, dense green part is obtained.

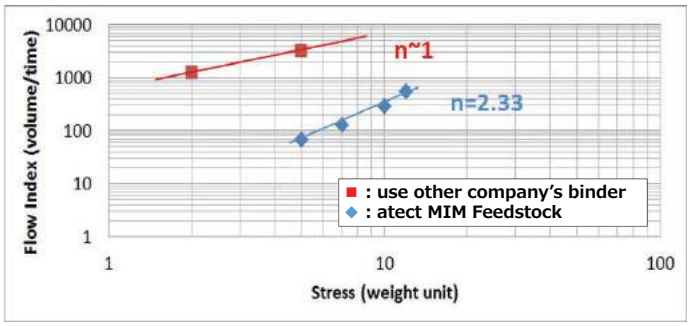

Fig.2 Flow characteristic compared with pellets using the other company's binder

※With our binder, it is possible to obtain precise green part because material easily expands in the mould.

atect corporation
3275-1 Kamihaneda Higashiohmi Shiga
Tel: 074-820-3400 Fax: 074-820-3401

www.atect.co.jp
Email :pimsales@atect.co.jp
takehiko.kitamura@atect.co.jp

create enough local impact force to create a micropit, whilst texturing with a small-sized needle, such as 5 and 10 µm, on the tough Ni foil causes needle breakage. Thus, micro-texturing with the 100 µm and 200 µm-sized WC needles was found to be optimum in controlling the position of the micropits, and microtextures of various sizes could be produced for both rectangular and circular shaped mould inserts.

In the injection moulding process the Ni mould insert containing the designed micropits was placed in the rectangular/circular mould cavity, replicating the green MIM part with micropillars. Conversely, Ni mould inserts with the micropillars could be used to produce the green MIM parts with micropits. The stainless steel feedstock granules were injected with a pressure of 450 bar and an injection time of 8 s for the rectangular mould cavity. For injection moulding of circular specimens, a pressure of 450 bar and an injection time of 4 s were used.

The researchers reported that the key to the successful fabrication of the final MIM stainless steel microtextures is complete filling of the metal powder feedstock within the very small and narrow micropits. The feedstock viscosity and the powder particle size have a major influence on the complete filling of the feedstock, and the authors found that the smaller the metal powder size, the smoother the surface and the better the surface roughness after sintering. Therefore, to ensure sufficient surface properties, powder size for MIM should be below around 20 µm in order to fill micropit cavities with a size of 100 and 200 µm. For easy and complete demoulding, the MIM feedstock should also have low affinity for the mould insert material so that the feedstock does not stick to the mould surface. Moreover, the mould insert should possess high tensile strength to avoid mechanical damage to the microtextured surface. Fig. 2 shows SEM images of PIM stainless steel microtextured surfaces in the sintered state which shows complete filling and demoulding of the stainless steel feedstock using Ni inserts.

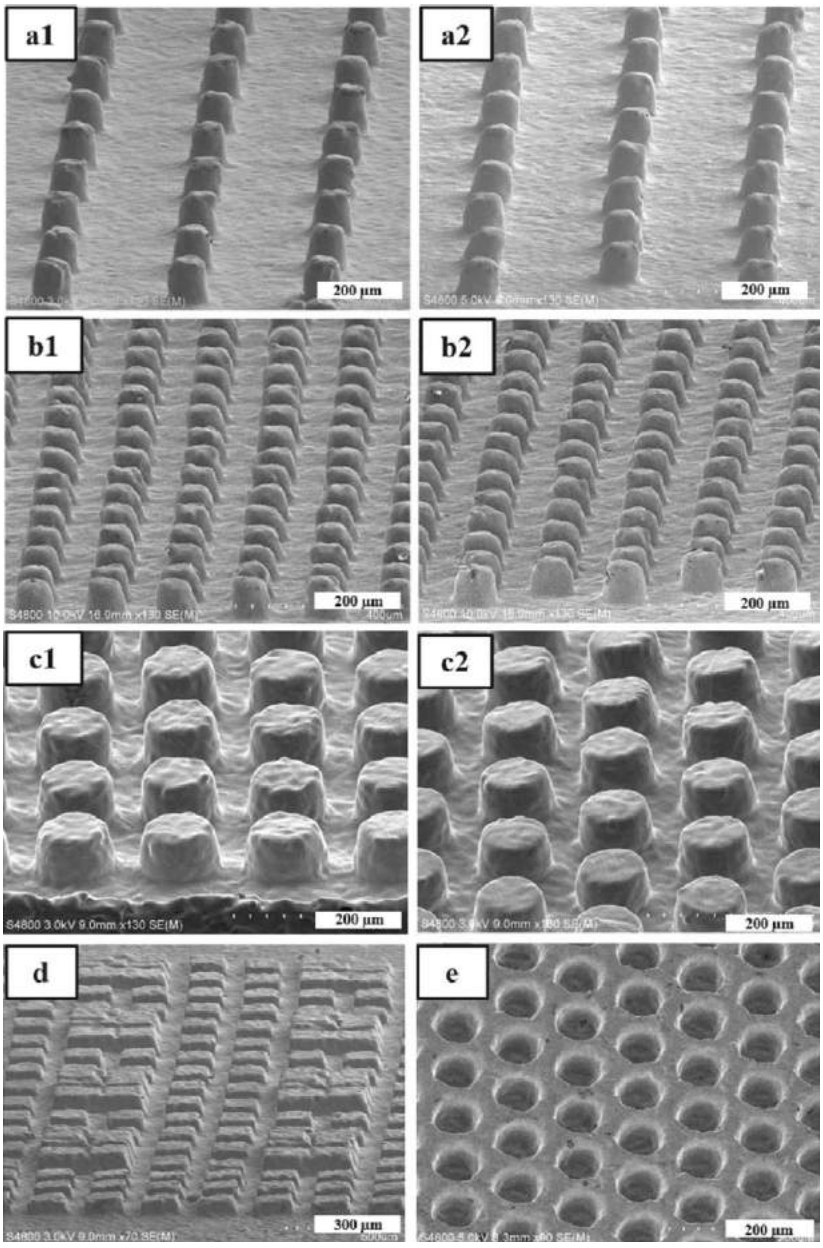

Fig. 2 SEM images of sintered 17-4PH stainless steel round shaped micropillars with a structure size of around (a1–b2) 100 µm sized (a) low density and (b) high density, and (c) 200 µm with (1) square and (2) hexagonal arrangements, (d) square-shaped micropillars with protective pillars, and (e) round shaped micropits. (From paper: 'Precise fabrication of microtextured stainless steel surfaces using Metal Injection Moulding', by L Ammosova, et al. Precision Engineering Vol. 62, 2020, pp 89-94)

It can be seen that the micropillars have a truncated cone shape with the size differing between the top and the bottom of the pillars. Thus the green MIM micropillars fabricated with the 200 µm sized needles have an average size of 215 µm at the top and 240 µm on the bottom. The bottom size of the micropillar is controlled by the impact force of the needle when the needle hits the Ni foil. The larger the impact force of the

needle, the deeper the micropits, and thus the larger the bottom size of the micropillar. Shrinkage during sintering of micropillars, calculated from parameters collected from ten random micropillars, is approximately 20%. This leaves the average size after sintering at the top of 170 µm and on the bottom at 205 µm.

The authors stated that pillar-like micro-textures can significantly reduce the contact area with a counter body in a controlled way, which suggests potential applications in controlling surface friction between sliding materials. However,

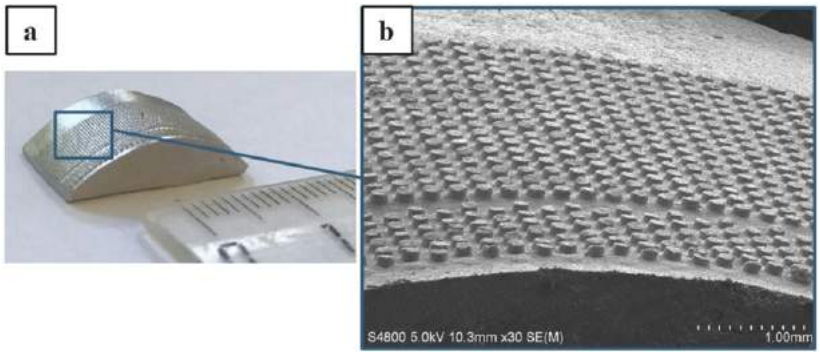

Fig. 3 (a) Curved MIM 316L SS surface containing micropillars and (b) its SEM image. (From paper: 'Precise fabrication of microtextured stainless steel surfaces using metal injection moulding', by L Ammosova, et al. Precision Engineering, Vol. 62, 2020, pp 89–94)

apart from their tribological properties, these micro-textured stainless steels could also serve as a new platform for the fabrication of substrates with controlled wettability, such as superhydrophic and ice-repellent surfaces. Other potential applications were also cited including those for micropits (Fig. 2(e)) which have the potential to act as reservoirs for both solid and oil lubricants for low friction applications. Moreover, micropits can act as a protective vessel for locating and growing cells and various particles, and can be used as protection from environmental damage. In addition, micropits on a metallic support can be used as a corrosion resistant durable microreactor for loading of catalysts and transformation of exhaust gases.

As mentioned earlier it is possible to fabricate these Ni mould inserts not only in planar but also curved shaped surfaces, as shown in Fig. 3. It can be seen in this figure that the quality of the replicated micropillars on the curved surface is relatively good, giving such MIM micro-textures the potential to reduce surface friction between moving parts such as bearings.

Research was funded by Business Finland/ERDF (European Regional Development Fund) project 'Multi-functional powder metallurgical products.'

www.uef.fi

https://www.journals.elsevier.com/precision-engineering

RENISHAW
apply innovation™

Racing ahead with additive manufacturing

AM has the power to disrupt, enabling innovative product designs and new agile business models

Atherton Bikes is taking advantage of these capabilities to break free from the rigid, labour-intensive conventional bike manufacturing mould. AM gives Atherton Bikes the flexibility to hone their race bike designs, and to make high performance custom bikes accessible to enthusiasts.

To find out more about the capabilities of our AM systems visit: www.renishaw.com/amguide

Renishaw plc Brooms Road, Stone Business Park, Stone, Staffordshire, ST15 0SH, United Kingdom
T +44 (0)1785 285000 F +44 (0)1785 285001 E additive@renishaw.com
www.renishaw.com

formnext

International exhibition and conference
on the next generation of manufacturing technologies

Frankfurt, Germany, 10 – 13 November 2020
formnext.com

Do you belong to the world of additive manufacturing?

In a world where AM applications are increasing rapidly, solutions are needed along the entire process chain. Become an exhibitor at Formnext. Present your expertise in the manufacturing process and secure your place in Frankfurt.

Where ideas take shape.

Offical event hashtag #formnext

mesago
Messe Frankfurt Group

Metal Injection Moulding in China: Market opportunities and research activities

Despite a broad economic slowdown, manufacturing in China is transitioning to an innovation-driven model. The country's Metal Injection Moulding industry has grown rapidly with the demand for high-performance products; currently, over four hundred Chinese MIM companies are active, producing a range of small, complex parts. New production equipment is also constantly emerging and a number of research institutions have invested in this field, further promoting the development of the industry. Prof Yimin Li, of China's State Key Laboratory of Powder Metallurgy and Research Centre for Materials Science and Engineering, along with associates, reviews the markets, application fields, technology and research status of the MIM industry in China.

Current MIM parts sales in China are valued at an estimated 7 billion RMB, accounting for approximately 40% of MIM parts sales worldwide. Among the MIM parts sold in the country, the consumer electronics sector, which includes smartphones, wearables, laptops and cameras, accounts for the largest proportion of production - approximately 80%. Other applications for MIM parts in China are in the automotive, power tools, communications, firearms and medical device industries.

In recent years, the market for consumer electronics has continued to expand, in part thanks to a growth in domestic consumption. The transfer of foreign manufacturers to China has also played a major role.

The number of mobile phone shipments in China in 2018 reached approximately 1.8 billion, thereby maintaining high production levels. Simultaneously, the market for thinner and lighter consumer electronics products, such as smartphones and wearable devices, continues to evolve. The core components of such products are becoming ever more complex and offer an important potential market for the MIM industry with a diverse range of opportunities.

Smartphones are now being developed with multi-lens modules which integrate lenses, sensors, an LED flash as well as other components firmly and securely. With the camera bracket being produced by MIM, this again brings opportunities and innovations to the MIM industry. The use of multi-camera lenses implies that more geometrically complicated

Fig. 1 Various MIM smartphone components, including SIM card trays, camera module frames and buttons (Parts courtesy of Shenzhen Shindy Tech. Co., Ltd)

Fig. 2 A Huawei Mate X folding smartphone. The new generation of folding smartphone designs presents high-value opportunities for the use of MIM hinge and drive mechanisms (Courtesy Huawei)

camera brackets will be needed, with higher requirements for wall thickness, flatness and contour (Fig. 1). The MIM process has unique advantages in processing near-net shaped parts with complex geometric shapes, uniform structure and excellent performance. In terms of materials, the use of high-nitrogen, non-magnetic, nickel-free stainless steel brings good biocompatibility as well as desirable non-magnetic properties, high strength and good corrosion resistance.

A new generation of smartphones with folding screens is currently being developed, again offering new opportunities for the MIM industry. To enable the foldable design, the hinge in middle core needs to be lightweight, flexible, thin and reliable. Whist this has high tolerance and strength requirements, its complexity and size fall within the optimum size range for MIM production. MIM, of course, also has the advantage of high manufacturing efficiency, low cost, excellent batch to batch repeatability and high quality.

" A new generation of smartphones with folding screens is currently being developed, again offering new opportunities for the MIM industry. To enable the foldable design, the hinge in middle core needs to be lightweight, flexible, thin and reliable."

The MIM process is also used in the smartphone sector to manufacture high-precision micro gears, shafts, guide rails and other components such as the smartphone camera lifting device as shown in Fig. 3. This high-precision assembly of MIM parts has to be extremely wear- and fatigue-resistant in an application in which a small defect will lead to device failure. The i-bar of the connecting rod is processed solely by MIM, with no machining required after sintering. The design of the device is very complex and conventional processes simply could not produce such assemblies in the required volumes. Through MIM processing, the gear can be formed in one step and meets the necessary mechanical and physical properties required. The system has been proven on smartphones manufactured by major Chinese brands OPPO and Vivo, with Vivo performing 50,000 lifting cycles and OPPO performing 300,000 sliding durability verification tests for its Find X device.

Automotive parts

In the field of automotive parts manufacturing, the MIM process, as a net-shape process, can offer significant savings in materials, production costs and weight. The reduction in material wastage and the ability to lightweight an application can be regarded as important environmental benefits. Thus, the technology has been highly valued by the automotive industry. Automotive companies now use MIM technology to produce complex shapes, bimetal parts and groups of micro and small parts such as turbocharger parts, adjusting rings, injector parts, blades, shift levers, locks, sensors, air bags parts, seatbelt adjusters, ignition switches, reverse gear components, cabriolet roof parts and power steering components. Fig. 5 shows an automotive sensor bracket manufactured by MIM, which offers a weight reduction of more than 50% as compared with conventional sensor brackets.

Fig. 3 MIM micro gear transmission system show on a nano-SIM card

Medical parts

Medical devices, including orthopaedic devices and minimally invasive surgical (MIS) components, provide great opportunities to the MIM industry in China. Typical orthopaedic procedures include the implanting of orthodontic stents and buccal canals. It is estimated that the value of MIM orthopaedic tools may double or triple in the next few years. Because there are hundreds of millions of children and teenagers in China, the orthopaedic devices market is expected to maintain rapid growth in the coming years. The working heads of MIS instruments, including fixed and dissecting forceps, scissors, biopsy forceps and needle holders, have increased the sales of medical equipment. In China, disposable MIS equipment has been widely accepted by both doctors and patients because they eliminate cross-infection. As the population grows and the quality of life improves, the demand for MIS instruments will also increase rapidly in the coming years.

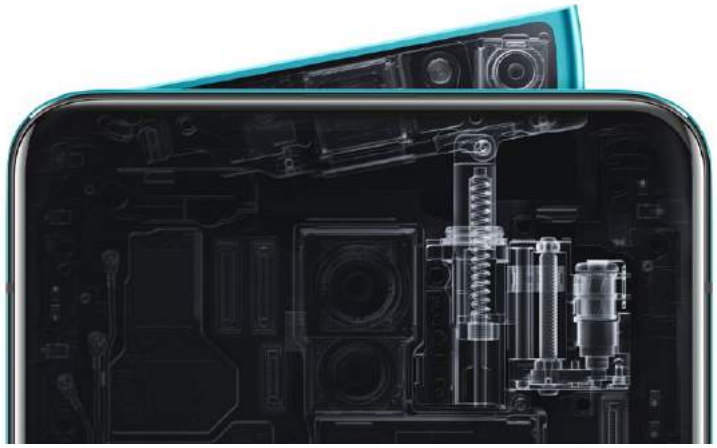

Fig. 4 Interior composite image of the Oppo Reno phone with the camera system raised. The operating mechanism and micro-gear reduction module can be seen on the right (Courtesy Oppo)

Tools

Tools are also an important application field in the MIM industry in China. As designers become more familiar with MIM, these applications continue to expand. As shown in the trigger in Fig. 6, the original design of this type of part needed to be connected by multiple studs and screws to the body. When the MIM process was used to make the part, reliability of the application increased. When designing such mechanical structures, designers can consider integrating the functions of multiple parts into one, which brings significant design freedom and potential cost reductions. In this application, 440C stainless steel was chosen as a material whose hardness can reach HRC55 or above,

Fig. 5 An automotive sensor bracket produced by conventional manufacturing (left) and MIM (right), with MIM offering substantial material and weight savings

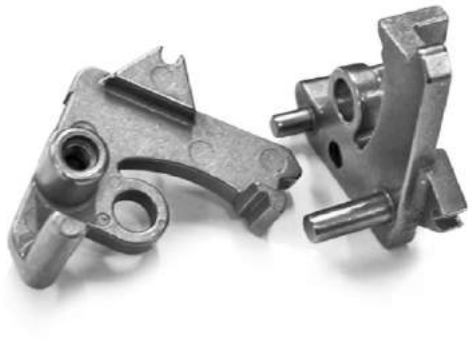

Fig. 6 MIM 440C stainless steel tool trigger. MIM's ability to integrate the functions of multiple parts into one component brings significant design freedom and potential cost reductions

Fig. 7 Lock cylinder made by MIM. In this application, M2 or T15 high-speed steels can be used, resulting in a hardness of HRC50, thereby significantly increasing the lock's anti-drilling performance and wear resistance

which meets the requirement of wear resistance better under the working condition of the parts.

In the lock application shown in Fig. 7, in order to develop lock cores with enhanced hardness materials such as M2 or T15 high-speed steels, resulted in a hardness of HRC50, thereby significantly increasing anti-drilling performance and wear resistance - effectively improving the safety performance of the lock.

Research trends

In recent years, two-material Powder Injection Moulding (2C-PIM), micro Powder Injection Moulding and PIM process simulation have moved to the forefront of industrial research.

Two-material Powder Injection Moulding

Co-injection moulding two different materials is a novel process that combines the advantages of polymer co-injection moulding and Powder Injection Moulding. It allows the fabrication of parts consisting of two layers with different properties. According to different injection methods, it can be divided into three types: rotating mould injection, simultaneous injection and sequential injection.

During the sequential injection process, the 'skin' and 'core' feedstocks are injected sequentially in one moulding machine through a single injection route. The first forms the outer layer and the second forms a core encapsulated by the skin. In this process, the breakthrough phenomenon (where the 'core' feedstock penetrates the outer 'skin' feedstock, as seen in Fig. 8a and b), as well as the homogeneity of skin feedstock, plays a critical role in the properties and cost of the final part. The effects of processing parameters on the profiles of the two feedstock layers during moulding have been studied. In the green part without breakthrough, the interface between the core and skin feedstocks exhibited an arched shape in the transverse plane and a V shape in the longitudinal plane.

The penetration length and thickness of the core feedstock are influenced by injection parameters, such as the pre-filling volume of skin feedstock, injection temperature of core feedstock and the injection rate of the skin feedstock. The occurrence of the breakthrough phenomenon primarily depends on the pre-filling volume of the skin feedstock [1, 2].

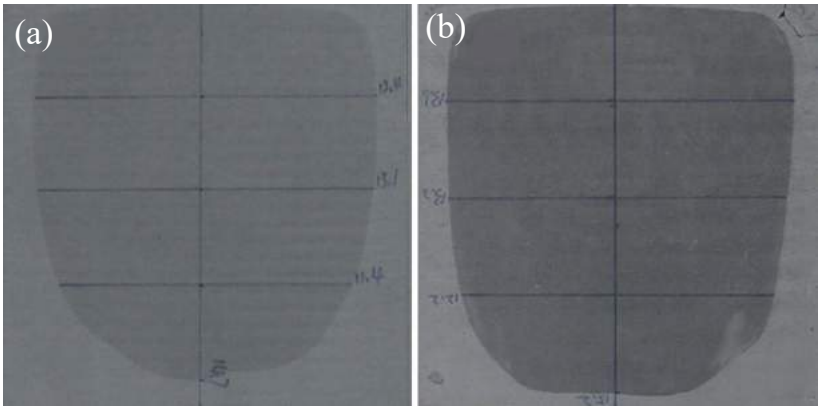

Fig. 8 Pictures of mid-cross-section of the sample polished from the transverse plane: a) green part without breakthrough phenomenon and b) green part with breakthrough phenomenon

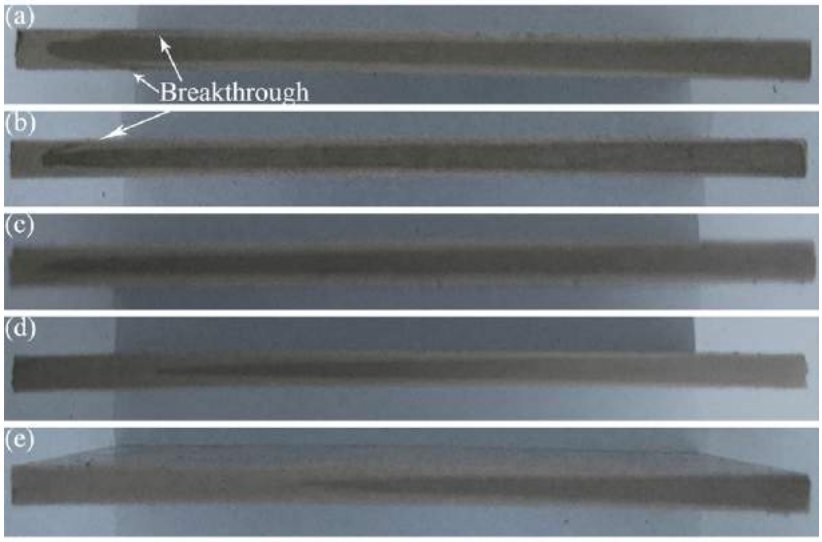

Fig. 9 Pictures of mid-cross-section of the sample polished from the longitudinal plane (Pre-filling volume of skin feedstock: a-40%; b-50%; c-60%; d-70%; e-80%)

Micro Powder Injection Moulding

The miniaturisation of complex components is becoming ever more important in a number of sectors, including consumer electronics, automotive, telecommunications, chemical industries and environmental technologies and medicine. Micro Powder Injection Moulding (μPIM), adapted from standard PIM, with the advantages of high-volume production capability at low cost, is currently the most promising micro-manufacturing technology for metals and ceramics.

Micro Powder Injection Moulding shares its overall process steps with conventional PIM, but there are also fundamental differences when the process has to be adapted to the micro-scale. To manufacture micro-components, whose masses are in the order of milligrams, or standard-sized components featuring micro-structured regions or dimensional tolerances in the micrometre range, special micro tooling processes and new design approaches must be adopted. Liu Lin from the University of Science and Technology, Beijing, fabricated a 17-4PH electromagnetic pilot valve for hydraulic support systems whose size was 1/20th that of conventional valves, with a micro post of φ500 μm [3]. Meanwhile, the effects of size reduction on deformation, microstructure and surface roughness were also studied.

The same author fabricated micro pillars with a depth of 0.5 mm and varying diameters of 0.2, 0.5 and 1 mm to investigate the powder-binder segregation during injection moulding [4], and separately developed the solvent debinding mechanism and fabricated 3Y-ZrO_2 micro-gears ranging from 200 to 900 μm [5].

Junhu Meng developed a micro-mixer silicon mould insert with 24 continuous channels and replicated the 316L stainless steel micro-mixers while maintaining a good shape without any visible defects; the width and depth of the channels were 129 and 105 μm, respectively [6]. Liu Chao from the China Iron and Steel Research Institute fabricated titanium micro-components for biomedical application with a yield strength of 450 MPa, ultimate tensile strength of 565 MPa, elongation of 18% and relative density of 97.3% [7].

Process modelling to predict density variation in the PIM process

Density variation is an inherent problem in the Powder Injection Moulding of metal and ceramic powders. The continuum model assumes that the feedstock maintains a constant density during moulding and, thus, it cannot predict the density variation. A bi-phase model treats the flow of feedstock as the addition of two distinct but coupled flows characterised by the viscosities of the binder and powder.

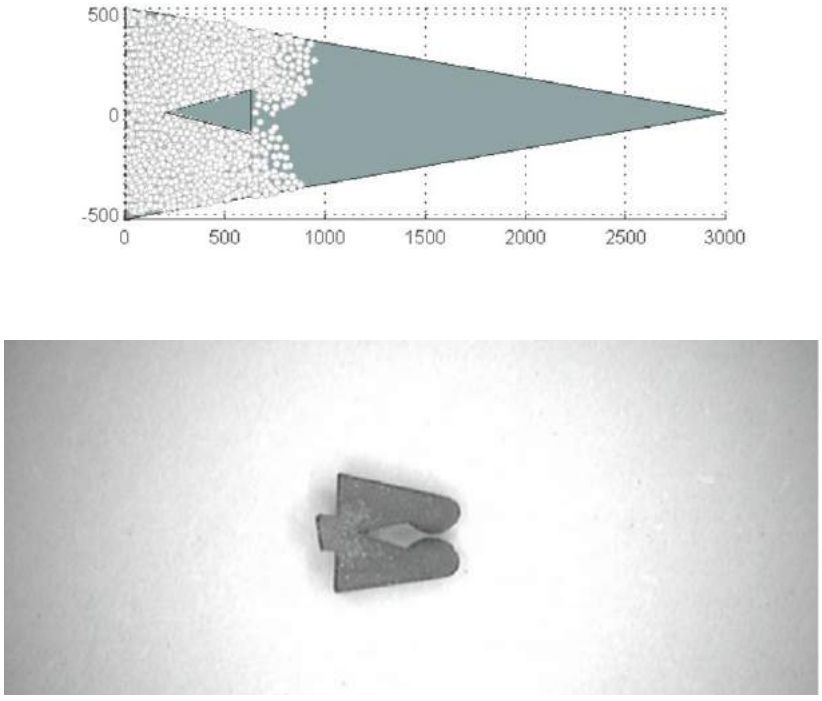

Fig. 10 Partial injection moulding of a sample with injection velocity = 6 m/s: top; simulated prediction of density variation in filling process using granular modelling with interstitial power-law fluid, and bottom; the as-moulded part [8]

However, powder particles are theoretically incapable of being treated as a continuous phase. Recently, a granular model with an interstitial power-law fluid was proposed to simulate the injection moulding process. The density variation was predicted and validated through comparison with experiments. The effects of different injection parameters, such as injection velocity, injection temperature, particle size and powder loading, were investigated.

The injection process was simulated and the simulation results were found to be consistent with the experimental results for two moulds with specific geometries. Because the viscosity of the metallic phase was not required, only a small amount of simulation was needed in the granular model. However, the simulation of a mould with a large or complicated shape still takes a very long time, mainly because a large number of particles needs to be calculated.

Material systems and products: Iron and nickel-based materials

Iron-based materials are an important area of research for injection moulding material systems. However, the research topics have expanded from traditional low-alloy steels, austenitic stainless steels 316/304, precipitation strengthened 17-4PH stainless steel and soft magnetic alloy to ferritic/martensitic 4-series stainless steel [9], M2 and other tool steels [10], superalloys [11] and other iron-based materials. Zhang Lin *et al* [12] used the MIM213 alloy to prepare a hollow turbine with a relative density of 96.6%; its tensile properties were significantly better than those of the same grade cast alloy.

Simultaneously, some researchers began to study the influence of interstitials (C, O) on the sintering process in detail in an attempt to improve the properties of sintered alloys or control the structure by adding alloying elements. An *et al* [13] found that, in the early stage of sintering of 420 stainless steel, the increase in C content can promote the reduction of oxides and accelerate densification; however, it separates the grain boundary and aids pore separation during sintering, thereby reducing the sintered density. Adding Nb is beneficial in reducing this trend and increasing the sintered density while strengthening the precipitation of carbides. The addition of Nb can also improve the corrosion resistance of MIM 420 stainless, steel but the strengthening effect is limited at high carbon content [9]. Lou *et al* [14] found that the residual carbon (< 0.1 wt.%) in MIM 17-4Ph alloys causes distortions in the martensite lattice, while the amount of copper atom precipitation is small (as shown in Fig. 11). Eventually, the strength and hardness of the alloy increased significantly, but its plasticity considerably decreased.

For soft magnetic materials, some work has been carried out on Fe-Ni alloys. Xiong Liang *et al* [15] prepared Fe-50% Ni alloy via MIM. It was found that porosity is the main factor affecting its saturation magnetic induction intensity and the two have a linear relationship. Porosity, impurities and grain size affect the magnetic permeability and coercive force. As the porosity and impurity mass decrease and the grain size increases, the magnetic permeability gradually increases and the coercive force decreases. Zhu *et al* studied the MIM Fe-50% Ni alloy in different cooling methods [16]. It was found that the cooling rate has limited effects on the density, impurities and grain size, but strongly affects the magnetic properties. With the acceleration of cooling rate, the coercive force increases first and then decreases. After liquid nitrogen

cooling, the saturation, magnetic induction, coercivity, maximum magnetic permeability and initial magnetic permeability of the alloy were 1.45 T, 7 A/m, 72.47 mH/m and 10.12mH/m, respectively. Ordered phases of metastable Fe-Ni were found in the Fe-50% Ni alloy cooled by oil and liquid nitrogen, which greatly improved the magnetic properties.

For Ni-based superalloys, Hu *et al* [17] prepared Inconel 718 alloy via MIM and studied the influence of sintering temperature, Hot Isostatic Pressing and heat treatment on its performance. The experiments showed that a density of more than 98% can be obtained at 1275°C and the material can be fully dense after Hot Isostatic Pressing. The strength and elongation at room temperature were 1250 MPa and 21.7% on sintering at 1275°C, while those at 650°C were 1177 MPa and 16.6%, respectively. The performance exceeds that of the forged alloy of the same grade.

Titanium and nitinol alloys

Titanium and titanium alloys have the advantages of high specific strength, excellent corrosion resistance and good biocompatibility, which has, for many years, attracted the attention of researchers. However, owing to the high cost of powder production and the challenges of processing – including the challenge of oxygen pick up in the forming process, their applications remain limited. Liu *et al* successfully prepared MIM titanium products using a water-soluble injection material system and atomised titanium powder [18]. The oxygen content, compressive strength and elongation of the samples were 0.228 wt.%, 554 MPa and 20.9%, respectively. The elongation of TC4 alloy reached 12% [19] and the overall performance of the sample satisfied the standards of ASTM Metal Injection Moulding for pure titanium and TC4 components. In addition, other scholars have studied beta titanium alloys, such as MIM nitinol alloys [20], titanium aluminium [21] and Ti-12Mo [22]. Zhou *et al* [23] added Nd to

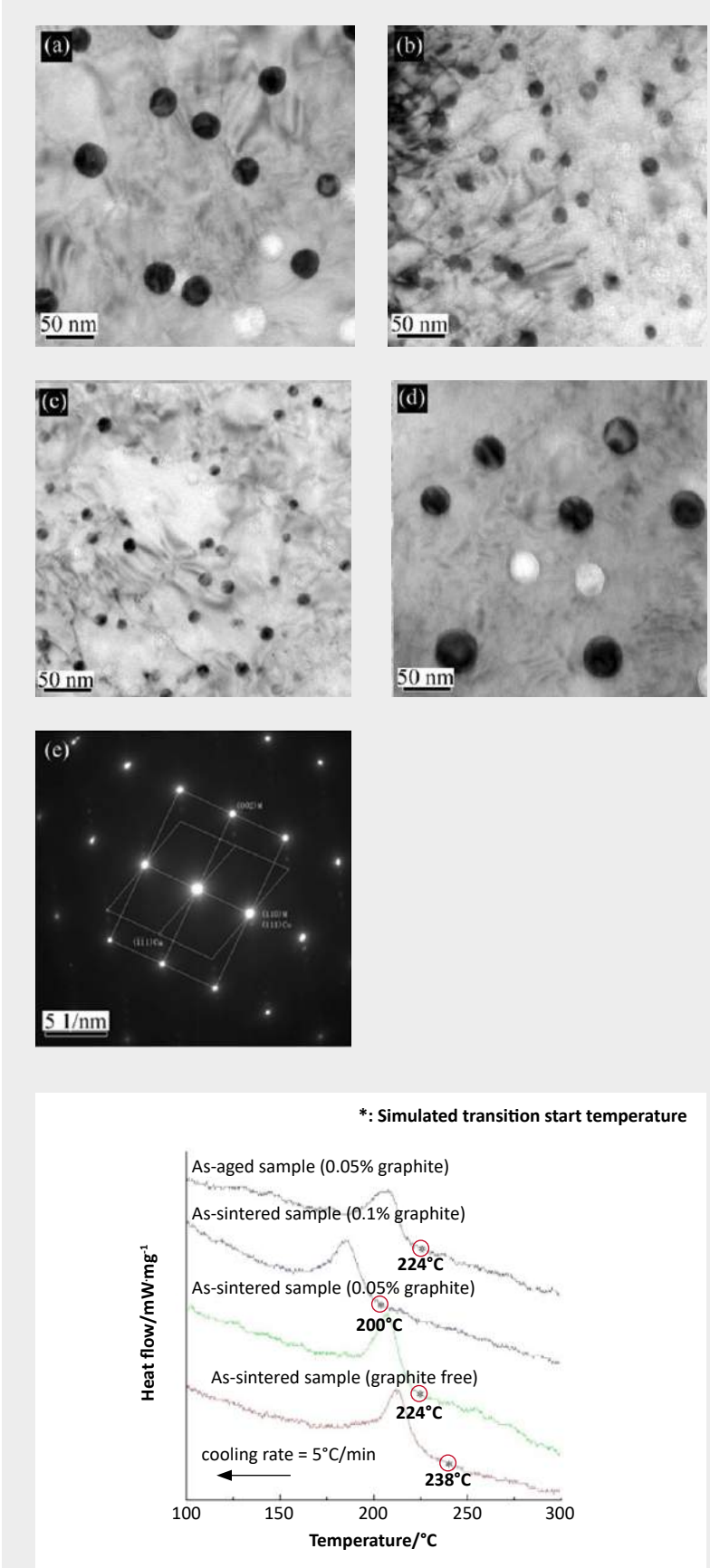

Fig. 11 Effect of carbon content on the size and phase temperature of nano copper phase in MIM 17-4PH stainless steel

titanium alloy to improve the oxygen distribution and mechanical properties of injection moulded products.

Tungsten and hard alloys

With the rapid development of the tungsten and hard alloy industries in China, MIM hard alloys and refractory alloys continue to be a research focus. Cemented carbides are generally produced by traditional powder metallurgical 'press and sinter' methods and the product geometries are quite simple. For products with complex shapes, semi-finished product machining or sintered product grinding is required, both of which have several disadvantages, including low material utilisation, high energy consumption and high costs. This route is also unsuitable for large-scale production, especially of ultra-fine cemented carbides.

"With the rapid development of the tungsten and hard alloy industries in China, MIM hard alloys and refractory alloys continue to be a research focus"

The use of MIM is solving the challenge of processing complex shaped carbide parts. During the MIM process, many factors can affect the properties of the finished products, including powder characteristics, binder formulations, rheological properties, uniformity of feed, mould design, injection parameters, debinding parameters and the sintering process. Zhou *et al* prepared WC-10%Co cemented carbide blades via MIM and systematically studied the effects of injection pressure, injection temperature and holding pressure on the injection process to optimise the injection parameters [24]. Luo *et al* studied the compatibility of pure tungsten binder components and the rheological properties of wax-based binders with different formulations [25]. Li *et al* used Jetmill to modify the powder; the powder loading capacity of tungsten feeding reached 65%. The density of pure tungsten reached 97.3% at 1900°C [26]. Shang *et al* prepared ultrafine-grained cemented carbides with a grain size of only 0.465 μm [27].

W-Cu composites are widely used in high-voltage switch electrical contacts, resistance welding, processed electrode materials, high-temperature materials for aerospace equipment, electronic packaging and thermal deposition materials. This is thanks to its high hardness, high strength, good conductivity, high thermal conductivity, low expansion system, resistance to arc erosion, resistance to high temperature oxidation and other characteristics. Among them, MIM W-Cu materials have also been used in other applications, such as a W-Cu shape charge liners. Wu *et al* developed a MIM ultra-fine W-25Cu liner. The density and strength of the liner reached 14.75 g/cm^3 and 822.4 MPa, respectively. It was found to have better stability in penetration tests [28]. He *et al* prepared a MIM W-20Cu liner with a relative density of only 55%; its penetration performance was more than 20% better than a spinning liner with the same conditions. The influencing mechanism of copper content and porosity on penetration performance remains to be further studied.

Owing to the large volume of binders used in the MIM process, the porosity of the sample after debinding usually reaches 40–60%, which causes significant post-sintering shrinkage. Most tungsten-based alloys require liquid phase sintering to obtain a fully-dense product. The non-uniform flow of the liquid phase under the action of gravity makes the product shrinkage more complicated. Guo *et al* prepared MIM W-4Ni-3Fe small-sized threads to study the influence of sintering temperature on the density and sintering shrinkage of the material [29]. The study found that solid-phase sintering was not performed at 1400°C and liquid phase sintering began at 1445°C. The W particles were significantly coarsened at 1480°C. Finally, the radial and axial shrinkage rates were 19% each. Luo *et al* studied the effects of Ni and Y_2O_3 on the activation sintering of MIM pure tungsten [30]. The study indicated that Ni can significantly promote the densification of W products at low temperature, but no promoting effect was observed when the sintering temperature exceeded 2050°C. However, Y_2O_3 evidently promotes densification at high temperatures. Y and W generate $Y_2(WO_4)_3$ at the interface at high temperature, which can reduce the free energy to promote densification. Jiang *et al* reported the application of ultra-fine MIM tungsten products in nuclear fusion devices [31]. It is considered that ultra-fine MIM W parts are suitable for Langmuir probe protective parts, while rare earth oxide dispersion enhanced W-1.2 Y_2O_3 is suitable for manufacturing helium cold strainer structural parts. Li *et al* researched the preparation of MIM porous W cathode substrates for electron emitters [32]. The study found that the MIM porous W parts, sintered at 1900°C, had uniform pores of 24.58%. The pore connectivity was good and satisfied the requirements of an ideal cathode substrate.

Conclusions

Metal Injection Moulding in China has developed significantly, to the point where it is now a globally competitive industry and an important contributor to the growth of Chinese manufacturing. It is, however, still not sufficiently stable

and faces great risks and challenges. This requires practitioners to constantly explore new application areas, develop new material systems to overcome various technical challenges,and further exploit the advantages of Metal Injection Moulding in the preparation of small, complex, high-precision components.

At the same time, MIM still has some way to go in terms of quality and process refinement, including density, precision control, impurity content and other aspects. Domestic enterprises need to continuously improve their management and technical levels, as well as strengthening scientific research and taking advantage of theoretical guidance from scientific research institutes. However, with the development of China's economy and the continuous progress of science and technology, Metal Injection Moulding remains an industry with high potential for a wide range of applications in medical devices, 5G communications and artificial intelligence, among other fields. Therefore, it can be expected that the future of China's MIM industry is bright.

Authors

Yimin Li*[a,b] Yong Yu[a], Hao He[b], Jia Lou[c], Chen Liu[b], Dongyang Li[a]

[a] State Key Laboratory of Powder Metallurgy,
Central South University
Changsha 410083
China

[b] Research Centre for Materials Science and Engineering
Guangxi University of Science and Technology
Liuzhou 545006
China

[c] School of Materials Science and Engineering
Xiangtan University
Xiangtan 411105
China

*Corresponding author: Dr Yimin Li, liyimin333@163.com

References

[1] J. Lou, Y. Li, H. He, D. Li, G. Wang, J. Feng and C. Liu, "Interface Development and Numerical Simulation of Powder Co-Injection Moulding. Part. I. Experimental Results on the Flow Behaviour and Die Filling Process", *Powder Technol.*, 2017, vol. 305, pp. 405–410.

[2] L. Jia, L. Yimin, H. Hao, L. Dongyang, W. Guangyao, F. Juan and L. Chen, "Interface Development and Numerical Simulation of Powder Co-Injection Moulding. Part II. Numerical Simulation and Experimental Verification", *Powder Technol.*, 2017, vol. 305, pp. 357–363.

[3] L. Lin, X.D. Wang, L. Xiang, X.T. Qi and X.H. Qu, "Effects of Size Reduction on Deformation, Microstructure, and Surface Roughness of Micro Components for Micro Metal Injection Molding", *Int. J. Min. Met. Mater.*, 2017, vol. 24, no. 9, pp. 1021–1026.

[4] L. Liu, M.X. Qi, Z.Q. Xie, Z.Y. He and F. Ming, "Filling of Microarray Fabricated by Micro Powder Injection Molding", Mater. Sci. Forum, 2017, vol. 898, pp. 1171–1176.

[5] L. Liu, Y. Chen, X.L. Ni, H.Q. Yin and X.H. Qu, "Investigation of Debinding and Sintering of 3Y-ZrO2 Gear Fabricated by Micro Powder Injection Molding", *Mater. Sci. Forum*, 2013, pp. 378¬–386.

[6] J. Meng, N.H. Loh, G. Fu, S.B. Tor and B.Y. Tay, "Replication and Characterization of 316L Stainless Steel Micro-Mixer by Micro Powder Injection Molding", *J. Alloys Compd.*, 2010, vol. 496, no. 1–2, pp. 293–299.

[7] L. Chao, K. Xiang-ji, W. Shengwen and K. Chun-jiang, "Research on Micro Metal Injection Molding of Titanium for Biomedical Applications", *Powder Metallurgy Industry*, 2017, vol. 27, no. 1, pp. 22–26.

[8] H. He, Y. Li, J. Lou, D. Li and C. Liu, "Prediction of Density Variation in Powder Injection Moulding-Filling Process by Using Granular Modelling with Interstitial Power-Law Fluid", *Powder Technol.*, 2016, vol. 291, pp. 52–59.

[9] W. Junfeng, H. Hao, L. Yimin and C. Shiqi, "Effect of Nb Addition on Corrosion Resistance of Metal Injection Molding 420 Stainless Steel", *Guangdong Chemical Industry*, 2019, vol. 46, no. 3, pp. 3–7.

[10] Z. Zhigang, L. Yimin, H. Hao and H. Zheyu, "The Study of Injection Forming High Speed Steel Performance after Various Heat Treatments", *Metal Materials and Metallurgy Engineering*, 2017, vol. 45, no. 3, pp. 31–35.

[11] L. Zhang, D. Li, X. Chen, X. Qu, M. Qin, X. He, Z. Li and F. Yang, "Microstructure Characterization and Tensile Properties of MIM418 Superalloy", *Powder Metall.*, 2016, vol. 58, no. 5, pp. 354–362.

[12] L. Zhang, D. Li, X. Chen, F. Yang, J. Wang, B. Chen, X. Ma and X. Qu, "Preparation of MIM213 Turbine Wheel with Hollow Internal Structure", *Mater. Des.*, 2015, vol. 86, pp. 474–481.

[13] A. Chuanfeng, H. Hao, L. Yimin, Y. Jian, L. Jia and Y. Yong, "Effect of Carbon and Nb on Sintering Densification and Mechanical Properties of MIM 420 Stainless", *Journal of Guangxi University of Science and Technology*, 2018, vol. 29, no. 2, pp. 63–69.

[14] J. Lou, H. He, Y. Li, H. Zhang, Z. Fang and X. Wei, "Effects of Trace Carbon Contents on Lattice Distortion and Nano-Copper Phase Precipitation in Metal Injection-Molded 17-4PH Stainless Steel", *JOM*, 2019, vol. 71, pp. 1073–1081.

[15] X. Liang, L. Yimin, H. Hao and Z. Zhaoyi, "Effects of Microstructure and Impurity on Magnetic Properties of Metal Injection Molding Fe-50%Ni Alloy", *The Chinese Journal of Nonferrous Metals*, 2011, vol. 21, no. 4, pp. 821–828.

[16] Z. Caiqiang, F. Zhijian, H. Hao, X. Liang and L. Yimin, "Effect of Heat Treatment Mode on Magnetic Properties of MIM Fe-50%Ni Alloy", Materials Science and Engineering of Powder Metallurgy, 2013, vol. 18, no. 3, pp. 390–397.

[17] Y. Hu, Y. Li, H. He, J. Lou and X. Tong, "Preparation and Mechanical

Properties of Inconel718 Alloy by Metal Injection Molding", *Rare Metal Mat. Eng.*, 2010, vol. 39, no. 5, pp. 26–31.

[18] L. Chao, K. Xiang-ji and K. Chun-jiang, "Research on Powder Injection Molding of Grade 2 CP-Titanium for Biomedical Application", *Powder Metallurgy Technology*, 2016, vol. 34, no. 4, pp. 281–284.

[19] L. Chao, K. Xiang-ji, W. Sheng-wen and K. Chun-jiang, "Study on Powder Injection Molding of Ti6Al4V Alloys for Biomedical Application", *Powder Metallurgy Industry*, 2019, vol. 29, no. 2, pp. 7–11.

[20] Z. Lixiang and H. Guoxin, "Experimental Investigation on Porous NiTi Shape Memory Alloy by Metal Injection Molding", *Journal of Shanghai Jiaotong University*, 2008, no. 1, pp. 87–90.

[21] Z. Liming, Q. Xuanhui, H. Xinbo and L. Shiqiong, "Sintering of TiAl Injection Molding", *Chinese Journal of Rare Metals*, 2008, no. 2, pp. 180–184.

[22] Z. Lingling, L. Xin, S. Bo, Y. Yu, L. Chengcheng and Q. Xuanhui, "Friction and Wear Performance of Ti-12Mo Alloy by Powder Injection Molding", *Rare Metal Mat. Eng.*, 2017, vol. 46, no. 3, pp. 675–679.

[23] Z. Rui, H. Hao and L. Yimin, "Effect of Nd on Oxygen Distribution and Mechanical Properties of Metal Injection Molding Ti Alloy", *Materials Science and Engineering of Powder Metallurgy*, 2014, vol. 19, no. 3, pp. 401–407.

[24] Z. Hongcui, F. Jinglian, C. Huichao and L. Sunhe, "Study on Optimization of Injection Moulding Parameters of WC-Co Cemented Carbide Insert", *Cemented Carbide*, 2013, vol. 30, no. 4, pp. 210–216.

[25] L. Tiegang, Q. Xuanhui, Q. Mingli and D. Yinghu, "Optimization of Binder and Research of Rheological Property for Metal Injection Molded Pure Tungsten", *Journal of Xi'an Technological University*, 2010, vol. 30, no. 4, pp. 361–366.

[26] R. Li, M. Qin, C. Liu, H. Huang, H. Lu, P. Chen and X. Qu, "Injection Molding of Tungsten Powder Treated by Jet Mill with High Powder Loading: A Solution for Fabrication of Dense Tungsten Component at Relative Low Temperature", *Int. J. Refract. Met. H.*, 2017, vol. 62, pp. 42–46.

[27] S. Feng, F. Jie, Q. Bin, L. Huaqiang, C. Zhenwei and S. Wei, "Study on Injection Molding Process of WC-10Co Ultrafine Grained Cemented Carbide", *Rare Metal Mat. Eng.*, 2017, vol. 45, no. 5, pp. 63–68+73.

[28] W. Huanlong, P. Kepu, X. Xu, W. Wei and S. Jiupeng, "Development and Performance Test of Tungsten-Copper Shaped Charge Liners by Metal Injection Moulding of Ultrafine Composite Powder", *Mater. Sci. Technol.*, 2017, vol. 25, no. 4, pp. 91–96.

[29] G. Yajie, D. Junqi, C. Junzhi and P. Xiaodong, "Effect of Sintering Temperature on Injection Molding of Small Size Screw of 93W-4Ni-3Fe Alloy", *Hot Work. Technol.*, 2014, vol. 43, no. 10, pp. 88–90+100.

[30] L. Tiegang, C. Yixiang, Q. Xuanhui and Q. Mingli, "Research of Active Sintering Densifying on Powder Injection of Molding Pure Tungsten", J. Mech. Eng., 2013, vol. 49, no. 18, pp. 63–68.

[31] J. Xiangcao, "Application of Ultrafine Metal Powder Injection Moulding on Tungsten Components in Fusion Devices", *Powder Metallurgy Technology*, 2018, vol. 36, no. 4, pp. 279–286.

[32] L. Rui, Q. Mingli, C. Pengqi, Z. Huailong, Z. Shang-jie, C. Zheng and Q. Xuanhui, "Preparation of Porous Tungsten Matrix of Cathode by MIM", *Vacuum Electronics*, 2016, no. 5, pp. 45–47.

formnext
SOUTH CHINA

Powder Metallurgy EXPO SOUTH CHINA

Shenzhen International Additive Manufacturing,
Powder Metallurgy and Advanced Ceramics Exhibition
深圳国际增材制造、粉末冶金与先进陶瓷展览会

Explore endless possibilities

9 – 11 September 2020

Shenzhen World Exhibition & Conventional Center
Shenzhen, China

www.formnext-pm.com

UNIRIS EXHIBITION SERVICE

messe frankfurt

HANNOVER MESSE 2020

TRANSFORMATION IS EVERYWHERE. ITS HEART BEATS IN HANNOVER.

For over 70 years we have driven, inspired, led and accompanied the course of industrial transformation. HANNOVER MESSE serves as a window revealing the world of tomorrow.
Be part of it: **hannovermesse.com** **#HM20**

NEW DATE: 13 – 17 JULY 2020

MAKING INDONESIA 4.0
PARTNER COUNTRY 2020

HOME OF INDUSTRIAL PIONEERS

HANNOVER MESSE

A beginner's guide to three leading sinter-based metal Additive Manufacturing technologies

To overcome the limitations of currently available Additive Manufacturing technologies for metals, sinter-based AM methods are seeing increasing attention for the single-piece and small- to medium-scale production of precision parts. Current development efforts are concentrated on Material Extrusion, Binder Jetting and Vat Photopolymerisation, which may also have potential to open up the closely related Metal Injection Moulding market for smaller quantity production runs. This is particularly the case in applications where the amortisation of MIM tooling costs is a commercial issue. Prof Dr Carlo Burkhardt presents an overview of how these technologies work and highlights their current strengths and weaknesses.

Additive Manufacturing is a relatively recent manufacturing process which has become a key area of interest in multiple industrial sectors. Deriving from digital models (CAD data or 3D scans), the process can be used to create solid yet highly complex parts by joining materials, usually layer upon layer – thus 'adding' material to build a part, as opposed to removing material as in subtractive manufacturing methods. AM's advantages, such as freedom of design, increased part complexity, lightweighting, multiple part consolidation and design for function are garnering particular interests from the aerospace, oil and gas, marine and automobile sectors and enable the push towards a tool-less manufacturing environment.

There are many metal AM process available which use powders. These can be broadly categorised into fusion-based and sinter-based processes. Fusion-based processes are categorised under the term Powder Bed Fusion (PBF) and include Laser and Electron Beam Powder Bed Fusion (L-PBF and EB-PBF). Whilst these names are now recognised by the International Organization for Standardization (ISO), there is an often confusing plethora of alternative or proprietary names, for example Selective Laser Sintering (SLS), Direct Metal Laser Sintering (DMLS), Laser Metal Fusion (LMF) and Electron Beam Melting (EBM). Sinter-based processes include Material Extrusion (MEX), Binder Jetting (BJT) and Vat Photopolymerisation (VPP) technologies. These

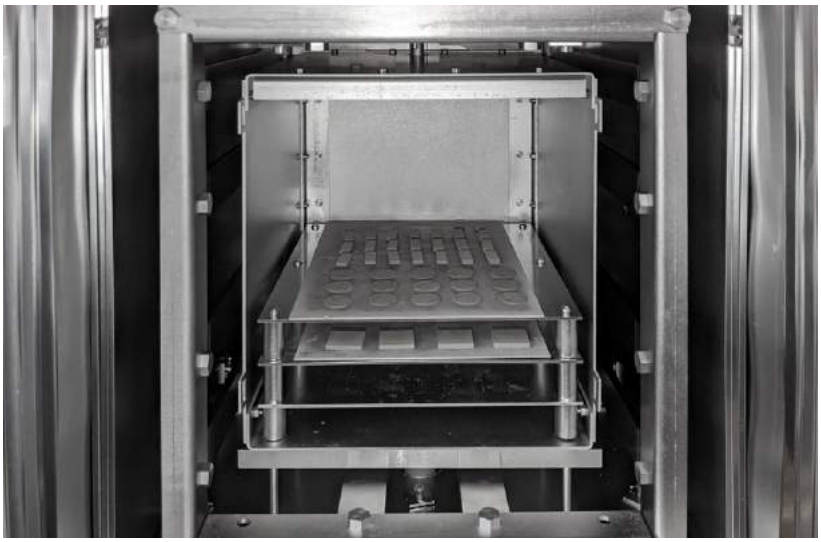

Fig. 1 It is the sintering process, typically undertaken in an industrial vacuum furnace such as this, that separates the sinter-based AM technologies from fusion-based processes such as L-PBF and EB-PBF

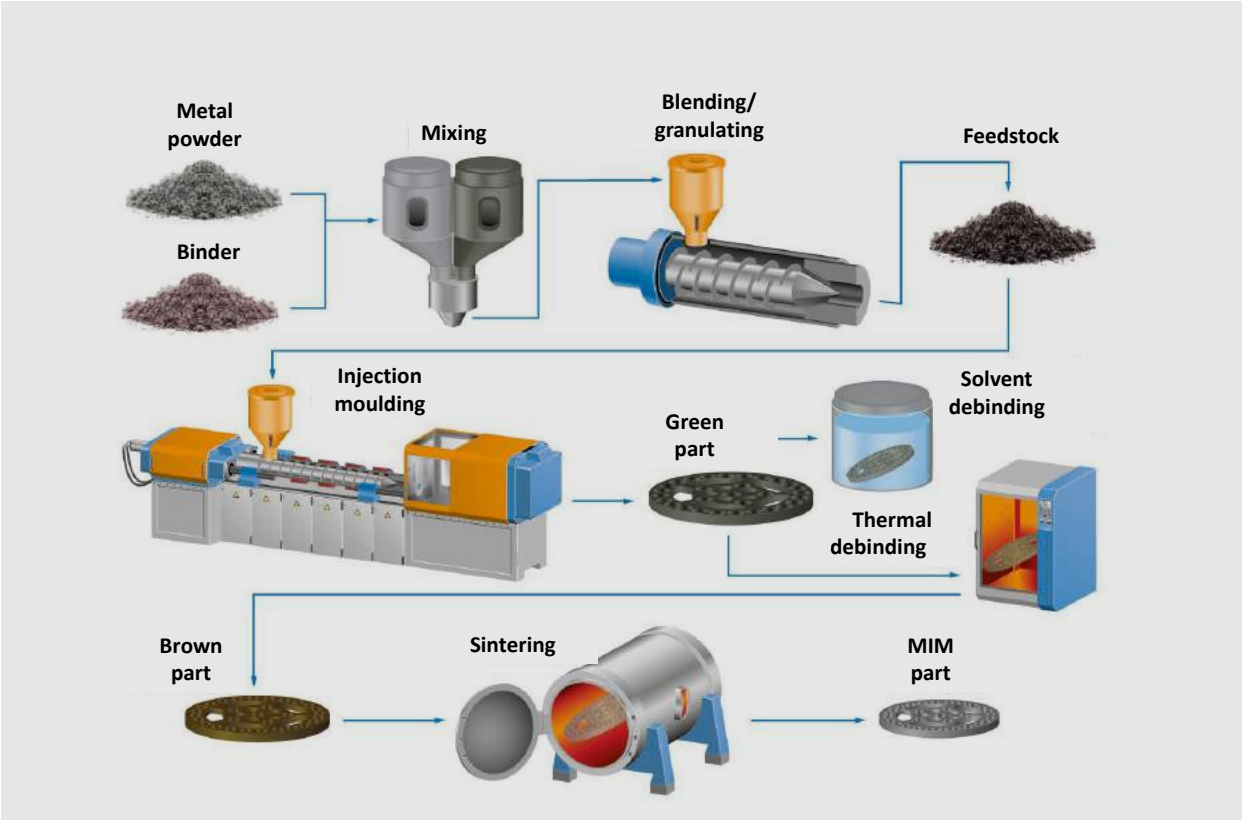

Fig. 2 A schematic of the Metal Injection Moulding process [8]

processes can also have a number of alternative or proprietary names, including Bound Metal Deposition (BMD) and Atomic Diffusion Additive Manufacturing (ADAM).

L-PBF technologies have enjoyed significant successes in the market for the production of complex-shaped metal parts. In L-PBF, a high-power laser is used to melt and fuse metallic powders together to create both prototypes and serial parts, often with thin walled features, hidden voids or complex cooling channels. Applications are typically characterised by low lot sizes.

However, because of the complex nature of the technology, where many parameters govern the process of producing components and consequently affect the quality of surface and mechanical properties, progress for small metal precision parts with high tolerances and/or high surface requirements is relatively slow.

The relationship between the powder size, laser beam power, process time, powder feed rate, beam patch overlap and layer thickness [1-3] involves significant development work to improve the accuracy and surface quality of the parts [4-7], particularly of 'downskin' surfaces. Whilst finer powder generally delivers better properties, the costs and handling of such powders, especially from a health and safety perspective (fine powders are pyrophoric and their particles are respirable and may therefore be carcinogenic) have led to challenges in the larger-scale adoption of L-PBF in the wider precision component producing industries.

These constraints are exacerbated by the need for support structures in the L-PBF process, which function as anchors and support overhanging structures, dissipating heat and thereby helping to control the thermal distortion associated with these parts. As the materials used for the support structures must be manually removed after the build process, the reworking of the attached surfaces and the remelting/reprocessing of the used material can substantially increase manufacturing time and costs.

Thus, in a world where consumers require products to be delivered ever quicker and where industries need to be more efficient, there is a need for alternative AM solutions to produce higher volumes of small, high-precision parts.

Sinter-based metal Additive Manufacturing and MIM

Sinter-based metal Additive Manufacturing technologies are an evolution of AM processes originally developed for polymer parts, combined with some processing steps from Metal Injection Moulding.

Metal Injection Moulding

MIM gained recognition throughout the 1990s as a technology capable of improving the cost efficiency of complex-shaped metal parts by offering high-volume production to

net shape, negating costly additional operations such as machining. The MIM process steps, as illustrated in Fig. 2, involve combining metal powders with polymers such as wax and thermoplastic binders to produce a feedstock mix that is injected as a liquid into a mould using a modified polymer injection moulding machine. The moulded green part is then cooled and ejected from the mould. Next, a portion of the binder material is removed using solvent, thermal furnaces, catalytic process, or a combination of these methods. The resulting fragile and porous part is referred to as the brown part.

This brown part is then heated to temperatures near its melting point in a protective atmosphere furnace to densify the particles using capillary forces, in a process called sintering. Due to the small particle size of the powders, diffusion rates are high, leading to reproducible shrinkage rates of between approx. 15 and 25%, depending on the feedstock system employed, and densification in the range of 96–99% density. The solid metal end-product has comparable mechanical and physical properties with parts made using conventional metalworking processes. Post-sintering heat treatments for MIM are the same as with other fabrication routes and, with high density, the MIM component is compatible with standard finishing processes such as plating, passivating, annealing, carburising, nitriding, precipitation hardening, etc.

The window of economic advantage in MIM parts lies in a combination of high design complexity and high production volumes for small-size parts and final products are used in a broad range of industries, including medical, dental, firearms, aerospace, consumer electronics and automotive applications [9]. The increased costs for part complexity that are associated with conventional manufacturing methods, such as for internal/external threads, miniaturisation, or identity marking, typically do not increase the cost in a MIM operation due to the flexibility of injection moulding.

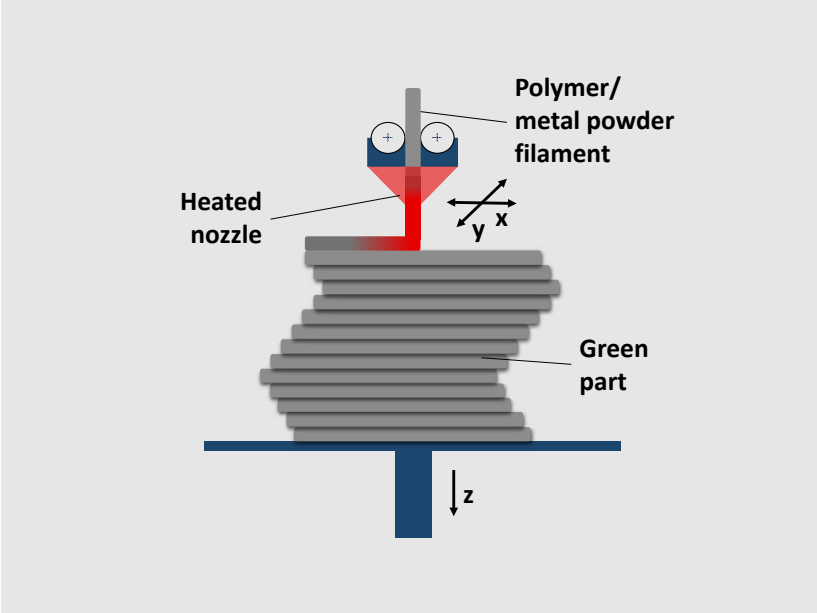

Fig. 3 The Material Extrusion process, in which filament is extruded onto a build plate one horizontal plane at a time to form the desired shape

However, as the high initial costs of the injection moulding tool limit the field to high-volume applications, sinter-based Additive Manufacturing processes are looking to replace the injection moulding step of MIM by Additive Manufacturing the individual green part.

Shaping of green parts with Material Extrusion

Material Extrusion (MEX) is today the most popular AM process by number of machines worldwide. Other terms commonly used for this process are Fused Filament Fabrication (FFF) and Fused Deposition Modelling (FDM). Fused Deposition Modelling, however, is now a Stratasys brand name and can no longer be used as a descriptive term for the process itself. Advantages of MEX processes are, for example, low machine costs, ease of operation and the uncomplicated change of filament material. To date, however, low geometrical precision and poor surface quality compared with other AM processes have limited the field of application.

MEX typically uses a continuous filament made from a thermoplastic material. The filament is fed from a coil, through a heated extruder head, as illustrated schematically in Fig. 3. Molten material is forced out of the extruder head's nozzle and deposited on the growing workpiece. The head is moved, under computer control, to define the part shape. Usually the head moves in two dimensions (x,y) to deposit one horizontal plane at a time, before the ground plate moves downwards (z) to begin a new slice. The speed of the extruder head may also be controlled, to stop and start deposition and form an interrupted plane without 'stringing' between sections.

To shape metallic green parts on standard MEX machines, tailored metal-based MEX filament material with a volume content of approx. 50–60% powder is used. Some MEX machines designed for metal use feedstock bars [26] or micro-extruders to process granulated MIM feedstock [27] and are designed to use that form of feedstock only.

Metal-based filament needs suitable viscosity and mechanical properties to be processed on the MEX machine; however, due to the higher temperature conductivity of the metal-filled filament compared to 'pure' thermoplastic, the extruder head must allow a reliable

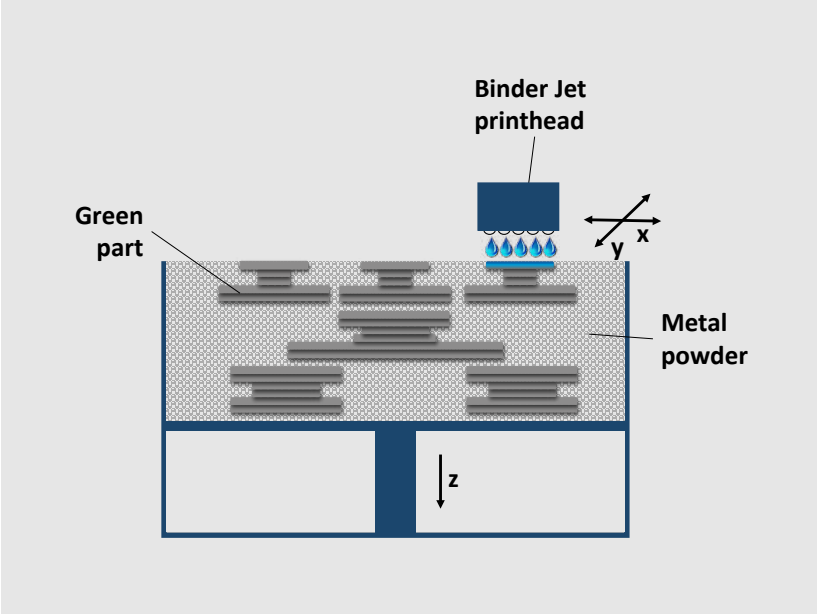

Fig. 4 The Binder Jetting process, in which a liquid binding agent is jetted into a powder bed

transportation of the softening material through the extrusion nozzle to ensure high-quality results. Machines with filament transportation units very close to the heated nozzle may not be suitable to process metal filaments and will need modifications such as cooling of the transport rollers or belt drive systems. Also, because of the higher temperature conductivity of the metal-containing green parts, special attention needs to be given to the temperature in the build chamber, as a non-uniform distribution during the shaping process may lead to distortion/warpage of the green parts due to thermal stresses [12]. Temperature controlled build chambers are therefore preferable and may allow faster build speeds.

For reliable part production, viscosity, flexibility and the surface of the filament are also important properties. If not suitably tailored to the technology, filaments may break during transportation, will not be transported in a continuous manner and can also block the extrusion nozzle, leading to geometric and surface imperfections or machine jamming. Nozzle diameter and layer thickness define the precision of the green part, with smaller values leading to higher precision. The minimum nozzle diameter is, of course, limited by the powder particle size and powder volume content of the filament and typically ranges from 0.1 to 0.5 mm.

As with L-PBF, each new layer of the part must be supported by the layer beneath it. Thus, larger overhangs, internal cavities and bridges must be supported with additional support structures to ensure a successful build. If the machine employs a multi-extrusion head, the support structures can be made from another (non-metallic) material. In this case, however, these support structures may need to be removed before sintering.

Shaping of green parts with Binder Jetting

Binder Jetting produces metal parts by selectively inkjet 'printing' a liquid binding agent into a powder bed, as illustrated in Fig. 4. The jetted binder droplets wet the powder particles and bond them into a cohesive, cross-sectional layer.

Once a layer of binder is printed, a new layer of powder is recoated on top of the previous layer, which is then bonded to the previous layer by the jetted binder. The layer-by-layer process is repeated to create the complete green part. Binder Jetting offers high throughput enabled by the inkjet printing technology. Moderate heat (70°C) is employed to set the binder and, therefore, the risk of warpage during production is believed to be low; however, no studies on the subject could be found to date.

The powder bed acts as support for the green compacts, so that no additional support structures are needed in the case of overhangs, bridges, etc, and several layers of parts can be produced in the same job. While some manufacturers favour a scalable single-pass strategy, both concepts offer initially good prerequisites for large scale production.

After completion of the process, the parts are cured at temperatures of 200–400°C to increase green compact strength by evaporating the solvent binder components. This is typically done with the parts still embedded in the powder bed to prevent mechanical damage. The parts are then removed from the powder bed with the help of compressed air, brushes and other manual processes, which currently limits the productivity of the process substantially.

In contrast to MIM and MEX parts, green parts produced by BJT are not fully dense, as only between approximately 2 and 8 vol.% of binder is jetted onto the powder. As the powder packing density in the powder bed is, depending on particle size and particle size distribution, only between 50 and 65 vol.%, this leaves the green part with an open porosity and approx. 30–40 vol.% of air. Without thermal curing, part removal from the powder bed is impossible and, even after curing, green part strength is low. This makes the handling of BJT green parts more challenging than with any other metal AM technology. A high degree of automation in the removal of the green parts from the powder bed is therefore a major challenge

and to date includes a high potential green part failure rate, especially where parts incorporate delicate features and thin-walled areas.

Another challenge with Binder Jetting is to achieve a homogeneous powder bed density with maximum packing, to minimise geometric deviation. Approaches to overcoming such restraints include vibration of the spreading tool [28, 29], the application of acoustic energy [30], double smoothing or multi-stage compaction systems, comprising at least one spreading and one compaction roller to densify the powder bed [28, 31]. Maximum packing, however, is limited by the risk of green part displacement and/or destruction due to external forces exerted by the compaction system.

In contrast to MEX and VPP, BJT involves the handling of fine powders during printing and removal of the parts from the powder bed. The increased effort in handling potentially flammable and carcinogenic powders implies considerable disadvantages compared to both MEX, where the powder particles are bound in the filament, and VPP, where the feedstock slurry prevents the particles from spreading.

Shaping of green parts with Vat Photopolymerisation

Vat Photopolymerisation, also known as stereolithography and Lithography-based Metal Manufacturing (LMM), is a process which employs a metal-photopolymeric feedstock containing polymers that are sensitive to ultraviolet light. In its cooled state, the feedstock has a 'butter-like' texture, but liquifies when heated, meaning that it can be finely distributed with the help of a heated blade to the surface of the working chamber (layer thickness typically between 20–50 µm). A digital light processor (DLP) projects a pre-programmed shape on to the surface of the photohardening binder (Fig. 5). In the exposed areas, the binder is photochemically solidified and forms a single layer of the desired object. The build platform then lowers one layer and the heated blade recoats the surface with feedstock. This process is repeated for each layer of the design until the 3D object is complete. Because of the layerwise DLP exposure, multiple parts can be built at one time without increasing cycle time.

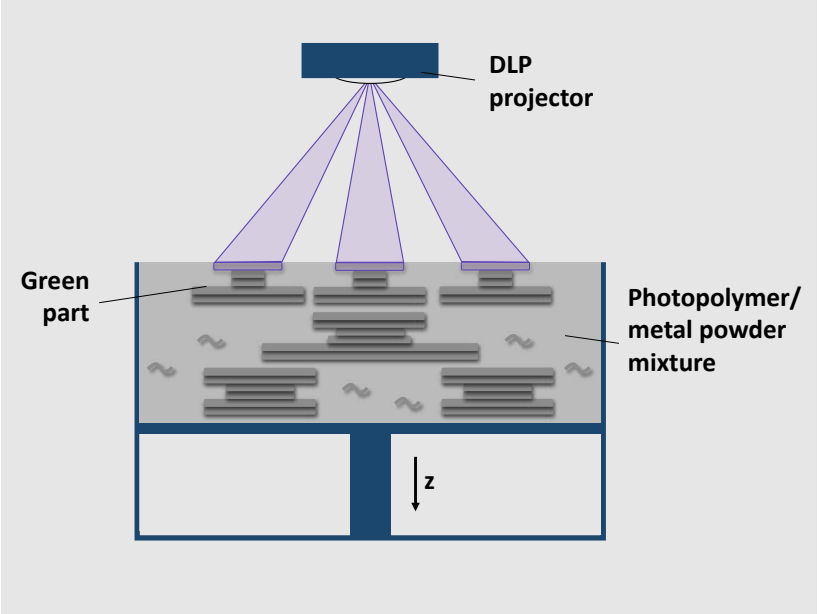

Fig. 5 The Vat Photopolymerisation (VPP) process, in which a digital light processor projects a shape onto a metal-photopolymeric feedstock one layer at a time, causing it to photochemically solidify in the desired shape

When the build job is finished, the cooled and hence solid feedstock block is removed from the VPP machine. It is heated to ~50°C, when the non-exposed material liquifies and can be collected for direct reuse. The remaining green parts are cleaned in an ultrasonic bath or with the help of a tailored air-brush system to remove residues of non-exposed material (~2–5 vol.%). This material goes through a filtering system, wherein the metal powder is collected and can be used for feedstock production without further reprocessing. Therefore, VPP has a near-to-100% material efficiency, which qualifies the process for precious metals and other supply-critical materials.

The green compacts have a very high strength, thus requiring no extra care during handling. As VPP does not use heat to process material, there is no risk for warpage during a build. As with BJT, VPP requires no additional support structures and several layers of parts can be built in the same job, as the feedstock in its cooled state has a strong supporting function. This allows even smaller distance between the parts (1 mm) compared to BJT and allows maximum use of the build chamber.

Particular challenges for VPP are the solid loading of the feedstock with metal powder (typically ~50 vol.%) and the process-reliable penetration of the feedstock mixture for the UV light to achieve a cohesion between the layers of the green compact without delamination.

Debinding and sintering of green parts

Whereas all three of the described sinter-based AM processes share the initial concept of using a metal-polymer mixture as starting material and to shape the green compact by curing a polymer while leaving the embedded metal powder 'unaffected', the debinding strategies of the three processes differ fundamentally due to their distinct binder composition.

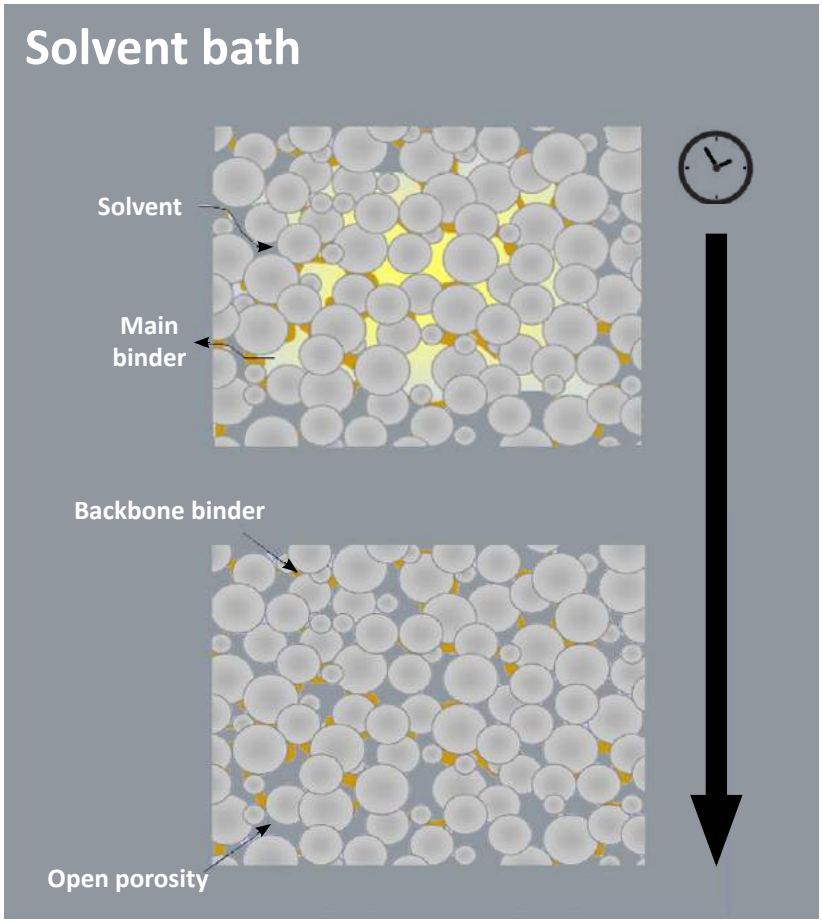

Fig. 6 The solvent debinding process leaves behind an open-pored material structure

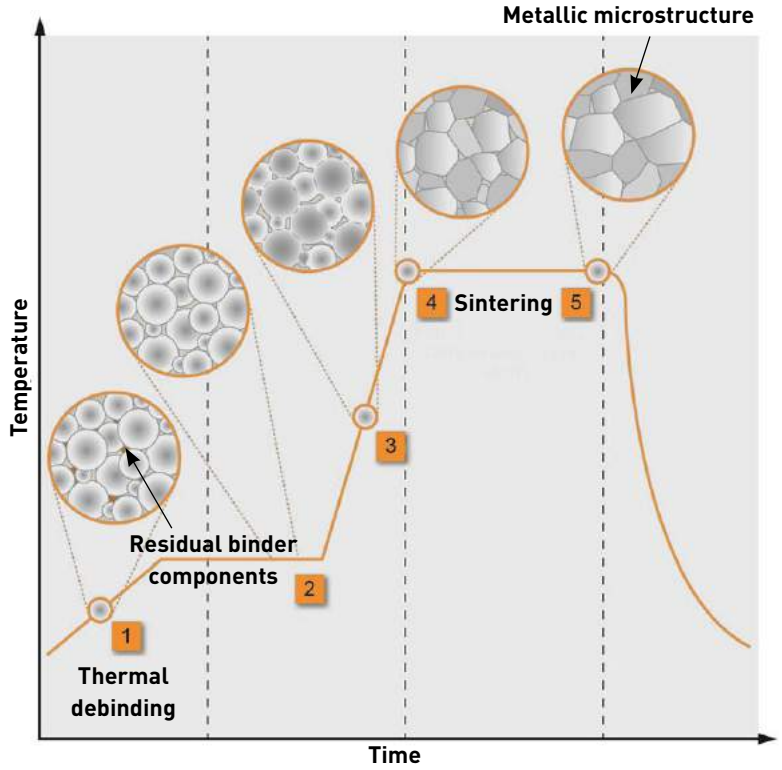

Fig. 7 Temperature vs time diagram of a typical sinter-based AM debinding and sintering run

Debinding of green parts produced by Material Extrusion

MEX feedstock filaments are based on multi-component binder systems [15]. The main binder allows the production and handling of the filament, ensuring good flowability while shaping, whereas the backbone binder gives the resulting brown part enough strength to be handled for the sintering procedure. Similar to the MIM process, the main binder is removed in MEX green compacts either thermally or with the help of solvents.

In solvent debinding, the green part is exposed for a certain time (typically several hours, depending on part size) to a solvent that dissolves the main binder component, leaving an open-pored structure, as illustrated in Fig. 6. The backbone binder is insoluble in the solvent used and therefore keeps the powder particles together for sintering. Depending on the solvent, debinding can also take place at elevated temperature or under high pressure, where the component is then exposed to a solvent vapour similar to that used in thermal debinding.

MEX-filaments made for catalytic debinding are also commercially available. Here, the main binder (usually polyacetal) is depolymerised in nitrogen atmosphere at elevated temperature in the presence of a catalyst (for example nitric acid) and then removed by the controlled exchange of the gas atmosphere. Such systems have a backbone binder which is not affected by the catalytic reaction. The main advantage of this method is the fast debinding time; however, the respective debinding units require very stringent health and safety measures that are more appropriate for a laboratory or production environment. Solvents cannot be used as debinding agents for ME-filaments which are designed for catalytic debinding.

Debinding of binder jetted parts

Binder Jetting technology employs a different strategy than Material Extrusion and, simply stated, applies only the 'backbone' binder to the

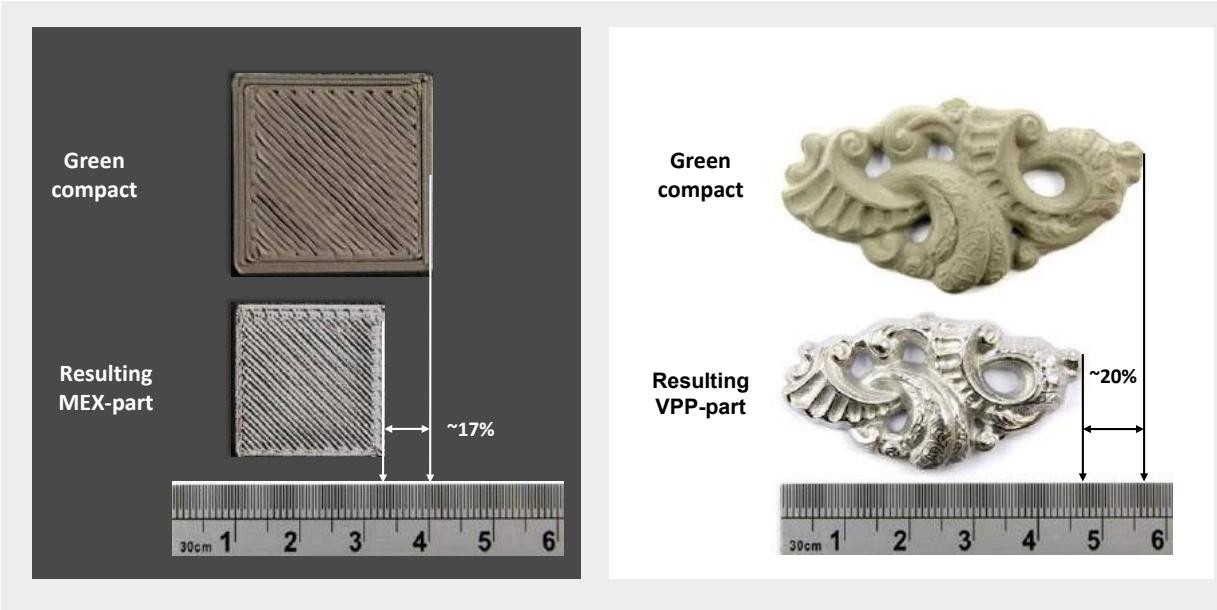

Fig. 8 Sintering factor of (left) MEX and (right) VPP parts

powder. Technically, BJT produces a brown rather than a green part and, therefore, no 'main' binder has to be removed by solvent or catalytic debinding. All remaining binder is removed in the sintering furnace.

Debinding of VPP green parts

The same is true for VPP, but for different reasons. Due to its chemical structure, the employed photopolymer cannot be removed by solvents or in a catalytic reaction and has to be removed during a thermal procedure that is integrated in the sintering run. Thus, when adhering to MIM terminology, all binder in VPP parts is 'main' binder and no 'backbone' binder is employed.

Thermal debinding and sintering of sinter-based AM parts

For all three described sinter-based AM technologies, the remaining binder is removed in a thermal procedure as part of a two-step operation in a MIM sintering furnace under protective atmosphere. The parts are held at temperatures suitable to fully decompose the used polymers thermally, typically in a range of approx. 200–350°C. Depending on geometry, but also on the employed feedstock system, the holding times will vary significantly, with VPP (~50 vol.% binder content) having longer debinding times for a geometrically similar part than BJT (2–8 vol.%).

A constant flow of protective gas ensures that the decomposed binder residues are removed from the samples and transported outside the sintering retort through a piping and exhaust system. As illustrated in Fig. 7 with the help of a temperature vs time diagram, in the sintering step the parts are quickly heated to a temperature near the melting point of the material to densify the particles using capillary forces. Reduction of the surface free energy alters the geometry of the dense object by non-densifying and densifying mechanisms [32]. This results in nearly pore-free samples with complex shapes and fine-grained microstructures for all three compared technologies.

The sintered parts are about 14–22% smaller than the green compacts [33], with the exact sintering shrinkage factor depending on the green part density of the material and manufacturing technology used (Fig. 8).

For MEX and VPP, the shrinkage factor itself is highly reproducible, with shrinkage being similar in all three dimensions [12, 34]. This allows a simple scaling of the CAD-drawing or scanned data as part of the construction step, as is well known from MIM products. For BJT, there are strong indications that the shrinkage is larger in the z-axis, leading to anisotropic sintering behaviour [35, 36, 37], which is more difficult to address in the design stage. The reason for this may be complex fluid/powder interactions during the Binder Jetting procedure.

As has long been recognised in MIM production, it is preferable for parts made by all three technologies to have at least one flat surface for support during the sintering process to prevent distortion. If a chosen geometry does not allow such support, a matching sintering support may be needed. The support must be made from the same material as the desired part. It must also be in the green state before sintering, as sintering shrinkage has to be taken into account.

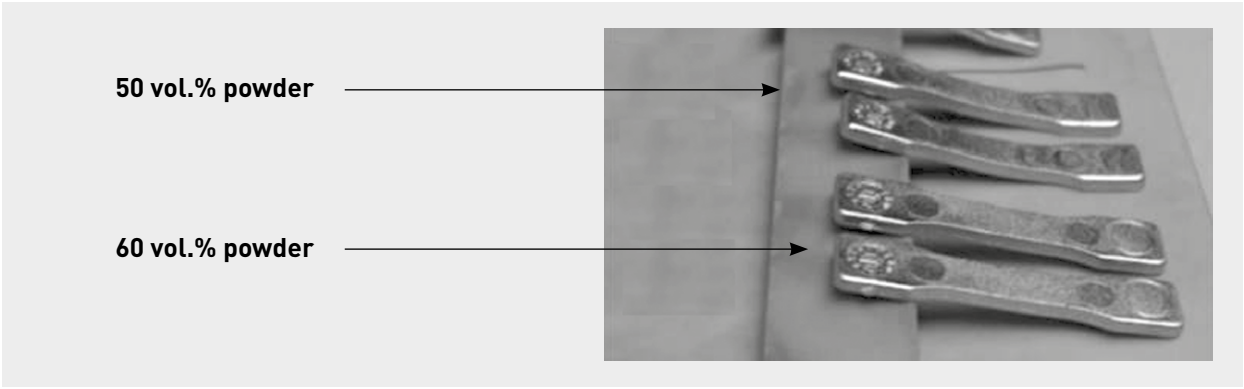

Fig. 9 Sintered tensile bars made from feedstock with different powder filling ratio

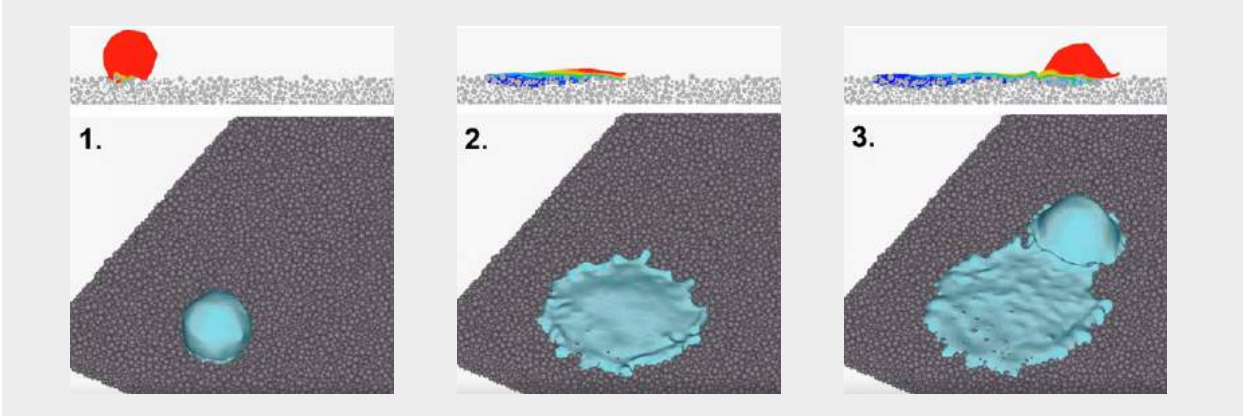

Fig. 10 Examples of Binder Jetting flow simulation [38]

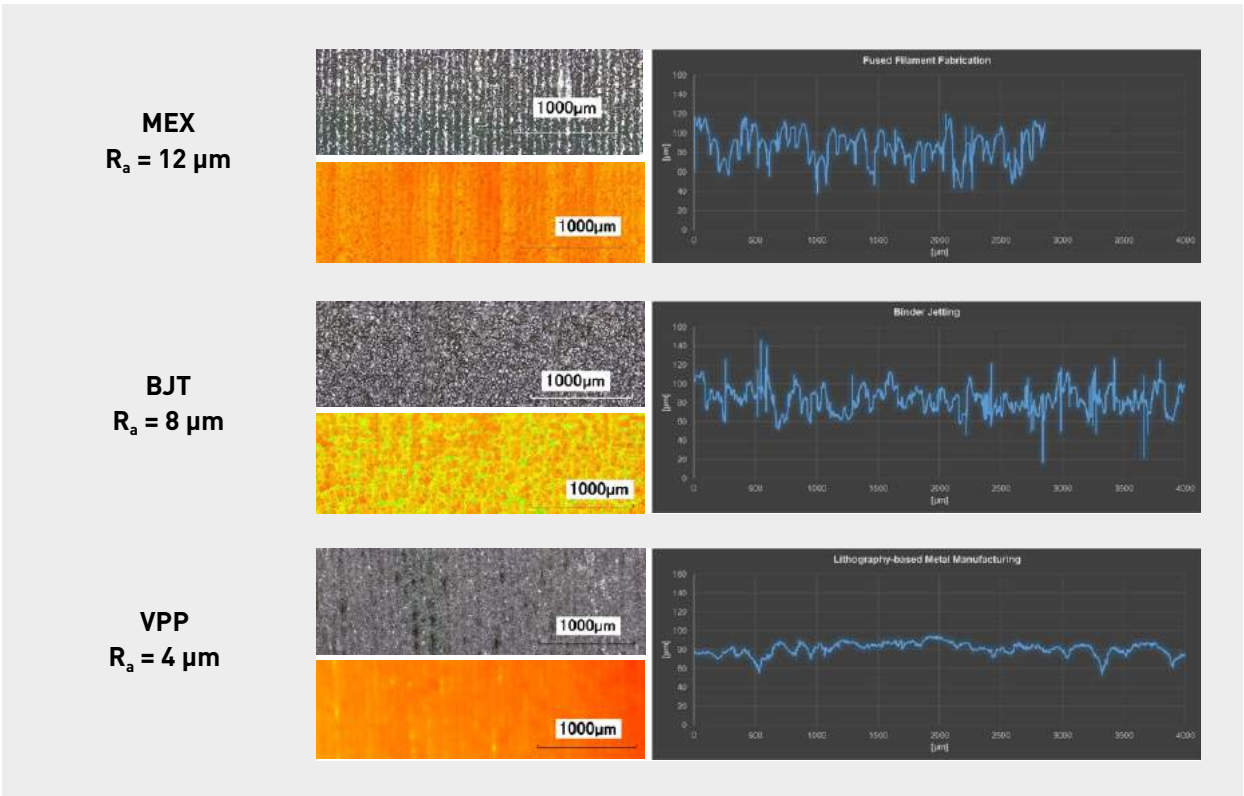

Fig. 11 Typical surface structures of MEX, BJT and VPP samples

In contrast to MIM, where secondary tooling is needed, with sinter-based AM it is much less costly to build a matching sintering support. In the case of MEX, support structures needed to build the part may also be used for sintering. To avoid labour-intensive efforts to remove them after sintering, incorporating a thin ceramic layer between part and support with ceramic filament from a second extruder head during the build may be a viable alternative. As the powder filling ratio of all currently available sinter-based AM feedstocks is lower than in commercial MIM feedstocks (typically in the range of 50–55 vol.% for current AM technologies compared with > 60 vol.% with MIM), sintering distortion may be greater than with MIM parts, as shown in Fig. 9 for tensile bars sintered under same conditions. It can be seen that the sintered bars with a higher powder loading keep their original shape, whereas those with lower powder loading show considerable distortion.

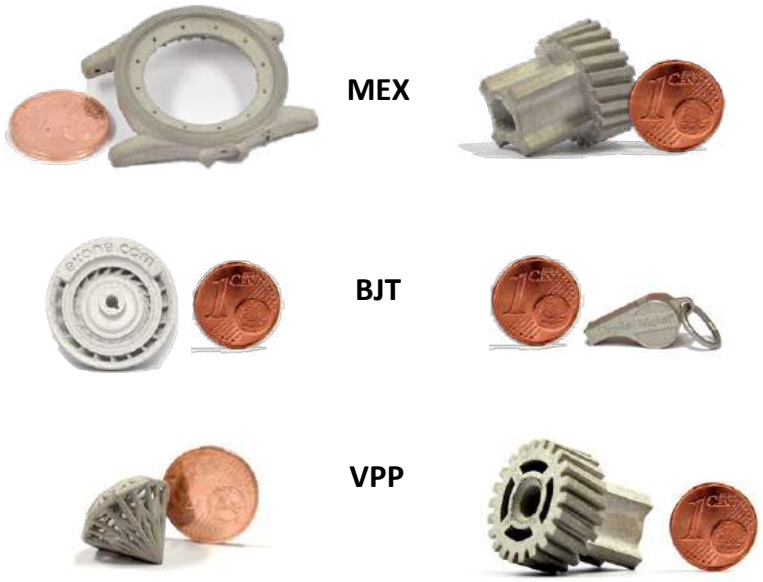

Fig. 12 Selected MEX, BJT, and VPP parts

Surface quality of sinter-based Additive Manufacturing methods

The achievable surface quality of the three investigated technologies differs significantly, with Material Extrusion having the roughest surface topography and VPP having the smoothest. Due to the forming technology of ME, the build lines on the surface of the green part are quite pronounced. They do not disappear during the sintering process, leading to a high surface roughness with a regular appearance (Fig. 8).

In Binder Jetting, the product quality depends on the nature of the interaction between the binder droplets in and with the powder, which is a complex and highly dynamic process. The interactions can vary significantly with the density, size, shape, powder and printing patterns. Specific combinations of powders and printing patterns generate a remarkable edge quality [35], but, in general, the capillary forces of the powder particles do not allow the formation of sharp edges when the binder is distributed (Fig. 10), thus giving BJT parts generally a slightly rough, 'sand-blasted' surface appearance.

With VPP, the digital light processing allows the exposure of sharp contours [34], leading to the best surface properties of the three compared sinter-based AM technologies. Typical as-sintered surface structures (printed z-axis) can be seen in Fig. 11, as measured with non-contact roughness depth and profile measurement on a Confocal 3D laser scanning microscope.

Conclusion

Sinter-based AM technologies are of significant promise for single-piece and medium-scale production of precision parts. MEX, BJT and VPP are highly innovative AM processes for metals that may have the potential to penetrate the MIM market for smaller quantities in applications where the amortisation of MIM tooling costs is a commercial issue.

However, this is associated with expenditure: each of the processes involves a whole array of complex manufacturing steps (shaping, cleaning, debinding, sintering), with strong mutual interdependencies, targeted coordination and optimisation require considerable development effort. Each individual process has its own challenges that need to be addressed and resolved; none of the three technologies can currently report 'mission accomplished'.

While MEX has the longest way to go to become a real MIM competitor in terms of dimensional accuracy and surface quality, the results achieved so far by BJT and VPP are promising. While BJT has clear advantages in terms of build process time and binder constituent costs, VPP may currently provide better dimensional accuracy and surface quality in the sintered parts, combined with technological advantages in green part cleaning, powder handling and equipment costs.

A variety of intensive development efforts in both industry and academia make rapid progress likely and point towards opportunities for future advancement and commercial success of sinter-based AM technologies.

Contact

Prof Dr Carlo Burkhardt
Head of Institute for Precious and Technology Metals (STI)
Pforzheim University
Germany
carlo.burkhardt@hs-pforzheim.de

References

[1] M. Król, L.A. Dobrzanski, L. Reimann, I. Czaja, Surface quality in selective laser melting of metal powders, *Archives of Materials Science and Engineering* 60/2 (2013) 87-92.

[2] A.B. Spierings, N. Herres, G. Levy, Influence of the particle size distribution on surface quality and mechanical properties in AM steel parts, *Rapid Prototyping Journal* 17/3 (2011) 195-202.

[3] E. Yasa, J. Deckers, J.-P. Kruth The investigation of the influence of laser re-melting on density, surface quality and microstructure of selective laser melting parts, *Rapid Prototyping Journal* 17/5 (2011) 312-327.

[4] R.J. Wang. L. Wang, L. Zhao, Z. Liu, Influence of process parameters on part shrinkage in SLS, I*nternational Journal of Advanced Manufacturing Technology* 33 (2007) 498-504.

[5] X.C. Wang, T. Laoui, J. Bonse, J.P. Kruth, B. Lauwers, L. Froyen, Direct selective laser sintering of hard metal powders: experimental study and simulation, *International Journal of Advanced Manufacturing Technology* 19 (2002) 351-357.

[6] A. Sachdeva, S. Singh, V.S. Sharma, Investigating surface roughness of parts produced by SLS process, *International Journal of Advanced Manufacturing Technology* 64 (2013) 1505-1516.

[7] C. Sanza, V. Garcia Navasa, O. Gonzaloa, G. Vansteenkiste, Study of surface integrity of rapid manufacturing parts after different thermal and finishing treatments, *Procedia Engineering* 19 (2011) 294-299.

[8] C. Burkhardt, Metallpulverspritzguss In: Die Bibliothek der Technik 237. *Süddeutscher Verlag onpact*, München 2013, ISBN 978-3-86236-056-7.

[9] https://www.epma.com/metal-injection-moulding, [accessed 29.12.2019]

[10] G. Wu, N. A. Langrana, R. Sadanji, S. Danforth, Solid freeform fabrication of metal components using fused deposition of metals, *Materials and Design* 23 (2002), pp. 97-105

[11] S. Masood and W. Song, Development of new metal/polymer materials for rapid tooling using Fused deposition modelling, *Materials & Design* 25 (7) (2004) pp. 587–594

[12] C. Burkhardt, P. Freigassner, O. Weber, P. Imgrund, S. Hampel, Fused Filament Fabrication (FFF) of 316L Green Parts for the MIM process, Proceedings EURO PM 2016, Barcelona (2016)

[13] C. Kukla, J. Gonzalez-Gutierrez, I. Duretek, S. Schuschnigg, C. Holzer, Effect of particle size on the properties of highly-filled polymers for fused filament fabrication, AIP Conference Proceedings 1914, 190006 (2017)

[14] J. Gonzalez-Gutierrez, D. Godec, C. Kukla, T. Schlauf, C. Burkhardt, C. Holzer, Shaping, Debinding and Sintering of Steel Components via Fused Filament Fabrication, 16th Int. Scientific Conference on Production Engineering, CIM2017, Zagreb (2017)

[15] C. Kukla, I. Duretek, S. Schuschnigg, J. Gonzalez-Gutierrez, C. Holzer, Properties for PIM Feedstocks Used in Fused Filament Fabrication, Proceedings EURO PM 2016, Barcelona (2016)

[16] P. K. Gokuldoss, S. Kolla, J. Eckert, Additive Manufacturing Processes: Selective LaserMelting, Electron Beam Melting and BinderJetting—Selection Guidelines, Materials 2017, 10, 672

[17] H. Miyanaji, M. Orth, J. M. Akbar, L. Yang, Process development for green part printing using Binder Jetting Additive Manufacturing, *Front. Mech. Eng.* 2018, 13(4): 504–512

[18] S. Shrestha, G. Manogharan, Optimization of Binder Jetting Using Taguchi Method, *JOM*, Vol. 69, No. 3, 2017

[19] Y. Bai, G. Wagner, C. B. Williams, Effect of Particle Size Distribution on Powder Packing and Sintering in Binder Jetting Additive Manufacturing of Metals, *Journal of Manufacturing Science and Engineering*, Vol. 139 (2017) / 081019-1

[20] J. W. Lee, I. H. Lee, D. Cho, Development of micro-stereolithography technology using metal powder, *Microelectronic Engineering* 83 (2006), pp. 1253–1256

[21] P.J. Bartolo, J. Gaspar, Metal filled resin for stereolithography metal part, *CIRP Annals - Manufacturing Technology* 57 (2008), pp. 235–238

[22] M. Roumanie, A. Badev, S. Cailliet, D. Vincent, R. Laucournet, Manufacturing of Metal Parts by Stereolithography, Proceedings EURO PM 2017, Milano (2017)

[23] G. Mitteramskogler, M. Schwentenwein, S. Seisenbacher, C. Burkhardt, O. Weber, Lithographic Additive Manufacturing of Metal-Based Suspensions, Proceedings EURO PM 2017, Milano (2017)

[24] G. Mitteramskogler, M. Schwentenwein, S. Seisenbacher, O. Weber, C. Gierl-Mayer, C. Burkhardt, Lithographic Additive Manufacturing of metalbased suspensions, *Metal Additive Manufacturing*, Spring 2018, 4 (1), (2018) pp. 131-134

[25] G. Mitteramskogler, M. Schwentenwein, C. Burkhardt, N. Cruchley, Lithography-based Metal Manufacturing (VPP) of 316L Powder, Proceedings EURO PM 2018, Bilbao (2018)

[26] I. Campbell, T. Wohlers, Markforged: Taking a Different Approach to Metal Additive Manufacturing. 2017 :113–115. *Metal AM* [Online] Available online: http://www.metal-am.com/wp-content/uploads/sites/4/2017/06/MAGAZINE-Metal-AM-Summer-2017-PDF-sp.pdf [accessed 18.01.2020].

[27] H. Gibertia, M. Strano and M. Annoni, An innovative machine for Fused Deposition Modeling of metals and advanced ceramics, MATEC Web of Conferences 43, 03003 (2016), DOI: 10.1051/matecconf/20164303003

[28] E. M. Sachs, Powder dispensing

apparatus using vibration, United States Patent, US 6,036,777, Mar. 14, 2000, filed Apr. 14, 1995

[29] K. J. Seluga, Three Dimensional Printing by Vector Printing of Fine Metal Powders, M.Sc. Thesis, Mechanical Enigeering, MIT, US, 2001

[30] C. Shu, Q. Yang, W. Zing-Fan, Z. Hong Hai, Experimnetnal and theoretical investigation on ultra-thin powder layering in three dimensional printing (3DP) by a novel double-smoothing mechanism, *J. Mater. Process. Technol.* 220 (2015) pp 231-242

[31] R. Lucas, K. Myers, Binder Jetting Process, Sinter-based Additive Manufacturing Workshop, IFAM Bremen (9/2019)

[32] W. Schatt, Densification mechanism in the initial stage of solid phase sintering, *Met. Powder Rep.* 50 (12) (1995), p. 53

[33] R.M. German, Sintering Theory and Practice, John Wiley & Sons, Inc. 1996, ISBN: 978-0-471-05786-4

[34] C. Burkhardt, G. Mitteramskogler, A. Baum, Advances in High Precision Lithographic Additive Manufacturing with Stainless Steel and Titanium Alloys, Proceedings TCT@formnext 2019, Frankfurt (2019)

[35] M. Ziaee, N. B. Crane, Binder Jetting: A review of process, materials and methods, *Additive Manufacturing* 28 (2019), p. 785-793

[36] S. Mirzababaei, S. Pasebani, A Review on Binder Jet Additive Manufacturing of 316L Stainless Steel, *J. Manuf. Mater. Process.* 2019, 3, 82; doi:10.3390/jmmp3030082

[37] A. Jansson, Scale factor and shrinkage in Additive Manufacturing using Binder Jetting, KTH, Examensarbete, Inom Teknik, Grundniva, 15 HP, Stockholm, Sverige, 2016

[38] Flow-3D Video, Oct. 2017, Available online: https://www.facebook.com/FLOW3D.CFD.Software/ videos/binder-jetting-fluid-flow-simulation/10154996020517452/ [accessed 18.01.2020]

PM CHINA 2020

The 13th Shanghai International Powder Metallurgy Exhibition & Conference

August 12th-14th, 2020

Shanghai World Expo Exhibition Center

Convergence of Cutting-edge Technology & Products

Organizer UNIRIS EXHIBITION SERVICE

Tel: +86 20 8327 6369/6389 +86 4000 778 909

Email: pmchina@unifair.com pmchina@unirischina.com

MIM superalloys: The effect of lower-cost nitrogen atomisation on properties of sintered IN713C

Metal Injection Moulded nickel base superalloy parts are today found in the most demanding service environments, including aerospace and power generation applications. In the automotive sector, MIM has been challenging investment casting for the production of IN713C turbocharger wheels. While MIM offers numerous advantages, powder cost is a major consideration, particularly where argon atomisation is needed for Ti and Al. Here, Sandvik Osprey and Chenming Electronic Technology Corp. (UNEEC) explore the effect of lower-cost nitrogen atomisation on properties of sintered IN713C. Elevated temperature tensile testing has been performed on sintered parts and the effect of nitrogen on microstructural development is compared with conventional argon-atomised IN713C.

Powder metallurgical processes are increasingly deployed for the manufacture of mechanical parts for numerous industrial and consumer applications. When suitably compounded with polymeric binder materials, these inorganic powders can be moulded in the same manner as thermoplastics. The most common example of this approach is Powder Injection Moulding for small dimensions, shape complexity and tight tolerances in high volume, although, for parts with simple shapes, extrusion or simple compression moulding may be used. Metal Injection Moulding, which is a segment of the broader field of PIM, is a relatively new technology that uses the shaping advantage of plastic injection moulding, but expands the applications to numerous high-performance metals and alloys. This advanced technology has grown in popularity in the past three decades as an effective means of producing complex near-net shape parts with high dimensional accuracy and excellent surface finish, and can make thin-walled parts to tight tolerances in a variety of industries, from consumer electronics and medical to automotive and aerospace [1–6].

The conventional PIM process comprises four main steps: mixing (kneading), moulding, debinding and sintering. In the first mixing step, the powder is dispersed in an organic medium (binder) to obtain a homogeneous feedstock, which is granulated ready for injection moulding to the designed geometry. The binder provides a uniform dispersion of

Fig. 1 A continuous sintering furnace at Chenming Electronic Technology Corp. (UNEEC), a Taiwan-based global OEM/ODM and a major MIM component producer with operations in Dongguan, China, since 2002

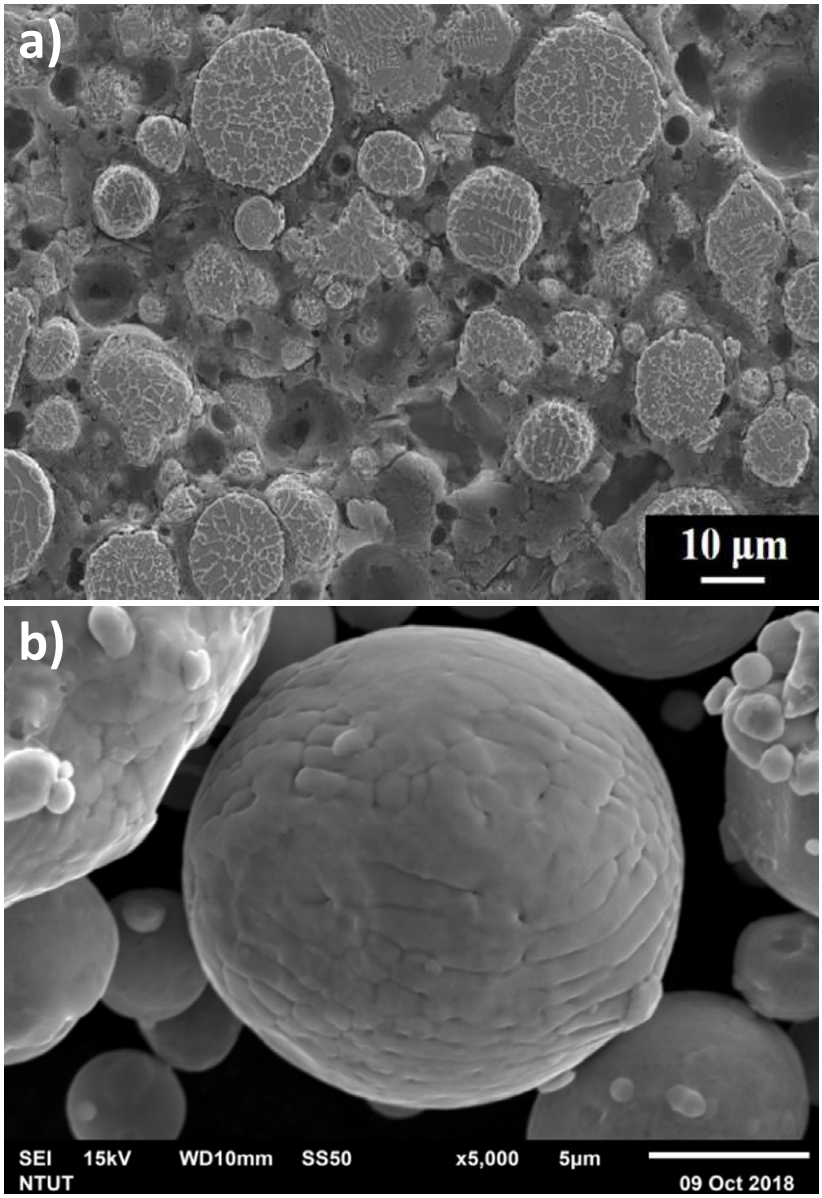

Fig. 2 SEM images of 90% -22 µm IN713C powders: (a) cross-section image (b) appearance image

powders for the subsequent injection moulding process. In addition, the binder provides sufficient green strength (shape retention) for handling during the binder removal and sintering operations.

The debinding method has evolved significantly since the early days of thermal debinding of PIM parts, with advances such as solvent debinding and catalytic debinding enabling parts producers to reduce operation costs, minimise distortion, improve dimensional stability and increase production yield. The final sintering step, either in vacuum or in a controlled atmosphere with different combinations of nitrogen, argon and hydrogen, is used to densify the part to the final form. The sintered parts are often subject to finishing operations, such as coining, CNC machining, plating and polishing to meet customers' stringent requirements, for example dimensional accuracy, corrosion resistance and aesthetic quality.

Knowledge of the role of the starting powder's (or binder's) characteristics on processing and sintering is essential to manufacture defect-free MIM products. It is generally accepted that gas atomised (GA) powders (Fig. 2) with spherical morphology, which can be packed to higher levels than irregular water atomised (WA) powders, enhance sintered density. Poorer packing of WA powder along with the presence of more surface oxide can limit densification. MIM components manufactured using GA powders generally exhibit superior physical properties to components made with equivalent WA powder including, for example higher density and correspondingly lower porosity [7].

Superalloys: overview

Applications in automotive, aerospace or energy generation often require high-temperature materials such as heat-resistant steels and superalloys. Superalloys are materials able to withstand extreme temperatures, particularly in challenging environments, that would destroy conventional ferrous and aluminium alloys. The term 'superalloy' was first used shortly after World War II to describe a group of alloys developed for use in turbo-superchargers and aircraft turbine engines that required remarkable high performance at elevated temperatures. The range of applications for which superalloys are used has expanded to many other areas and now covers aerospace, automotive, rocket engines, medical, chemical and petroleum plants.

Gas turbine applications

Superalloys are typically used in the hottest parts of gas turbines because they offer a unique combination of a high strength at elevated temperatures and considerable resistance to wear in corrosive and oxidising environments. They can be classified according to the main alloying elements in the composition, with the three base metals being nickel, iron-nickel or cobalt alloys. They contain variable amounts of chromium, tungsten, molybdenum and a range of other elements, including aluminium, titanium, tantalum and

niobium. While the term superalloy is nominally reserved for those alloys, which are used at service temperatures of above 800°C, they were developed for applications where high tensile, thermal, vibratory and shock stresses are encountered and where oxidation resistance is frequently required, particularly in the aerospace and energy industries.

The efficiency of turbines depends mostly on the inlet temperature, and the maximum temperature is limited by the alloy grade in the hot path of the turbine due to this temperature being dictated by the ability of the components used to maintain their performance, reliability and safety under imposed thermal and mechanical loads. Continued improvements in the properties of these materials have been possible through close control of chemistry and microstructure as well as the introduction of advanced processing technologies. Therefore, a more profound understanding of the material chemistry, microstructure, phase characteristics, high-temperature strength and oxidation behaviour is beneficial to ensure lifetime and safety, since material loss and surface degradation due to oxidation can ultimately lead to the failure of structural components.

The gas turbine engine, with its high temperatures and stresses, is a dominant application that drives the superalloy industry, continually demanding that the performance boundaries be advanced, especially for nickel-based superalloys. The emergence of this alloy type for the aerospace industry can be traced back to the development of the modern gas turbines where high-temperature resistant materials are greatly demanded to enable higher power output efficiency by operating the turbine at higher temperatures. They have been designed to withstand service temperatures beyond 540°C up to 1000°C, in particular when resistance to creep, corrosion and fatigue is required. Typical industrial nickel-base superalloys can be broadly classified into solid solution-strengthened and precipitation-hardenable varieties.

Alloys such as Inconel 600, Inconel 690, Inconel 625, Hastelloy X, etc., are solid solution-strengthened since this mechanism has the effect of decreasing the stacking fault energy (SFE) in the crystal lattice, leading to inhibition of dislocation cross slip. Inconel X-750, Inconel 100, IN713C (Inconel 713C), Astroloy, MarM-252, GMR-235, Nimonic 90, Nimonic 115, Nimonic PE16, Waspaloy, Udimet 700, CM 247LC, etc., are precipitation-hardenable types. MAR-M 246 is an equiaxed cast alloy and CMSX-10 is a single crystal superalloy, both being used in gas turbine engine components.

Compositions

Commercial nickel-based superalloys are composed of a carefully balanced combination of functional elements, usually containing significant amounts of up to ten alloying elements, including light elements like boron or carbon and heavy refractory elements like tantalum, tungsten, or rhenium, designed to perform in high temperature environments. Most nickel-based alloys contain 10 - 20% Cr, up to 8% Al + Ti, 5 to 10% Co and small amounts of B, Zr, and C to control grain structure. Refractory elements Mo, W, Ta, Hf, and Nb are added to enhance high-temperature durability. The continuous matrix of nickel superalloys is γ phase (face centred cubic, FCC crystal structure). The γ formers can be found in Groups V, VI and VII and are elements such as Co, Cr, Mo, W, Fe. The difference between the atomic diameters of these elements and Ni (the primary matrix element) is typically 3 to 13%. The γ′ formers come from group III, IV and V elements and include Al, Ti, Nb, Ta, Hf. The atomic diameters of these elements differ from Ni by 6 - 18%.

Most types of these superalloys are age-hardenable, with fine scale precipitation of γ′ particles in a γ matrix, even down to the nano-scale. The composition of γ′ phase is nominally Ni_3(Al,Ti) in an ordered FCC crystal structure, where Al and/or Ti atoms occupy the unit cell corners and Ni atoms occupy the centres of the unit cell faces. Properties of the superalloy depend on the size, quantity and the distribution of γ′ precipitates [8-10]. A uniform distribution of the precipitating phase improves significantly mechanical properties, such as the tensile strength, the fatigue lifetime, the creep rupture strength, etc. [11-12].

As for specific nickel superalloys, for example IN 718, a highly weldable superalloy, the primary strengthening mechanism is via niobium-strengthened body-centred tetragonal (BCT) γ″ -Ni_3Nb precipitates, which are coherent with the γ matrix, while inducing large mismatch strains (of the order of approximately 2.9%). γ′ and γ″, which are generally coherent intermetallic compounds, could confine the movement of dislocations. Movement of a dislocation in the matrix containing precipitates can only take place by cutting through or by bypassing the particles. However, the limitation for IN 718 is due to the γ″ strengthening phase, in comparison to γ′, having a lower solvus temperature. Alloys

"A uniform distribution of the precipitating phase improves significantly mechanical properties, such as the tensile strength, the fatigue lifetime, the creep rupture strength, etc."

	Ni	Cr	Al	Mo	Nb	Ti	Fe	Si	Zr	C	N	O	Cu	Mn	B
Spec. min	Bal	12.0	5.5	3.8	1.8	0.5	0.0	0.0	0.05	0.08	-	-	0.00	0.00	0.005
Spec. max		14.0	6.5	5.2	2.8	1.0	2.5	0.5	0.15	0.20	-	-	0.50	0.25	0.015
90% - 22 µm	Bal	12.5	5.7	4.2	2.1	0.8	0.5	0.2	0.11	0.10	0.04	0.014	0.01	0.01	0.008

Table 1 IN713C powder chemical specification and powder analysis (wt.%)

hardened through a γ″ strengthening phase have a rapid decrease in strength above 650°C, as it transforms to δ phase, and this limits the application temperature for IN718 to the low to intermediate temperature range. IN713C, which was developed in 1956 at Inco's US research laboratories, contains around 8% Al + Ti combined, leading to a high volume fraction of ordered γ′ -Ni_3(Al,Ti) as the major strengthening phase. This means that its service temperature extends to high operating temperatures in excess of 850°C.

This is an important consideration for components such as turbine wheels in gasoline turbochargers, which have to withstand temperatures above 1000°C, and thus IN713C is the preferred material for engine manufacturers. Cr and Al perform an important function in nickel superalloys, forming a protective, adherent oxide film on their surface comprising primarily Cr_2O_3 and Al_2O_3, respectively. This protective coating permits the use of nickel superalloys in a wide variety of applications that require resistance to aggressive high-temperature oxidising environments, to aqueous corrosion and sulphide attack. The oxidation rate is controlled by the diffusion of substrate elements in the alloy and the inward diffusion of oxygen through the porous oxide scale. Typically, two different types of alloys are distinguished: IN713C (Inconel 713 Carbon) with carbon contents in the range of 0.08 to 0.2 wt.% and IN713 LC (Inconel 713 Low Carbon) containing 0.03-0.07 wt.% carbon.

Processing routes

Investment casting, direct solidification, wrought, Powder Metallurgy via Hot Isostatic Pressing (HIP) and isothermal forging are often used to fabricate nickel superalloys [13–15], but can be costly. However, their high strength and hardness make them difficult to machine. Special equipment and experience for the machining itself are required. Therefore, any additional finishing step, especially for this class of material, should be avoided as part costs increase significantly. Besides, solidification in casting will easily create inhomogeneous elemental segregation and undesirable phases.

In order to overcome these limitations, an alternative process is MIM, which offers solutions to complex design geometries, minimum material loss, material variety, quick scale-up response time and significant cost reduction in large-scale industrial production. Components produced via MIM have a very homogeneous microstructure differing from investment casting components, owing to the finely dispersed powders used by MIM. Macrosegregation phenomena that occur during the solidification of high-strength nickel superalloys can be avoided. Moreover, unlike other powder metallurgical routes, it is not always necessary for MIM parts to be HIPed, since very high densities are already achieved in the as-sintered state. Therefore, MIM is one of the most promising and advantageous production routes for next-generation nickel superalloys, with geometrical near-net shape and homogeneous composition parts.

MIM materials

There is an increasing number of MIM materials for superalloys, such as IN713C (Inconel 713C) [16-24], Inconel 718 [16, 25-34], Hastelloy X [16, 26], Nimonic 90 [16], Inconel 100 [16, 19], Inconel 625 [26, 34], Inconel 706 [34], GMR-235 [16], Udimet 720 [18] , MAR-M 247 [19] and CM 247LC [33].These studies outlined some promising and successful results regarding superior mechanical properties at high temperatures, as well as good high-temperature oxidation behaviour. IN713C, among Ni-based superalloys, is one that possesses excellent mechanical properties and oxidation resistance at high temperatures. Investment cast IN713C is widely used in aircraft engines and gas turbines, albeit that casting is prone to defects and limits the section thickness that can be fabricated. This is one key reason to consider MIM processing of IN713C, which could offer homogeneous part properties

Powder Size	D10 [µm]	D50 [µm]	D90 [µm]	Apparent Dens [g/cm³]	Tapped Dens [g/cm³]	Pycno. Dens [g/cm³]
90% - 22 µm	6.1	12.1	21.5	3.30	4.55	7.8019

Table 2 Particle size distribution and density data for test powders (Malvern Mastersizer 2000)

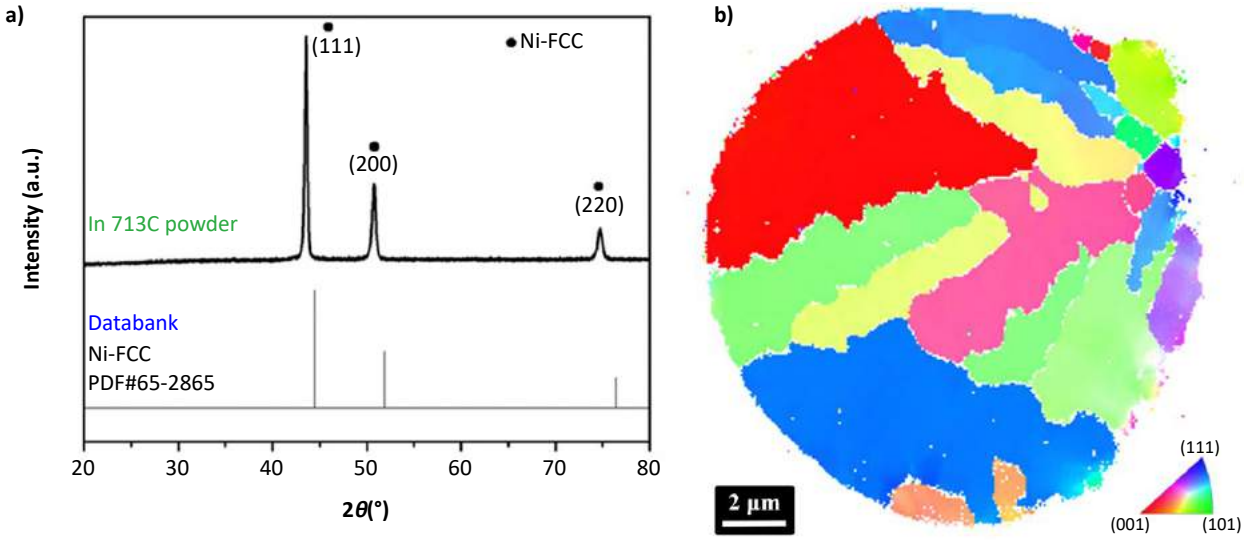

Fig. 3 90% - 22 µm IN713C powders (a) XRD patterns (b) EBSD Inverse Pole Figure (IPF) maps of FCC crystal structure

in thin-walled structures. Nickel superalloy powders for MIM are usually produced by argon inert gas atomisation to avoid oxidation of the alloy, because surface oxides would reduce the sintering activity leading to a lower density. A conventional argon gas atomisation process is usually preferred to minimise potential for reaction of N with Ti and Al, which could notionally reduce the volume fraction of γ′. In this article, an alternative atomisation of IN713C powders (nitrogen gas atomisation) will be explored and studied, especially in terms of high-temperature properties and microstructures, to assess the viability of a lower-cost powder feedstock for high-volume production, compared with the argon-atomised powder variant.

Experimental procedure

The IN713C pre-alloyed powder used in this study was manufactured by Sandvik Osprey using its proprietary gas atomisation technology. Powders were produced by the induction melting of raw materials and atomising using nitrogen. Feedstocks were compounded using a proprietary multi-component polyoxymethylene-based (POM) binder system using a Z-Blade mixer.

Tensile bar specimens were prepared by injection moulding under various conditions using a NISSEI NEX 50T machine. Moulded parts were then subject to a debinding process using a WINTEAM HT-220LTZL furnace in fuming nitric acid. Sintering trials were performed in a molybdenum line furnace using argon atmosphere with 5 K/min heating rate and a holding time of 3 h at the maximum temperature. In order to check the evolution of impurity element contents during Powder Injection Moulding and sintering processes, the chemical elements of C, N and O in raw powders and sintered parts were analysed by C/S analyser (EMIA-320V2, Horiba, Japan) and N/O analyser (EMGA-930, Horiba, Japan).

X-ray diffraction, XRD, (D2, Bruker, Karlsruhe, Germany) was applied for crystal structure identification. Element distribution was assessed via EPMA (JXA-8200SX, JEOL, Japan) with EDS (X-MAX 50, Oxford Instruments, UK). For morphological, microscopic and phase investigations, a FESEM (JSM-7800F Prime, JEOL, Japan) with electron backscatter diffraction (EBSD) detector (NordlysNano, Oxford Instruments, UK) was applied. Transmission Electron Microscopy, TEM (JEM-2100F, JEOL, Japan), with EDS (INCA X-sight, OXFORD, UK) was also applied.

IN713C powder characterisation

The chemical compositions of IN713C powder was measured via ICP and Leco analysis and is shown in Table 1. All measured values are within the theoretical ranges given for the IN713C composition.

Table 2 shows the particle size distribution data as measured via laser diffractometry (Malvern Mastersizer 2000). Also shown are apparent and tapped density values (ASTM B527). The corresponding microscopic morphology of cross section and appearance SEM images can be seen in Fig. 2.

The as-atomised IN713C powders' XRD pattern is shown in Fig. 3(a), which reveals the FCC crystal phase characteristics and a slight shift in 2 θ angle due to the effect of complex alloying (at least ten different elements) on the lattice constant. Fig. 3(b) shows the corresponding EBSD Inverse Pole Figure (IPF) maps of FCC crystal structure. As demonstrated, all the grains inside the IN713C powders are based on the FCC crystal structure and this result is in line with the XRD patterns aforementioned.

	Sintered density (g/cm³)	C (%)	O (%)	N (%)
Specification	-	0.08 - 0.20	Not specified	Not specified
1250°C - sintered	7.66 (96.5%)	0.12	0.0156	0.0172
1260°C - sintered	7.82 (98.6%)	0.13	0.0085	0.0095
1270°C - sintered	7.87 (99.2%)	0.13	0.0324	0.0096

Table 3 Sintered density of residue carbon, oxygen and nitrogen analysis

Results and discussion

Sintering results are summarised in Table 3. The density of the as-sintered parts was determined based on the Archimedes' immersion technique and it is shown to reach 96.5% of theoretical density when sintering takes place above 1250°C. The elemental analysis of the as-sintered part was within the theoretical specifications of the IN713C alloy. Tramp elements such as carbon, oxygen and nitrogen can play a critical role with regard to superalloy performance. The carbon specification is met by the standard. Nitrogen and oxygen are normally not specified; but it is evidently shown that the nitrogen is kept at quite low levels even though the raw IN713C powders are based on the nitrogen gas atomised route.

The progression of as-sintered microstructures, from 1250°C to 1270°C, was characterised by scanning electron microscopy (SEM) at high magnification in Fig. 4(a) to (c). These SEM images showed the white network-like γ continuous matrix with dark γ′ segregated precipitates embedded into the γ matrix. These images also confirmed the presence of a rather high volume fraction of cuboidal γ′ precipitates of approxi-

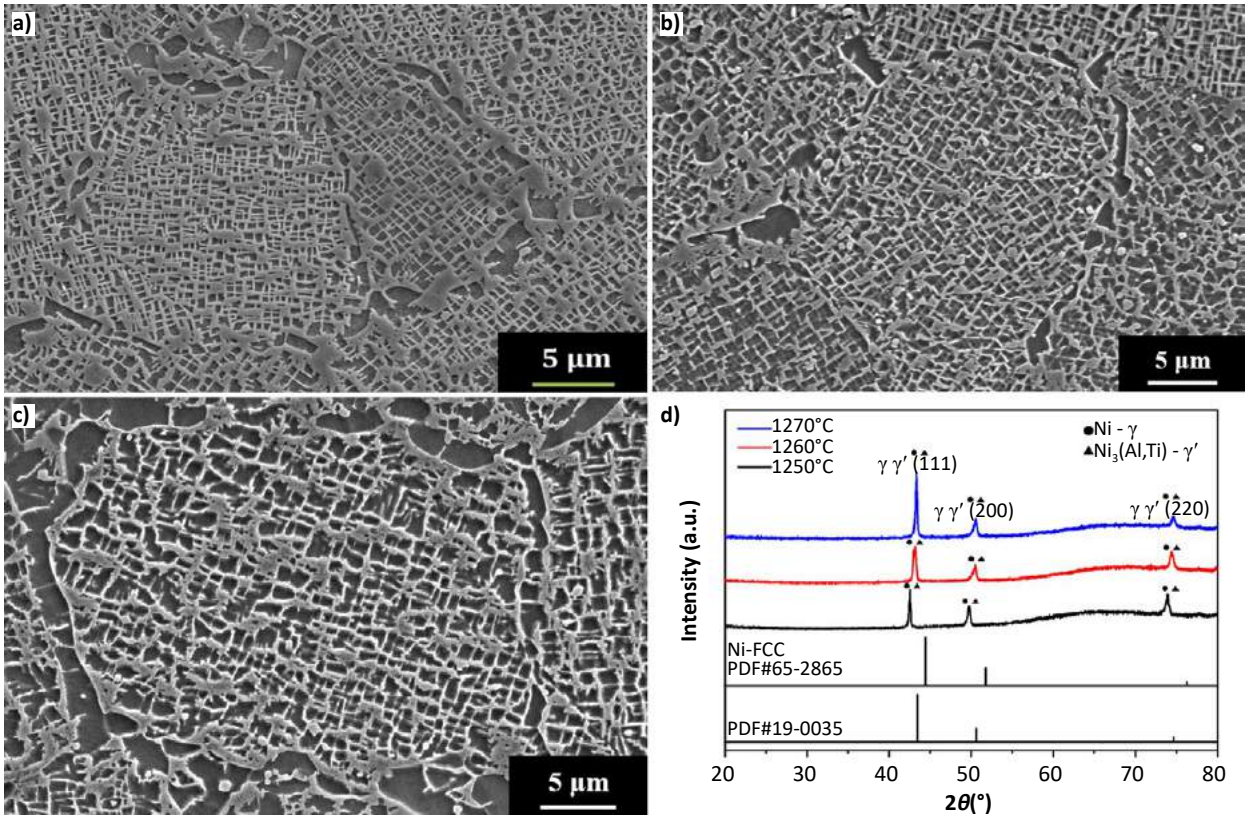

Fig. 4 (a) SEM image of 1250°C - sintered part, (b) SEM image of 1260°C - sintered part, (c) SEM image of 1270°C - sintered part, (d) XRD pattern for three sintered conditions

Composition (at %)	Ni	Cr	Al	Mo	Fe	C	Nb	Ti	Si	Zr	N
γ phase	66.77	16.53	8.98	3.35	0.97	0.35	1.56	0.99	0.48	0.02	0
γ′ phase	70.88	7.69	16.05	1.39	0.58	0.49	1.24	1.33	0.29	0.01	0

Table 4 EPMA quantitative composition analysis of γ and γ′ based on 1260°C - sintered condition

mate 0.5 μm size in the as-sintered state. Around the grain boundaries, coarser γ′ precipitates, 1 to 3 μm in size, are observed, confirming that nucleation and grain growth behaviour are more intensive at high angle grain boundaries. The crystal structure of the γ and γ′ phases in the sintered parts was identified by XRD as shown in Fig 4(d). Their diffraction peaks overlap and are indistinguishable since both γ and γ′ have an FCC structure with almost the same lattice constant (approximately 3.52 to 3.58 Å). As for the γ /γ′ interface coherency, we cannot precisely judge this from only XRD information due to the similar lattice constants. What we can conclude from XRD analysis is that γ′ might be either coherent or semi-coherent with respect to γ phase at the interface, rather than incoherent. γ /γ′ interface coherency will be further examined and discussed via High-Resolution Transmission Electron Microscope (HRTEM) analysis in the future. Besides, XRD analysis cannot exactly judge presence of carbides, since their volume fraction in the matrix is quite low.

The Electron Probe Micro Analyser (EPMA) quantitative chemical composition of 1260°C-sintered γ and γ′ is listed in Table 4. Cr, Mo and Fe are relatively higher in the γ phase, whereas Al and Ti are relatively high in the γ′ phase, which is in line with the literature, since Al and Ti are both essentially chemical elements for γ′-Ni_3(Al,Ti) formation. Other elements, such as Cr, Fe, Ni, and Mo will also enter into the γ′ phase.

EPMA and Energy-Dispersive X-ray Spectroscopy (EDS) elemental mapping are shown in Fig. 5 and Fig. 6, respectively. As shown, Cr, Fe and Mo amounts are relatively higher in γ phase, while Al, Ti and Ni amounts are higher in γ′ phase. This result is consistent with the EPMA quantitative chemical composition analysis shown in Table 4. We can also observe that the 0.2 to 0.4 μm spherical precipitates are based on C, Ti, Nb, and Mo abundant metal carbide. The exact structure is discussed later.

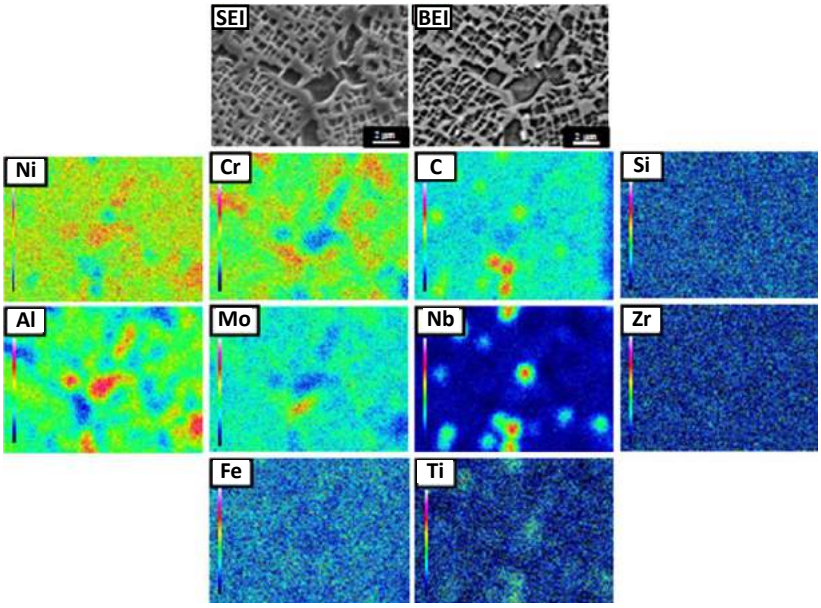

Fig. 5 EPMA elemental mapping based on 1260°C - sintered condition

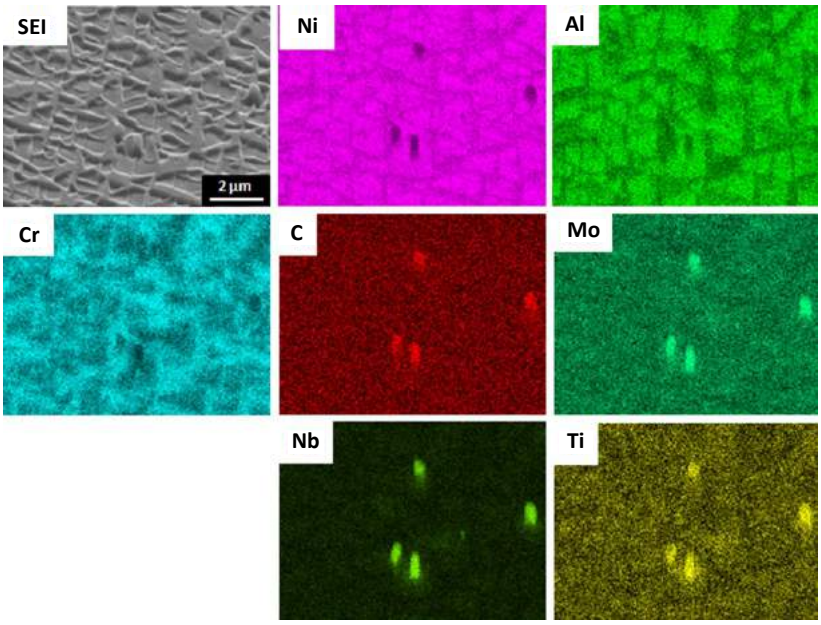

Fig. 6 EDS elemental mapping based on 1260°C - sintered condition

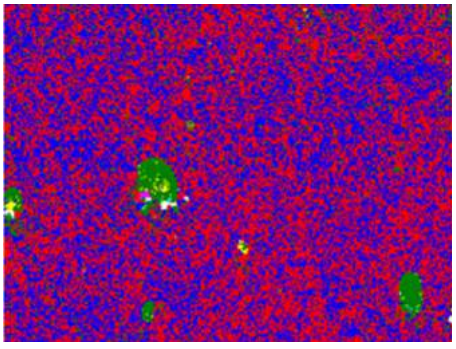

Phase	Fraction (%)
γ	47.55
γ′	45.78
MC	4.59
M_6C	0.03
M_7C_3	0.02
$M_{23}C_6$	0.02
MN	0.05
M_2N	0.05
Zero solution	1.82

Fig. 7 EBSD phase mapping image based on 1260°C - sintered condition

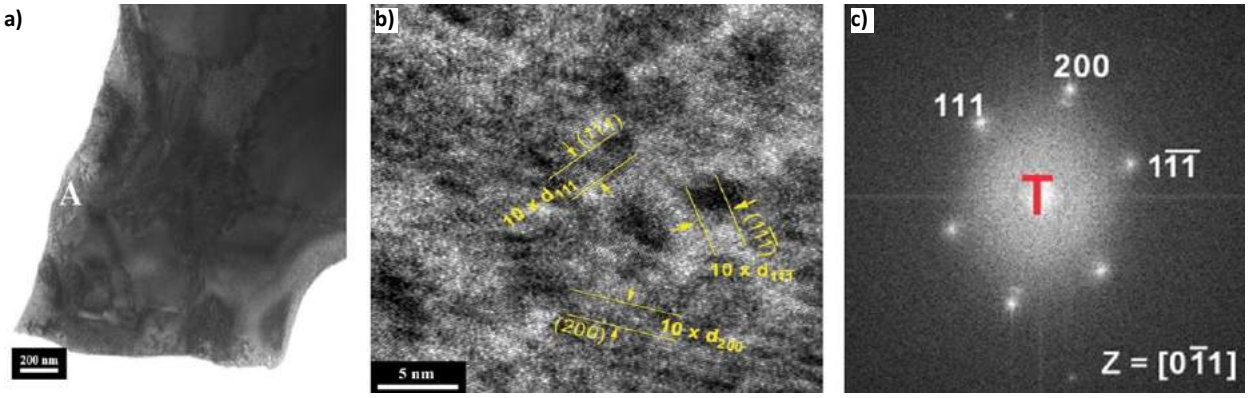

Fig. 8 HRTEM analysis of γ phase based on 1260°C - sintered condition (a) Bright field (b) High resolution image (c) Fast Fourier Transform, FFT

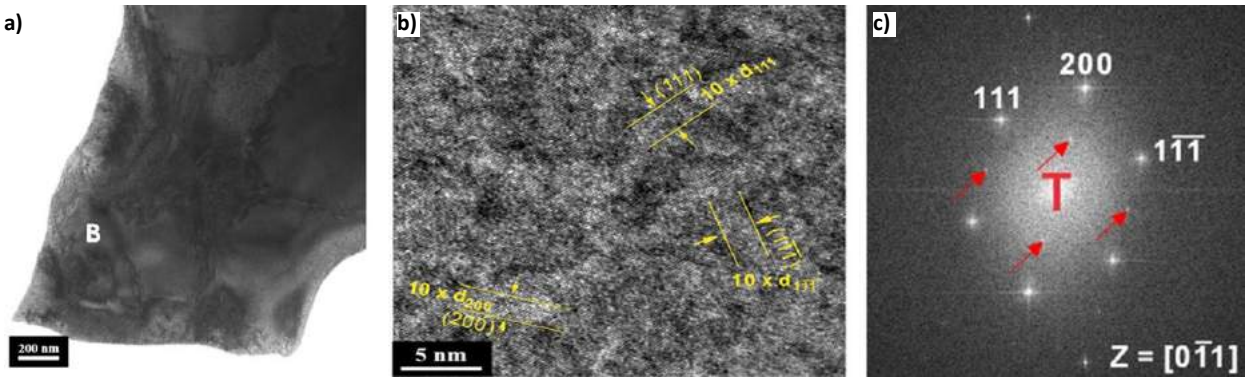

Fig. 9 HRTEM analysis of γ′ phase based on 1260°C - sintered condition (a) Bright field (b) High resolution image (c) Fast Fourier Transform, FFT

The EBSD phase mapping image based on 1260°C - sintered part is shown in Fig. 7. γ and γ′ phase identification is just for arbitrary reference since their lattice constants are quite similar and difficult to precisely verify via EBSD analysis. Nevertheless, this structure was confirmed by backscattered electron images (BEI), discussed earlier. In future, HRTEM analysis will be carried out to confirm and discuss in depth.

From SEM, EPMA and EDS mapping, we found that some dispersed spherical particles are based on Ti, Nb, and Mo abundant metal carbide, as shown in Fig. 5 and Fig. 6, respectively. From current EBSD mapping as a complementary tool, we can therefore judge that this carbide is based on the MC structure, that is, (Ti, Nb, Mo) C. Alongside the primary MC metal carbide, other M_6C, M_7C_3, $M_{23}C_6$ secondary carbides are not detected in 1260°C -sintered EBSD mapping. Similar results are also confirmed in 1250°C and 1270°C - sintered EBSD analysis. This implies that MC is stable during 1250°C to 1270°C sintering conditions, without further transformation into other M_6C, M_7C_3, $M_{23}C_6$ secondary carbides.

> *" ...nitride compounds, such as MN and M_2N are virtually absent in the sintered parts despite the fact that powders used in this study were made using a nitrogen gas atomisation process..."*

Because M_6C or $M_{23}C_6$ carbides contain large amounts of Cr, it is believed that the areas around these carbides are locally depleted of chromium and act as initiation zones for stress-corrosion cracking. MC carbides act as pinning agents (Zener pinning effect) [35–44] that delay significant grain growth during the sintering process. This is consistent with the microstructural images as revealed in Figs. 4(a)-(c). Furthermore, nitride compounds, such as MN and M_2N are virtually absent in the sintered parts despite the fact that powders used in this study were made using a nitrogen gas atomisation process. This was achieved by

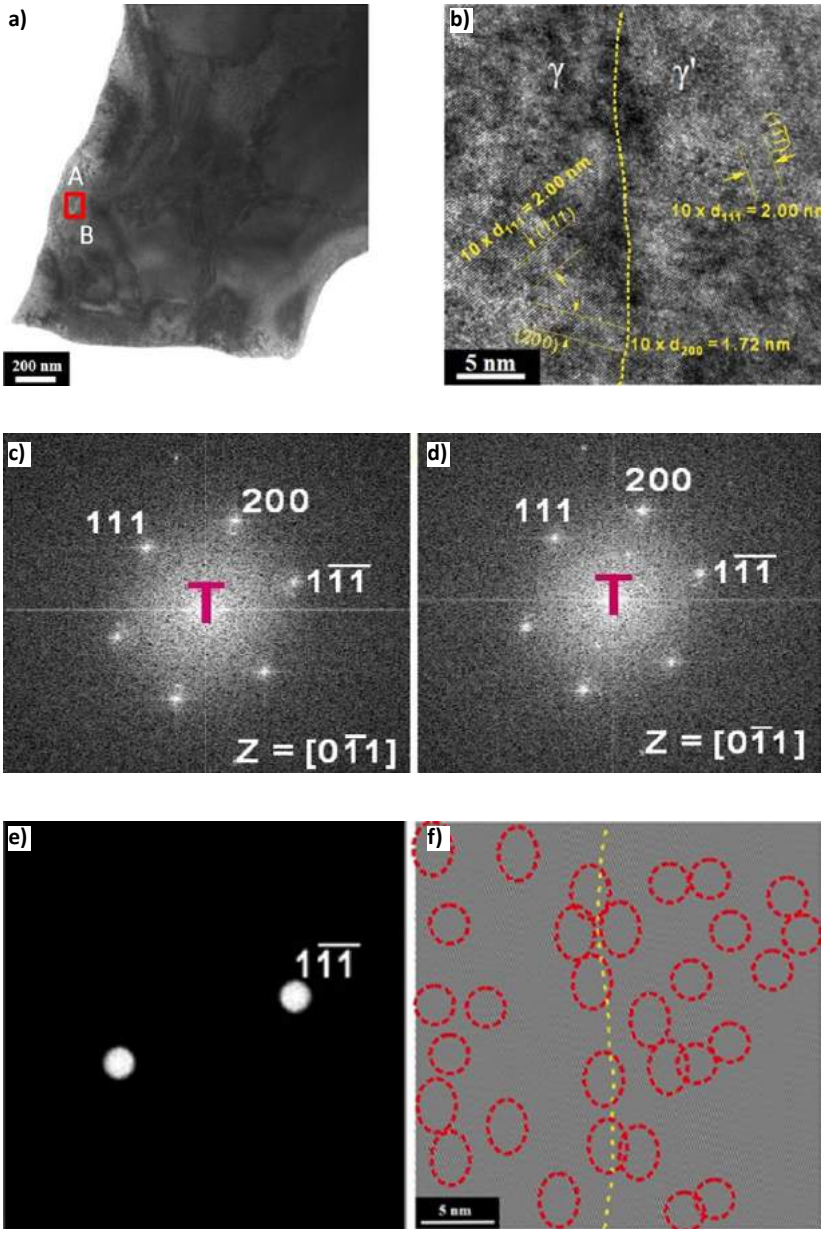

Fig. 10 HRTEM analysis of γ /γ′ interface based on 1260°C - sintered condition (a) Bright field (b) High resolution image (c) FFT of left hand side of Fig. 9(b) γ phase (d) FFT of right hand side of Fig. 9(b) γ′ phase (e) Diffraction vector, g = (1$\bar{1}\bar{1}$) (f) Inverse FFT Image, g = (1$\bar{1}\bar{1}$)

controlling impurity nitrogen content at quite low levels, using Sandvik Osprey's proprietary gas atomisation technology.

γ and γ′ phases could be identified and distinguished via HRTEM analysis, as shown in Fig. 8 and Fig. 9, respectively. As revealed in Fig. 9, zone B is identified as γ′ phase since it has a superlattice, identified from a Fast Fourier Transform (FFT) image. Instead, zone A in Fig. 8 does not have this characteristic and thus, in turn, is recognised as γ phase. As for the interface coherency between zone A (γ phase) and zone B (γ′ phase), shown in Fig. 10, based on the inverse FFT image of (1$\bar{1}\bar{1}$) reflection, some dislocations (as marked in the red circle) are observed near the γ / γ′ interface and it is rational to classify this type as a semi-coherent γ / γ′ interface.

The isothermal oxidation behaviour of 1260°C - sintered IN713C specimens was investigated in the temperature interval from 900°C to 1100°C for 100 h. Table 5 and Fig. 11 show that a homogeneous and

Oxidation Temperature (°C)	Percentage of weight gain (wt.%)
900	1.12
1000	1.46
1100	1.78

Table 5 Weight gain behaviour of 1260°C - sintered part for 100 h oxidation at various temperatures

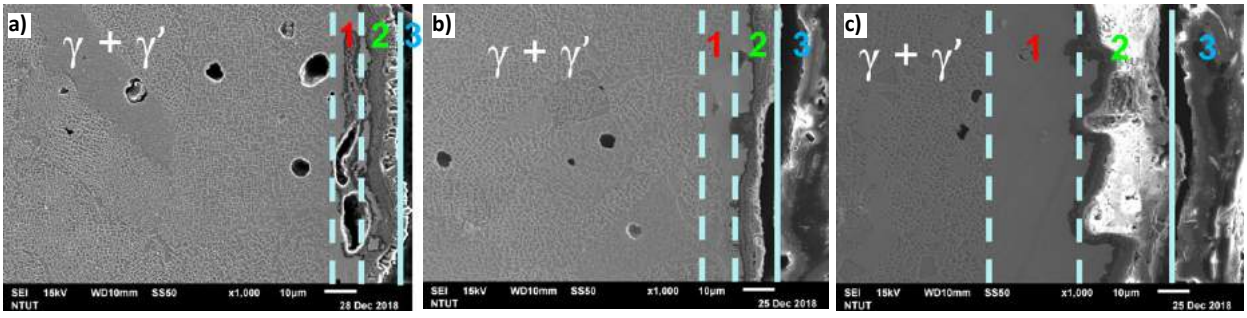

Fig. 11 SEM images after thermal oxidation, based on 1260°C - sintered part: (a) 100 h at 900°C ; (b)100 h at 1000°C ; (c) 100 h at 1100°C; Zone 1: γ′ depletion zone; Zone 2: oxide layer; Zone 3: bakelite mount

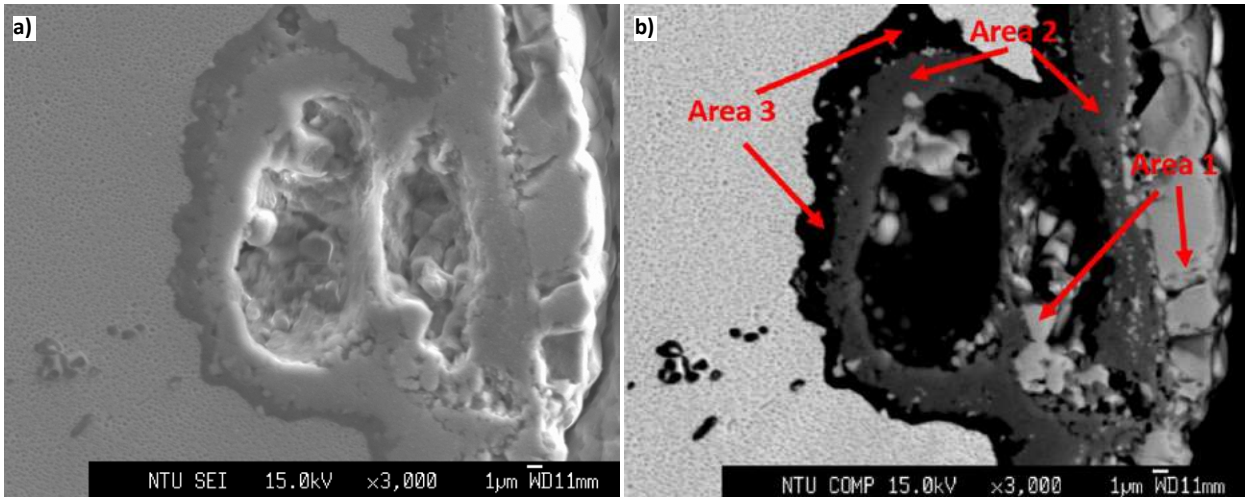

Fig. 12 (a) Microstructure of 1260°C -sintered part after 100 h oxidation at 1100°C Secondary Electron Image, SEI (b) Backscattered Electron Image, BEI from outer to inner layer sequence: area 1, area 2 and area 3

Composition (at%)	Area 1	Area 2	Area 3
Ni	52.86	13.73	0.85
Cr	0.24	1.23	0.15
Al	0.15	29.78	38.96
Ti	0.10	0.06	0.04
O	46.65	55.20	60.00

Table 6 EPMA quantitative analysis of area 1,2 and 3 as indicated in Fig. 12

slow-growing oxide layer occurred at 1000 to 1100°C. Analysis of oxidised samples was also conducted by SEM, EPMA, XRD and EBSD, as shown in Figs. 12 5 respectively. These results indicated that the presence of three distinct oxide layers are evident (from inner to outer oxide layer): inner layer is Al_2O_3; middle layer is a mixed oxide scale containing TiO_2 and spinel $NiAl_2O_4$, followed by NiO as the outer layer. Beneath the Al_2O_3 layer, a γ′ –depletion zone (precipitation free zone, PFZ) occurs, due to loss of Al from γ′- Ni_3(Al,Ti) precipitates, diffusing to the surface during the formation of Al_2O_3 as explained by Gesmundo and Gleeson [45]. If the depletion zone becomes too thick, the diffusion length for Al to diffuse to the surface to form Al_2O_3

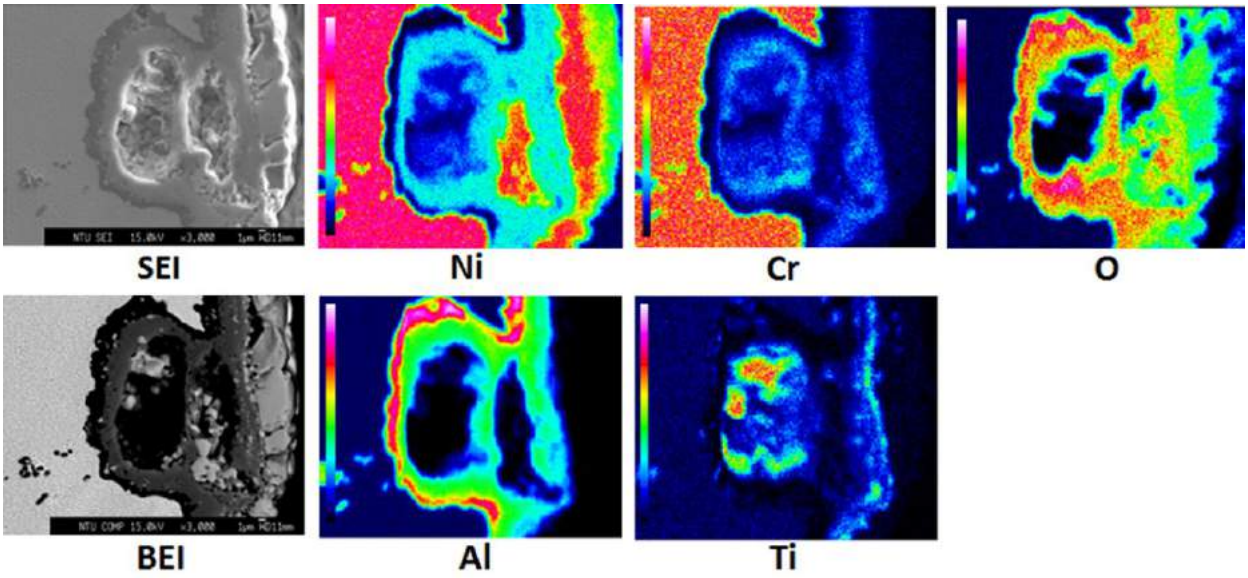

Fig. 13 EPMA qualitative analysis of 1260°C - sintered part (100 h oxidation at 1100°C)

increases. After long oxidation periods, the protective oxide layer can no longer be formed and the alloy fails. Without γ′ precipitates in the outer region of the sample, the alloy loses high temperature and creep strength [22].

Specimens sintered at 1260°C and 1270°C had been tensile tested at high temperature for ultimate tensile strength (UTS) and elongation measurement, as shown in Fig. 16 and Fig. 17, respectively. Fig. 16 showed that, for UTS performance, the 1260°C - sintered part is almost the same as 1270°C - sintered part from low to high temperatures and we also compared these results with other MIM data reported [18, 20-21]. Fig. 17 also showed the comparison of elongation values for this study with other MIM data reported [18, 21] , along with conventional cast process data for IN713C. As for elongation, a 1260°C - sintered part gives better values compared with a 1270°C - sintered part, due to slight coarsening in grain size for the 1270°C - sintered part, as outlined earlier in the SEM discussion. Furthermore, the 1260°C - sintered part is almost comparable with the cast grade.

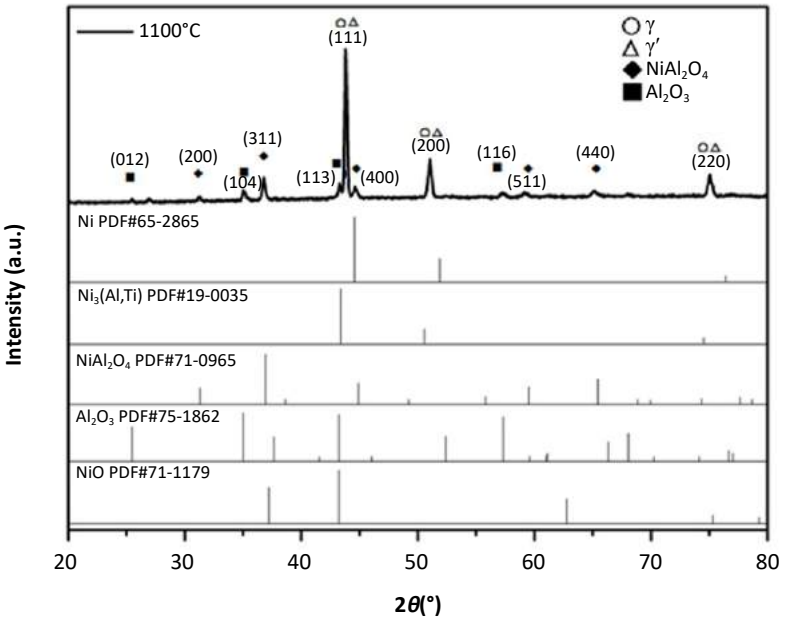

Fig. 14 XRD patterns of 1260°C - sintered part (100 h oxidation at 1100°C)

Summary and conclusions

In this investigation, a nitrogen gas atomised 90% -22 µm IN713C pre-alloyed powder has been successfully processed by metal injection moulding to characterise its microstructure and high temperature performance. The as-atomised powders' XRD and EBSD phase mapping demonstrated that the FCC crystal structure exists in the as-atomised state. The elemental analysis of the as-sintered composition was within the theoretical specification of the IN713C alloy. The as-sintered condition showed that 96.5% relative density can be reached

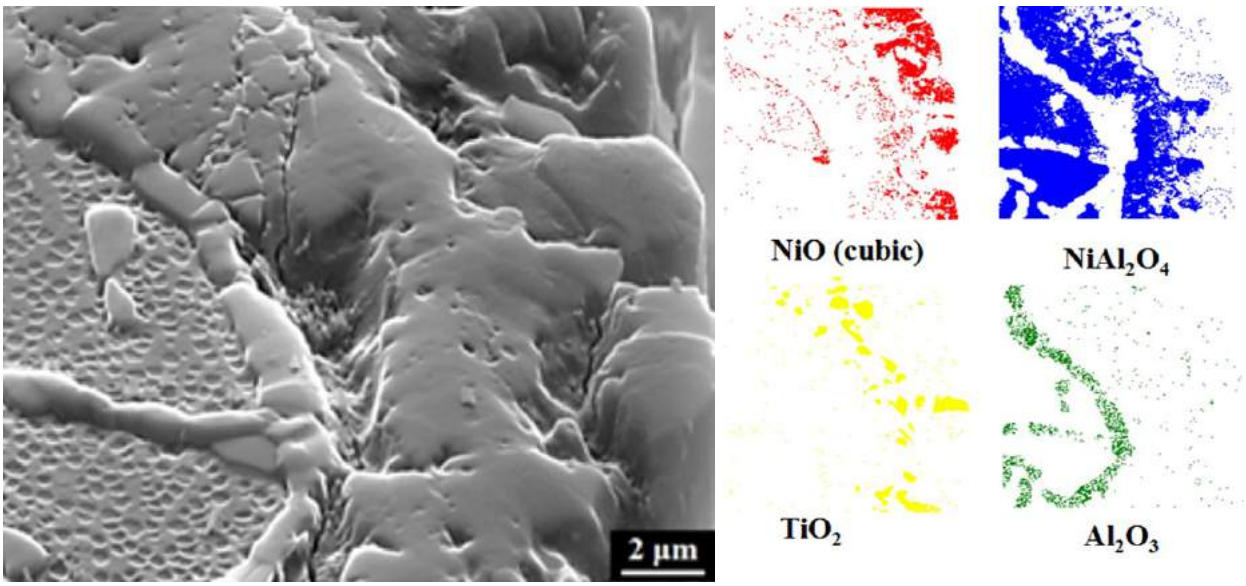

Fig. 15 EBSD phase mapping of 1260°C - sintered part (100 h oxidation at 1100°C)

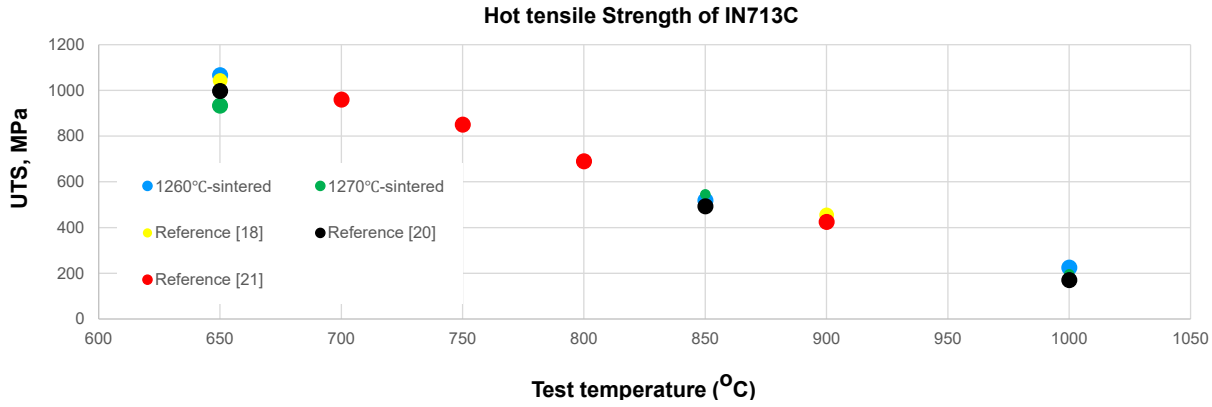

Fig. 16 Hot tensile strength of 1260°C - sintered and 1270°C - sintered IN713C

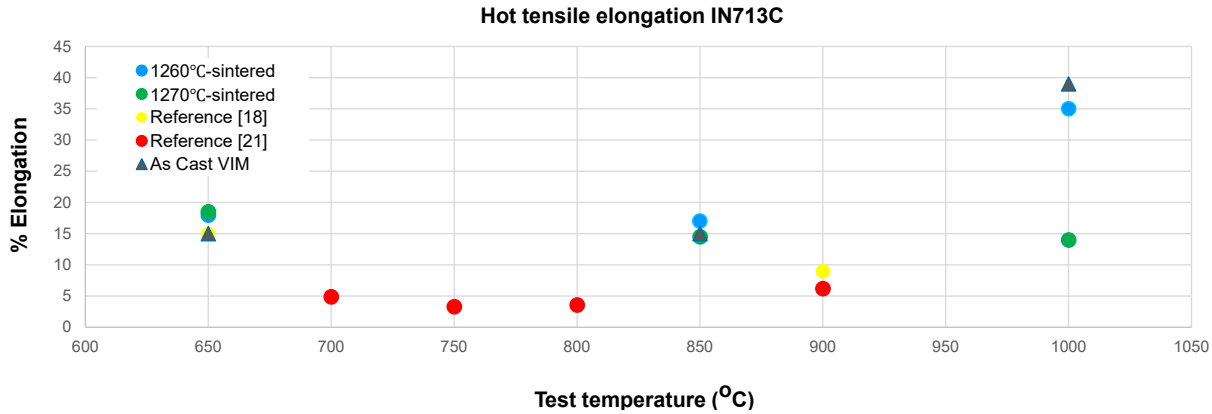

Fig. 16 Hot tensile elongation of 1260°C - sintered and 1270°C - sintered IN713C

by sintering above 1250°C. A good microstructure and a high density was reached within 1250°C to 1270°C sintering range and grain coarsening/growth is not so intensive within this temperature range, due to some MC carbide particles dispersed in the matrix, which followed the Zener pinning effect. SEM images showed the white network-like γ matrix phase and dark γ′ segregated precipitates surrounded by the white network. The images also confirmed the presence of a rather high volume fraction of cuboidal γ′ precipitates of around 0.5 μm in size in the as-sintered condition. These two phases form a semi-coherent interface, as deduced from HRTEM analysis. Besides, the residual carbon, oxygen and nitrogen after sintering could be controlled at quite low levels.

Besides this primary MC metal carbide structure, other M_6C, M_7C_3 or $M_{23}C_6$ secondary carbides are not detected from 1250°C to 1270°C, as indicated from EBSD phase mapping. This implied that MC is stable during 1250°C to 1270°C sintering conditions, without further transformation into other M_6C, M_7C_3 or $M_{23}C_6$ secondary carbides. Nitride compounds, such as MN and M_2N, are almost nonexistent in the sintered parts, even after we applied a nitrogen gas atomisation process to prepare the raw alloy powders in this study. This is due to the fact that the impurity nitrogen content was controlled at quite a low level using Sandvik Osprey's proprietary gas atomisation technology.

Also, in this work, the oxidation behaviour of IN713C, produced using nitrogen atomised MIM powders, is investigated in the temperature range of 900°C to 1100°C for 100 h duration. Microstructure analysis indicated three distinct oxide layers (in order from inner to outer oxide layer): Al_2O_3, a mixed oxide scale containing TiO_2 and spinel $NiAl_2O_4$, followed by NiO as the outer layer. For hot tensile strength and elongation results, the performance is even better than other MIM data reported. These results confirm this nitrogen-atomised based MIM route as an excellent choice for the production of advanced industrial components. Since the nitrogen gas atomisation process is relatively cost effective compared with conventional argon atomising, this study provides a promising and viable alternative for MIM material choice with improved, competitive solutions for next generation high temperature applications in automobiles, aero engines or stationary gas turbines.

Acknowledgements

The authors gratefully acknowledge Chenming Electronic Technology Corp. (UNEEC) and Sandvik Osprey

Ltd. We are thankful to all R&D centre colleagues, for sharing their pearls of wisdom during this research, assisting us at every point and, without whom, this task would not have been possible to accomplish.

Authors

Shu-Hsu Hsieh, Chung-Huei Chueh and I-Shiuan Chen
Chenming Electronic Technology Corp. (UNEEC),
2F, No. 27, Sec. 6, Minquan E. Rd.,
Neihu Dist., Taipei City 114,
Taiwan

Martin A Kearns, Paul A Davies, Keith Murray, Mary-Kate Johnston and Szymon Kubal
Sandvik Osprey Ltd.
Red Jacket Works, Milland Road,
Neath, SA11 1NJ
United Kingdom

References

[1] R.M. German, K.F. Hens: *Ceram. Bull.*, 1991, vol. 70, no. 8, pp. 1294–1302.

[2] R.M. German: *Powder Metall. Int.*, 1993, vol. 25, no. 4, pp. 165–169.

[3] K.M. Kulkarni: *Met. Powder Rep.*, 2000, vol. 55, no. 10, pp. 40 – 42.

[4] C. Ballard, M. Zedali: *Advances in powder injection molding, in: Annual Technical Conference–ANTEC*, Conference Proceedings, 1998, vol. 1, pp. 358–361.

[5] A. Hauck: *Int. J. Powder Metall.*, 2000, vol. 36, no. 3, pp. 29 – 30.

[6] R.M. German: *Int. J. Powder Metall.*, 2000, vol. 36, no. 3, pp. 31 – 36.

[7] H.O. Gulsoy, S. Ozbek & T. Baykara: *Powder. Metall.*, 2007, vol. 50, no. 2, pp. 120 - 126.

[8] S. Zhao, X. Xie, G.D. Smith, S.J. Patel: *Mater. Lett.*, 2004, vol. 58, pp. 1784 – 1787.

[9] H.Y. Li, X.P. Song, Y.L. Wang, G.L. Chen: *J. Iron Steel Res.*, 2009, vol. 16, pp. 81 – 86.

[10] S. Tian, X. Ding, Z. Guo, J. Xie, Y. Xue, D. Shu: *Mater.Sci. Eng A.*, 2014, vo. 594, pp. 7 – 16.

[11] K. Fuwei, C. Fuyang, Z. Xuemin, Y. Hongyan, F. Yicheng: *Rare Met. Mater. Eng.*, 2015, vol. 44, pp. 2965 – 2970.

[12] F.S. Qu, X.G. Liu, F. Xing, K.F. Zhang: *Trans. Nonferrous Met. Soc. China.*, 2012, vol. 22, pp. 2379 – 2388.

[13] F. Zupanic, T. Boncina, A. Krizman, F.D. Tichelaar : *J. Alloy. Compd.*, 2001, vol. 329, pp. 290 – 297.

[14] L. Chang, W. Sun, Y. Cui, R. Yang: *Mat. Sci. Eng. A.*, 2017, vol. 682, pp. 341 – 344

[15] M. Lachowicz, W. Dudzinski, K. Haimann, M. Podrez-Radziszewska: *Mater. Sci. Eng A.*, 2008, vol. 479, pp. 269–276.

[16] H. Wohlfromm, A. Ribbens, J. ter Maat, M. Blömacher: *Proc. Euro PM*, 2003, vol. 2003, pp. 207 – 215.

[17] D. Martischius, H. Wohlfromm, A. Kern, M. Blömacher, J. ter Maat, A.Thom, M. Blömacher: *PIM Int.*, 2009, vol. 3, no. 2, pp. 37 – 42.

[18] B. Klöden, U. Jehring, T. Weißgärber, B. Kieback, I. Langer, R.W.-E. Stein: *PIM Int.*, 2010, vol. 4, no. 4, pp. 63 – 67.

[19] A. Kern, M. Blömacher, J. ter Maat, A.Thom: *Metal Powder Report*, 2011, vol. 66, issue 2, pp. 22 – 26

[20] N. Salk, S. Schneider: *PIM Int.*, 2011, vol. 5, no. 3, pp. 45 – 48.

[21] K.S. Kim, K.A. Lee, J.H. Kim, S.W. Park, K.S. Cho : *Adv. Mater. Res.*, 2013, vol. 602 - 604, pp. 627 – 630

[22] B. Albert, R. Völkl, U. Glatzel : *Metall. Mater. Trans. A.*, 2014, vol. 45, pp. 4561 – 4571.

[23] H. Shinya, F. Kazushige, O. Ryutaro, N. Yoshimichi, I. Kenichiroh: *Proc. World PM 2018*, Beijing, China, 2018, pp. 586 – 591.

[24] S.F. Chen, C.K. Yao, W.P. Huang, H.L. Lee: *Proc. World PM 2018*, Beijing, China, 2018, pp. 677 – 682.

[25] A. Bose, J.J. Valencia, J. Spirko, and R. Schmees: *Adv. Powder Metal. Part. Mater.*, 1997, vol. 3, pp. 18.99 – 18.112.

[26] J.L. Johnson, L.K. Tan, P. Suri, R.M. German: *Adv. Powder Metal. Part. Mater.*, 2004, vol. 1, pp. 4.89 – 4.101.

[27] P.A. Davies, G.R. Dunstan, R.I.L. Howells, and A.C. Hayward: *Met. Powder Rep.*, 2004, vol. 59, pp. 14 – 19.

[28] H. Miura, H. Ikeda, T. Iwahashi, T. Osada: *PIM Int.*, 2010, vol. 4, no. 4, pp. 68 – 70.

[29] E.A. Ott, M.W. Peretti: *JOM.*, 2012, vol. 64, no. 2, pp. 252 – 256.

[30] Ö. Özgun, H. Ö. Gülsoy, R. Yilmaz and F. Findik: *J. Alloy. Compd.*, 2013, vol. 576, pp. 140 – 153.

[31] A.T. Sidambe, F. Derguti, A.D. Russell, I. Todd: *PIM Int.*, 2013, vol. 7, no. 4, pp. 81 – 85.

[32] I. Shuji, S. Shigeyuki, T. Nobuyasu, Y. Takashi, S. Masayuki: *IHI Engineering Review.*, 2014, vol. 47, no. 1, pp. 44 – 48.

[33] A.Meyer, E. Daenicke, K. Moor, S. Müller, I. Langer, R.F. Singer: *Powder Metall.*, 2000, vol. 36, no. 3, pp. 29 – 30.

[34] J.J. Valencia, T. McCabe, K. Hens, J.O. Hansen, and A. Bose: *in Superalloys 718, 625, 706 and various Derivatives*, E.A. Loria, ed., TMS, Warrendale, PA., 1994, pp. 935 – 945.

[35] D.Turnbull: *Trans ASME.*, 1951, vol. 191, pp. 661 – 665.

[36] T.Nishizawa: *Tetsu-to-Hagane.*, 1984, vol. 70, pp. 1984 – 1992.

[37] M.Hillert: *Inst Met.*, 1968, pp. 231 247.

[38] CS. Smith: *Trans AIME.*, 1948, vol. 175, pp. 15 – 51.

[39] T.Nishizawa, I.Ohnuma, K.Ishida: *Mat Trans JIM.*, 1997, vol. 38, pp. 950 – 956.

[40] T.Gladman: *Proc Roy Soc A.*, 1966, vol. 294, no. 1438, pp. 298 – 309.

[41] M.Hillert: Acta Metal., 1988, vol. 36, pp. 3177 – 3181.

[42] O.Hunderi, N.Ryum: *Acta Metal Mater.*, 1992, vol. 40, pp. 543 – 549.

[43] DJ. Srolovitz, MP.Anderson, GS.Grest, et al : *Acta Metall.*, 1984, vol. 32, pp. 1429 – 1438.

[44] MP.Anderson, GS.Grest, RD.Doherty, et al: *Scripta Metal.*, 1989, vol. 23, pp. 753 – 758.

[45] F. Gesmundo and B.Gleeson: *Oxid.Met.*, 1995, vol. 44, pp. 211– 237.

WorldPM2020 / MonTreaL

World Congress on Powder Metallurgy & Particulate Materials

Montréal / June 27–July 1, 2020 / Visit WorldPM2020.org

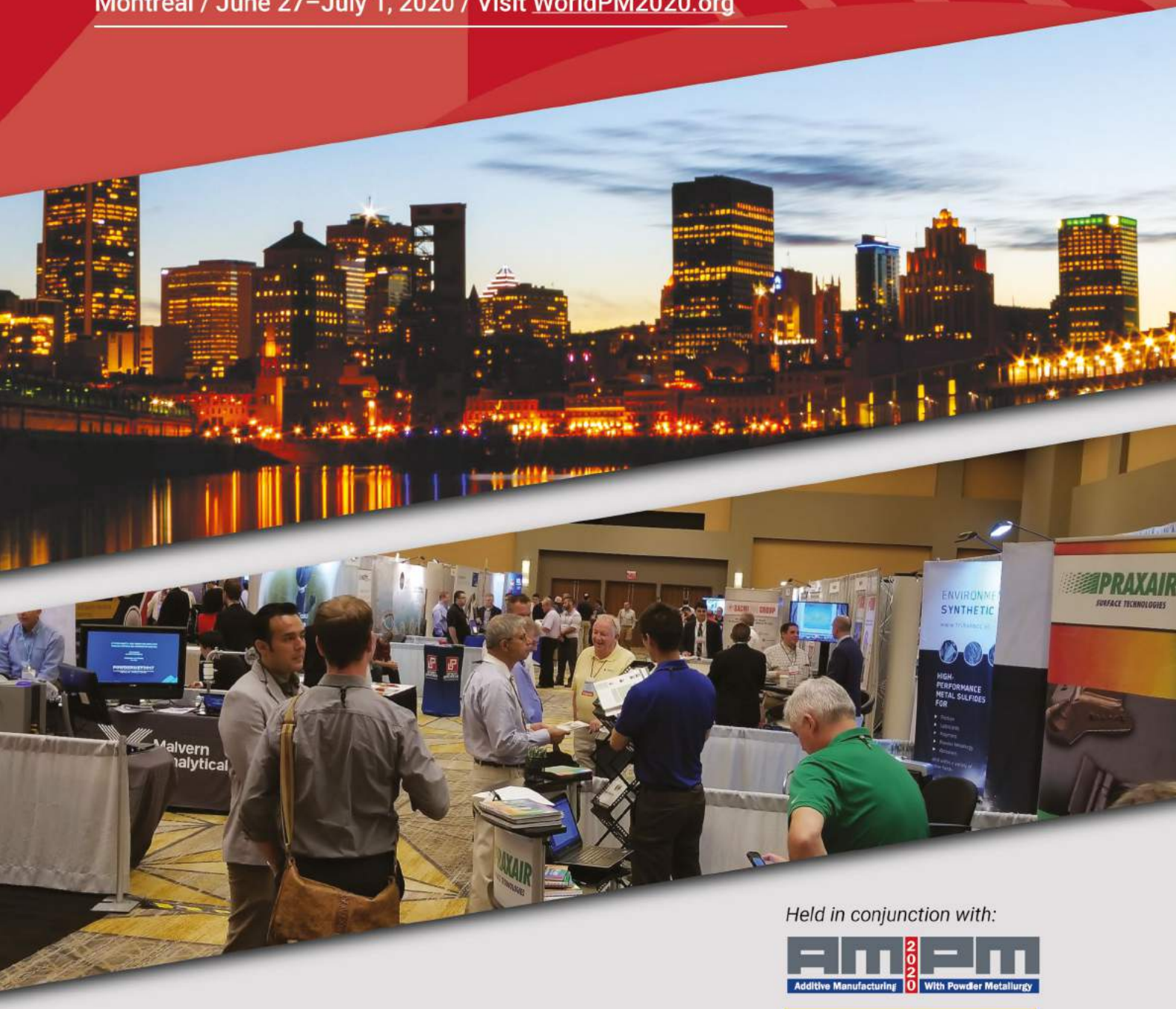

Held in conjunction with:

AM2PM 2020 Additive Manufacturing With Powder Metallurgy

Nb Mo Hf W Ta Ir Re Os
Tungsten, Refractory & Hardmaterials Conference

Metal Powder Industries Federation
APMI International

Euro PM2019: Innovations in Powder Injection Moulding process simulation and control

A technical session at the Euro PM2019 Congress, organised by the European Powder Metallurgy Association (EPMA) and held in Maastricht, the Netherlands, October 13–16, 2019, focused on aspects of process control, including process simulation, in Powder Injection Moulding. The session programme consisted of a number of papers from international academia and industry, looking at key areas such as numerical simulation and analysis with regard to sintering, debinding and other steps in the PIM process. Dr David Whittaker reports on behalf of *PIM International*.

Debinding and sintering investigations using optical dilatometry in combination with finite element analysis

A paper from Holger Friedrich, Heiko Ziebold and Friedrich Raether, of the Fraunhofer-Centre for High Temperature Materials and Design, Germany, reported on debinding and sintering investigations using optical dilatometry in combination with finite element analysis [1]. Powder-based processes such as Metal Injection Moulding, press & sinter Powder Metallurgy, and Additive Manufacturing processes such as Binder Jetting (BJT), all involve producing a preform consisting of the metal powder and organic process additives (binder). In these processes, the binder has to be removed before the green part is sintered. In the case of MIM, where binder contents of more than 40 vol.% are common, a two-step-process has been established. In the first step, part of the binder is removed by dissolution or chemical attack. In the next step of the debinding process, the residual binder is thermally pyrolysed. For BJT or pressed parts, where the binder content is much lower (< 5 vol.%), only thermal debinding is sufficient. During pyrolysis, the component is heated above the decomposition temperature of the organics, usually below 500°C. Depending on the chemical composition and the decomposition conditions (temperature and atmosphere), the binder is transformed into volatile species and residual carbon. The volatile products have to be transported from the origin of decomposition through the porous network to leave the compo-

Fig. 1 The EPMA's Euro PM congress and exhibition series is firmly established as the leading European technical conference on PM, MIM and metal AM (Photo Andrew McLeish / EPMA)

nent. Depending on permeability and the rate of gas formation, high local pressure can build up, which might lead to blistering or crack formation. Additionally, thermal gradients can lead to critical stresses. In order to avoid such detrimental effects, systematic optimisation of heating cycles is helpful. In order to obtain optimised cycles, a combined approach of precise experimental methods and finite element simulation, completely based on measurement data, has been developed. This approach has been successfully applied in several studies, showing that a prevention of defect formation and a significant reduction of debinding time and energy consumption can be achieved.

The experimental work reported in this paper included the determination of the debinding kinetics and measurement of the gas permeability and thermal diffusivity, which change during the progress of binder decomposition. In order to consider heat and gas formation, the exothermic and endothermic effects during binder decomposition, as well as the types of gases that are formed, were measured using differential scanning calorimetry and mass or FTIR spectroscopy. These data were then used to simulate the development of temperature, pressure and resulting stresses as well as the degree of conversion during a given time-temperature-profile. As a first iteration, conditions for constant debinding rates were determined using the so-called kinetic-field approach. As mass loss is usually not a linear function of temperature, more complex heating programs were necessary. In the next step, FE analysis was used to adapt this approach to larger components or higher amounts of binder, where heat transfer influences temperature distribution and thus the progress of binder decomposition, including gas formation. As a further refinement, the effects of heat transfer to the components via the atmosphere and kiln furniture, as well as the effects of the surrounding atmosphere (e.g. flow rate), can be integrated in the FE simulation, in order to account for the effects of real furnace conditions.

After debinding, consolidation of the powder compact is achieved in a sintering step. The sintered product should show a minimum of geometric distortion, a homogeneous microstructure with the desired amount of porosity and be free of flaws. In powder metal sintering, the small temperature interval between the onset of densification and deformation due to increased creep requires a well-defined heating profile.

Similarly to the case of debinding, a kinetic approach has been pursued in order to describe and simulate the sintering process. The experimental input was based on shrinkage data, viscous properties and thermal diffusivity. In the case of shrinkage, high accuracy and reproducibility were required. These data were obtained using special furnaces, called thermo-optical measurement (TOM) devices.

"In order to obtain optimised cycles, a combined approach of precise experimental methods and finite element simulation, completely based on measurement data, has been developed. This approach has been successfully applied in several studies..."

Two different TOM-devices have been installed to characterise the sintering behaviour of powder-metals: TOM_ac and TOM_metal. Both devices use graphite heated furnaces for sintering in vacuum, inert or reducing atmospheres. In the case of TOM_metal, additionally, pure hydrogen and over-pressure of up to 30 bar can be applied. The atmosphere conditions of most powder metallurgical heating processes can therefore be achieved. For process control, the atmosphere of the furnace is monitored.

Geometric changes of the samples have been determined using non-contact optical methods. Undesired external forces, as in a push rod dilatometer, can therefore be avoided. Based on defined heating cycles with varied heating rates, the kinetic field can be calculated. Additionally, the onset of deformation due to gravity can be determined. In order to measure the viscous properties of the material during sintering, the capabilities of forged sintering or cyclic loading have been achieved in the TOM-devices. Thermal diffusivity as a function of the state of sintering has been measured using laser flash methods.

For the experimental programme, additively manufactured samples were produced using ExOne Binder Jetting equipment and 420 stainless steel powder and binder, also supplied by ExOne. Cylinders with a diameter of 20 mm and a height of 25 mm were built in two different orientations, in order to investigate the influence of the build direction on sintering. Additionally, discs with a diameter of 12 mm and a thickness of 2 mm, as well as discs with a diameter of 40 mm and a thickness of 2.5 mm, were built for the measurement of permeability and thermal diffusivity, respectively. In these cases, the build direction was perpendicular to the cylinder axis. For comparison, the debinding behaviour of a MIM product, based on 42CrMo4 stainless steel, was analysed.

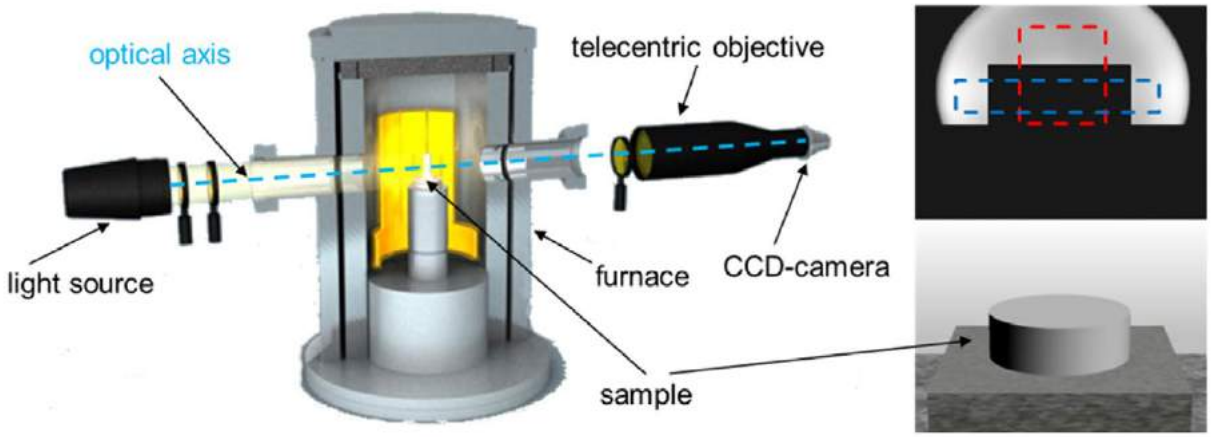

Fig. 2 Left: General set-up for the measurement of shrinkage and deformation during sintering using optical dilatometry. Right: A sample's shape (bottom) and achieved shadow (top) with indicated so-called measurement windows for in-situ determination of geometric changes [1]

Weight loss during debinding was measured by thermo-gravimetric analysis (TGA) under a flowing argon atmosphere. Basic chemical analysis was performed with respect to hydrogen, oxygen, nitrogen and carbon. Energetic effects during debinding were taken from the differential thermal analysis (DTA) curves of the TGA measurements. Permeability in the green state and after debinding was calculated from the flow of a test gas through the sample as a function of pressure gradient using small disc-shaped samples. The thermal diffusivity of the component as a function of temperature was measured in situ by the laser flash technique for both the debinding and the sintering steps.

Shrinkage was measured on additively manufactured cylinders with the TOM ac device. Cylinders, with their build directions parallel and perpendicular to the cylinder axis, were used. For the measurement of the viscous parameters, forged sintering was performed by applying a constant load of 100 N in the z-direction. In all measurements, in-situ shrinkage of width and height was determined using optical dilatometry, using a picture frame rate of ten pictures per second. A sketch of the set-up for optical dilatometry is shown in Fig. 2.

The numerical simulation of debinding and sintering behaviour was performed using COMSOL Multiphysics®. As different kinds of physical mechanisms and chemical reactions occur simultaneously and influence each other, a coupled multi-physical formulation of the problems was required.

In the case of debinding, the temperature distribution due to external heat transfer from the furnace and reaction energies from the combustion process were described using an energy conservation formulation. Flow of gases (volatile decomposition products and counter-diffusion of atmosphere) and build-up of local pressure was implemented based on Darcy's equation for flow in porous media. Finally, mass transfer due to chemical reactions and interdiffusion was considered.

For sintering, equations for heat transfer, sintering partial differential equations (PDE) and solid mechanics were coupled to simulate the shrinkage and deformation behaviour for a defined time-temperature cycle. With respect to the temperature distribution, thermal diffusivity, density and heat capacity were implemented. The PDEs for sintering considered strain due to free sintering as well as the contribution of viscous effects based on gravity and external forces. In addition, Young's modulus, Poisson's ratio and the coefficient of thermal expansion (CTE) were considered for solid mechanics. Whereas these material data were taken from well-established databases, all other input was based on precise in-house measurements. Data for the free shrinkage rate were generated from the TOM measurements using

"As different kinds of physical mechanisms and chemical reactions occur simultaneously and influence each other, a coupled multi-physical formulation of the problems was required."

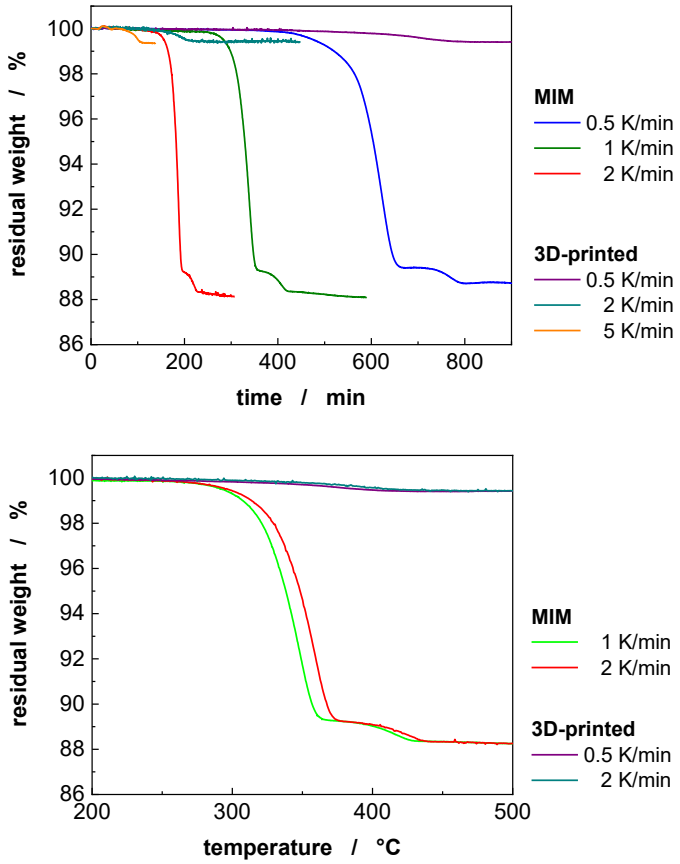

Fig. 3 Weight loss curves for the AM and MIM material during debinding, measured at indicated heating rates in flowing argon. Residual weight versus time (left) and for selected measurements versus temperature (right) [1]

optical dilatometry via the calculated kinetic field. Viscous properties were determined from forged sintering and cyclic loading using the optical dilatometry set-up of the TOM-devices. Thermal diffusivity as a function of the sintering state was measured using the laser flash method during sintering.

The weight loss curves of the AM and MIM materials are shown in Fig. 3. Measurements were run for three different heating rates. The total weight losses for AM and MIM samples were about 0.5 wt.% and 12.5 wt.%, respectively.

Depending on the heating rate, mass loss started in both cases between 200 and 250°C. Above 450°C, no further weight loss could be determined. With increasing heating rate, the curves were shifted to higher temperatures. The weight loss for the MIM material was much higher than that of the AM material due to a higher content of organic processing additives. The shapes of the weight loss curves for the two different materials also differed, based on their different compositions. Whereas a one-step mass loss took place for the AM material, a second step could be seen between 350 and 450°C for the MIM material. However, the main mass loss took place between 300 and 350°C.

Based on the measured TGA data, the kinetic field was set up and used to calculate required heating cycles for constant, but arbitrarily chosen, debinding rates. Depending on the chosen debinding rate, the time frame of the debinding process can vary strongly. Due to the different weight loss characteristics, the suggested heating cycles also differed considerably for the two materials.

The maximum acceptable heating rate can be determined experimentally using a special device called TOM pyr, where samples of up to 500 g can be debound under defined atmospheres and gas flow. The device aims at representing flow conditions in industrial furnaces more accurately. Cracking is monitored using sound emission analysis. Alternatively, a well-established heating cycle could be improved, based on the same total debinding time but adapted time-temperature intervals. Otherwise, FE analysis can be used to calculate the maximum stress occurring during the standard process. Subsequently, a time optimised heating profile is calculated, during which this acceptable stress is never exceeded. FE analysis is also used for more complex or larger components. In combination with elemental analysis for gas formation, heat transfer characteristics and gas permeability, the stress development during debinding is first simulated for defined constant debinding rates. Then the heating cycle is iteratively optimised with respect to stress minimisation. For industrial solutions, the component geometry, heat transfer conditions in the furnace and heat transfer due to the contact of the component with the kiln furniture should also be included in the simulation.

The shrinkage behaviour during sintering is shown in Fig. 4 for the additively manufactured material. Similar to the case of debinding, measurements with three different, constant heating rates were run in order to determine the sintering kinetics. Depending on the heating rate, sintering starts at a temperature of about 1050°C. The first indications of deformation can be seen starting above 1350°C. Additionally, the shrinkage curve of a vertically printed cylinder is included in Fig. 4 for comparison. As can be seen, the printing direction has an influence on the shrinkage behaviour. Therefore, for a comprehensive simulation, the sintering kinetics has to be measured in all directions.

Especially for metal powders, deformation due to plastic flow at increased temperatures has to be considered. The material behaviour is characterised by the viscous moduli. Experimental determination is usually difficult with standard push rod dilatometry, so optical dilatometry in combination with the option of applying defined external forces is an efficient solution. The measurement of the shrinkage curves under constant or cyclic loading and their comparison with shrinkage curves measured without load enables the calculation of the viscous moduli. The influence of a constant load on the sintering shrinkage is shown for an additively manufactured sample in Fig. 4. A constant force of 10 N was applied in the vertical direction. This leads to an increased shrinkage in the vertical and reduced shrinkage in the horizontal direction.

Fig. 5 shows the results of a sintering test for a T-profile made by AM in comparison with the simulation results. Despite small differences, the simulation demonstrates the problems, which arise during sintering. In a consecutive step, both the sintering profile and the shape of the additively manufactured green body can be adjusted in order to obtain an in-spec component in the first run. The advantage of this approach is that, based on the specific material data, any shape or component can be simulated, allowing high flexibility and efficiency, especially for prototype and small-series production.

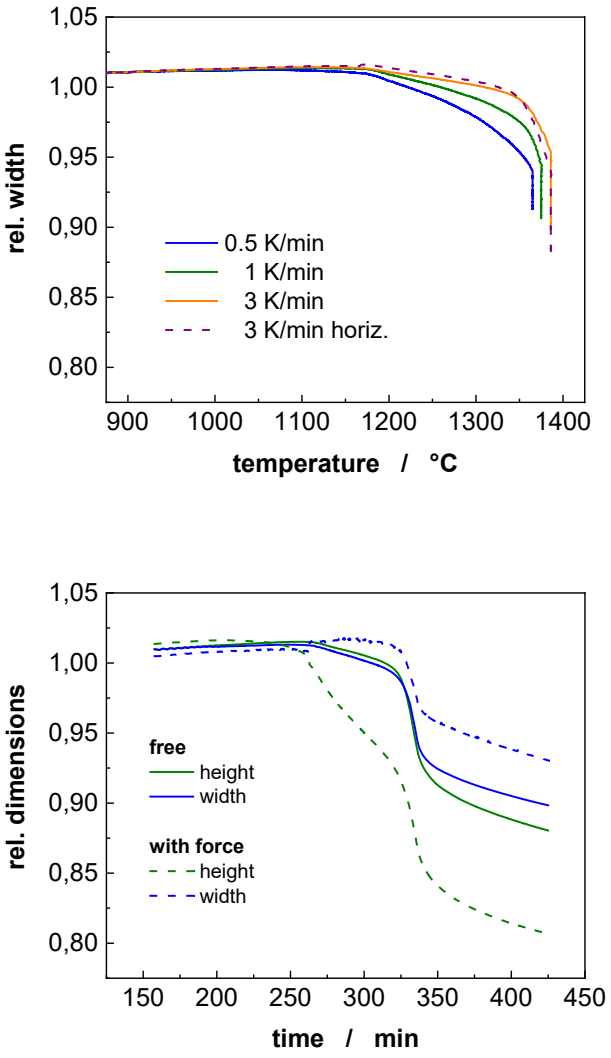

Fig. 4 Left: Shrinkage curves for the width of additively manufactured cylinders measured with indicated heating rates and adapted maximum temperatures and holding times. Additionally included is the shrinkage curve for a horizontally printed cylinder for demonstrating the influence of the build direction on the sintering characteristics. Right: Shrinkage behaviour with and without external force (10 N) in z-direction (forged sintering) [1]

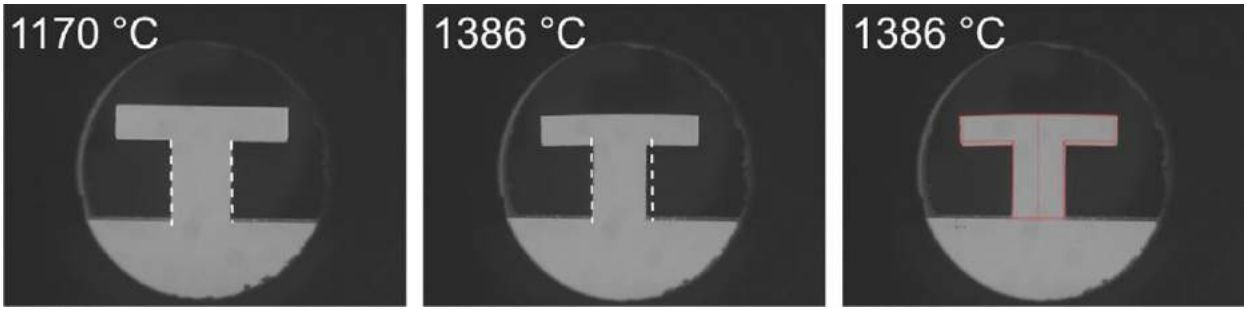

Fig. 5 Pictures of an additively manufactured T-shaped sample at 1170°C and at maximum temperature of the heat treatment together with indicators for shrinkage (white dashed lines) and the predicted shrinkage (red lines) based on FE simulation on the right [1]

Alloy	Fe	Cr	W	Mo	V	Co	Ni	Mn	Si	N	C	O	S	P
8620 PA	Bal	0.60	-	0.22	-	-	0.60	0.70	0.27	0.02	0.25	0.11	0.005	0.01
8620 MA	Bal	1.77	-	0.61	-	-	1.77	2.25	0.85	0.03	0.64	0.10	0.007	0.01
4140 PA	Bal	1.02	-	0.25	-	-	-	0.84	0.26	-	0.43	0.13	0.008	0.01
H11	Bal	5.35	-	1.28	0.45	-	-	0.46	1.09	0.05	0.37	0.12	0.008	0.01
H13	Bal	5.09	-	1.59	1.08	-	-	0.32	0.90	0.06	0.43	0.11	0.009	-
T15	Bal	4.63	12.6	0.50	4.88	4.91	0.05	0.38	0.34	0.07	1.63	0.11	0.024	0.03
CIP BC	Bal	-	-	-	-	-	-	-	-	0.01	0.035	0.20	0.001	-

Table 1 Chemical analyses of powders used in the reported study [2]

Review of sintering behaviour of different tool steels and low-alloy steels made by MIM

Next, Luke Harris, Martin Kearns, Paul Davies and Szymon Kubal, of Sandvik Osprey Ltd., UK, and Viacheslav Ryabinin and Erainy Gonzales, of TCK S.A., Dominican Republic, provided a review of the sintering behaviour of a number of tool steels and low alloy steels made by MIM [2].

Low alloy steels, for the purposes of this paper, were regarded as having up to ~0.5%C, with widespread use in general engineering, automotive and firearms parts, where their high strength and toughness provide cost effective solutions. Popular low alloy MIM steels include AISI8620, 4140, 4340 and 4605 with ~0.2-0.5%C. Tool steels typically have carbon content in the range 0.4 - 1.5% and, in traditional cast forms, heat treatments are designed to achieve the optimum distribution of matrix carbides to give the required balance of hard wearing properties. The choice of alloy for a specific application depends on cost, working temperature, required surface hardness, strength, shock resistance and toughness requirements. The sintering mechanisms in high-speed tool steels such as M2 and other high C tool steels is Super-Solidus Liquid Phase Sintering (SSLPS) and densification occurs rapidly once a liquid phase is formed at grain boundaries. Grain growth also tends to occur rapidly and, as the liquid film thickness increases, the likelihood of distortion also increases.

Material	Nominal psd	D10	D50	D90
H11 PA	90%-22 µm	4.05	10.16	20.97
H13 PA	90%-22 µm	4.06	9.95	21.17
T15 PA	90%-22 µm	5.47	11.95	21.93
4140 PA	90%-22 µm	4.40	10.50	21.50
8620 PA	90%-16 µm	3.72	8.39	15.65
8620 MA	90%-22 µm	4.50	12.94	21.81
CIP BC	90%-12 µm	2.60	5.60	11.20

Table 2 Particle size data for powders used in the reported study [2]

There is relatively little published information on the MIM processing of tool steels and one aim of this study was to compare such data with low alloy steels. In addition to AISI8620, the behaviours of H11, H13 and T15 tool steels were examined. H11 and H13 are tough, high-strength tool steels suited to hot work environments such as for extrusion and forging dies. T15 is a highly alloyed tool steel used in high-performance broaches and milling cutters. The high V level increases wear resistance and W and Co improve high-temperature performance.

Previous studies have shown the advantages that can be obtained via a masteralloy (MA) approach, including higher density and lower distortion. Recognising the criticality of carbon control on sintering behaviour and finished part properties, carbon loss was tracked during sintering and heat treatment to relate this to the chemistry of the starting powders. While this paper was focussed on MIM, part makers using binder jet Additive Manufacturing face a similar challenge in optimising the sintering of green parts.

In the reported experimental work, a series of PA and MA powders was produced by Sandvik Osprey's proprietary inert gas atomisation process using nitrogen gas. 'As-atomised' powders were air classified to 90% - 22 µm or 90%

- 16 µm size ranges. The chemistry and particle size distribution data of each powder batch used in the study are shown in Tables 1 and 2. In the case of 8620 MA, an addition was made of low C CIP (carbonyl iron powder). The MA has a three times concentration of the main alloying elements, including 0.7%C.

The CIP was significantly finer than the gas atomised powders and, when added to the MA, reduced the median size distribution to more nearly replicate a typical 90% - 14 µm powder size distribution but with a bimodal distribution. Both powder morphologies were essentially spheroidal.

Feedstocks were prepared by TCK using their proprietary binder formulation to achieve a powder loading level of 61.8%, corresponding to a 17.4% shrinkage factor. The feedstocks were moulded to produce green standard MIM tensile and Charpy test specimens.

Moulded green parts were then subjected to an initial solvent debind, followed by thermal debinding and sintering in a nitrogen atmosphere. The temperature profile adopted was to ramp to 750°C at 2°C/min (hold 1 h), ramp at 3°C/min to 1150°C (hold 1.5 h) and finally ramp at 5°C/min to sintering temperature (hold 3.5 h) followed by a furnace cool. Sintering was carried out at 1360°C, for all alloys other than T15, which was sintered at 1240°C. 4140 and 4340 were sintered at 1300°C to maximise mechanical performance. For each sintering run, Charpy impact bars were mounted on refractory supports, both cantilever style (15 mm overhang) and suspended across refractory supports (38 mm separation), to determine the extent of distortion as a function of alloy type and sintering temperature.

Table 3 shows the densities obtained for different alloys after sintering in nitrogen at 1360°C (T15 at 1240°C, 4140 at 1300°C). Except for T15, which achieved nearly full density (99.6% theoretical), the lower carbon tool steels showed modest final density levels, in the range 91-93%. 8620 pre-alloy achieved just over 93% density, while the same composition produced via a masteralloy route reached over 95% theoretical density. 4140 achieved a density of 92%, modest by MIM standards, but certainly comparable to or better than many press & sinter automotive parts.

Material	Nominal psd	Avg density (%)
H11 PA	90% - 22 µm	91.30
H13 PA	90% - 22 µm	90.85
T15 PA*	90% - 22 µm	99.60
4140 PA*	90% - 22 µm	92.60
8620 PA	90% - 16 µm	93.15
8620 MA + CIP	90% - 14 µm	95.25
*T15 at 1240°C, 4140 at 1300°C		

*Table 3 Densities of MIM specimens achieved after sintering in nitrogen at 1360°C (*T15 at 1240°C, 4140 at 1300°C) [2]*

Alloy	Start %C	Start %O	Sinter %C	ΔC start vs sintered	Molar ratio C/O_2
4140 PA	0.43	0.13	0.39	0.04	1.1
8620 PA	0.25	0.11	0.20	0.05	1.2
8620 MA + CIP	0.28	0.17	0.21	0.07	1.1
H11 PA	0.37	0.12	0.32	0.05	1.1
H13 PA	0.43	0.11	0.39	0.04	1.0
T15 PA	1.65	0.11	1.52	0.13	3.2

Table 4 Progression in %C, N, O levels from powder to sintered product and heat treated products [2]

Metallographic assessments showed that 8620 had a mixed ferrite and fine pearlite structure, with the MA variant exhibiting a lower level of porosity and a coarser grain size. Pores were fine and evenly dispersed. In comparison, the 4140 microstructure was almost fully bainitic. Optimisation of the sintering cycle is crucial to ensure the optimised microstructure for low alloy steels. H11 and H13 showed mixed martensite and bainite microstructures, while T15 showed a uniform microstructure of mixed carbides.

Table 4 shows that, during the sintering process, carbon was lost from each of the alloys and the amount lost was predictable, based on the amount of oxygen in the starting feedstock. The column showing the calculated molar ratio C/O_2 is close to unity in most cases, suggesting that carbon was lost as CO_2 and that, once the available oxygen had been consumed, the carbon level remained stable. Exceptional behaviour was shown by T15, whose C loss was far higher than expected, based on the oxygen level in the feedstock alone. Overall, the carbon losses across all tool steels were quite modest, predictable and could be compensated for as required.

Material	Nominal psd	Density (%TD)	0.2%PS (MPa)	UTS (MPa)	%El	VHN	HRC
4140 PA	90% - 22 µm	92.60	-	800	-	253	23
8620 PA	90% - 16 µm	93.15	280	507	15.0	138**	-
8620 MA + CIP	90% - 14 µm	95.25	339	585	13.8	164**	-
H13	90% - 22 µm	90.85	902	1600	4.3	402	42
T15	90% - 22 µm	99.60	1097	1280	0.8	550	52
*M2**	*80% - 22 µm*	*99.9*	*1230*	*1471*	*1.5*	*579*	*54*
**From ref 4; ** normally increased by case hardening (carburising)*							

Table 5 Mechanical properties of as-sintered specimens [2]

Table 5 shows the results of tensile and hardness testing of the different tool steel variants, including results from a previous study on M2. In the case of 8620, the MA variant provided a significantly higher strength and hardness level than the PA variant, without compromising ductility. In the case of 4140, previously reported work from this group had shown that an additional tempering step of 250°C for 1 h would be beneficial in effectively doubling the tensile performance. Elongation values for the 4140 low alloy steel are not presented, but were typically a few % only. T15 achieved high density after sintering at 1240°C in nitrogen and, with optimised heat treatment, higher strength and hardness values greater than the 65HRC achieved in this study should be possible.

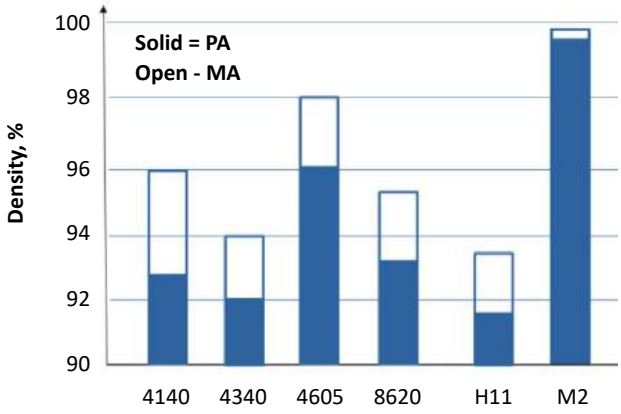

Fig. 6 Compilation of Sandvik Osprey/TCK Joint studies since 2010 highlighting density versus PA and MA production routes [2]

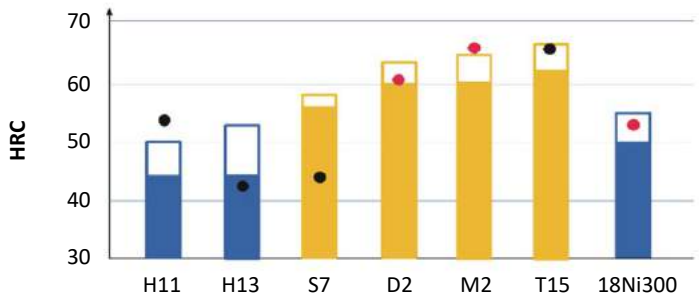

Fig. 7 Typical min/max working hardness ranges for different tool steels . Black symbols- values achieved in this study; green symbols (D2/SKD-11, M2 and 18Ni300) from previous studies [2]

For the remaining alloys in this study, density levels of 91–95% were relatively modest by MIM standards, but were in the range where post HIP treatment should enhance density and mechanical properties, if desired. In the case of 8620, the density and strength level values reported before heat treatment are in line with values reported by parts makers and, in practice, parts would likely be subjected to further treatments such as heat treatment and carburising to enhance surface hardness. Comparative data have shown that the MA approach, using a three times concentrated alloy, and compounding with 2 parts CIP is confirmed to be advantageous in achieving higher density, which could lead to enhanced mechanical properties and lower distortion than evident in a PA route, see Fig. 6. For binder jet AM, the CIP + MA option is not feasible and so there is a challenge to develop more readily sinterable PA low alloy steels.

Fig. 7 shows a summary of hardness values expected for popular tool steels, with the open ranges indicating the typical working hardness ranges. Superimposed on this, black symbols indicated the peak hardness values determined in this study. For

comparative purposes, hardness ranges for three other common tool steels (D2, M2, 18Ni300) have been shown, along with green symbols highlighting data obtained from other MIM studies featuring Sandvik Osprey gas atomised powders.

Hardness expectations were met in this study for T15, but not for H13. The reasons for this may be found in a lack of densification on sintering, inhibited to some extent by the nitrogen sintering atmosphere and by carbon loss on sintering. Indeed, the carbon loss on sintering itself is shown, in Table 4, to be quite modest and predictable based on the starting level of oxygen, in all cases except T15, where nitrogen substitution plays a significant part in carbon loss.

The fact that carbon control is predictable following the sintering stage is an important finding, confirming previous studies and highlighting the benefits of using gas atomised metal powders with relatively low and consistent oxygen levels. Variable carbon levels, within what is a narrow sintering window for tool steels and low alloy steels, would make control of hardness and part tolerances challenging.

Weld lines and their effect on the fatigue response of case-hardened MIM 8620 steel

Finally, a paper from Dr.-Ing. Markus Schneider, Johannes Bergfeld and Christian Simon, GKN Sinter Metals, Germany, explored the effect of weld lines on the fatigue response of case-hardened MIM 8620 products [3].

Weld lines are the result of two or more fill fronts where the feedstock flow splits and joins together during the filling process. Such weld lines can occur behind drillings or if the component is injection moulded with more than one gate. The plastic injection moulding industry has much experience with weld lines, and differentiates between weld lines formed due to different feedstock flow temperatures during fill front formation and weld lines formed by

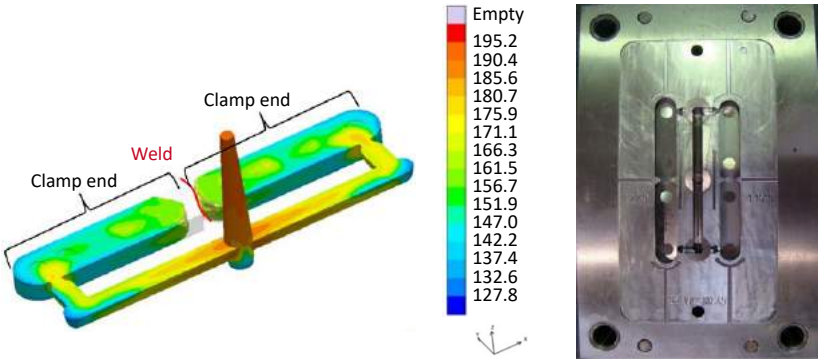

Fig. 8 Mould flow simulation of a twin-gated fatigue specimen with a notch radius of 0.45 mm (left) and tool cavity for fatigue specimens with a notch radius of 0.45 mm for two different offset factors and special adjustable valves (right) [3]

differently angle-orientated fill fronts. If two fill fronts meet each other with a certain angle, a blurred weld line can arise. The resulting part surface shows a local sink mark, which can be interpreted as a notch.

In the plastic injection moulding industry, a characteristic sink mark angle of 135° is used to differentiate between merged and conventional weld lines. In the past, tool designers of MIM parts have shifted the gates to positions that ensure that the weld lines are far away from highly-loaded part regions. Another option is to vary the gate diameter or the volumetric injection feedstock flow rate to guarantee a quick injection moulding process without strong cooling. Also, feedstock flow temperature or tool temperature can be increased to decrease the feedstock viscosity.

To analyse the injection moulding process in general and to investigate the resulting feedstock flow paths, a mould flow simulation is an often-recommended procedure. Fig. 8 (left) shows the weld line position of a fatigue specimen simulated with Sigmasoft Mold Flow. The tool designer can vary the gate position. However, the shifting of the weld line to uncritical part regions is not always possible, due to the complexity of the injection moulding tool (location of cooling channels, other cavities and length of the runner). Therefore, it is necessary to assume the worst-case scenario, where the weld line is located in the highly-loaded part region and the weld line is loaded with fracture opening mode 1. For the determination of material properties and to investigate the effect of weld lines, a new tool concept for fatigue specimens and conventional tensile test pieces was developed. Also, fatigue specimens were injection moulded with two different gate variants. For the investigation of the notch sensitivity and to derive the resulting support factor, three different tools with different cavities were designed. The un-notched fatigue specimen exhibits a waist with a radius of r=30 mm (K_t =1.04 for bending loading). Also, two further fatigue specimens with notch radii of r = 0.9 mm (K_t = 1.91 for bending loading) and r = 0.45 mm (K_t = 2.47 for bending loading) were produced. The corresponding stress concentration factors Kt were calculated numerically using FEA. The worst-case scenario was created with the tool cavity in Fig. 8 (right). With this cavity, it is possible to produce one-gated and twin-gated fatigue specimens by adjusting valves. Due to the symmetry of the runners, the resulting weld line of the twin-gated process is located at the notch root, as shown in Fig. 8 (left).

The injection moulding of all specimens was conducted with plant-specific parameters. The one-gated and twin-gated fatigue specimens were injection moulded with the

Geometry	r (mm)	Condition	σ_u (MPa), 1 gate	σ_u (MPa), 2 gates
DIN EN ISO 2740	∞	As-sintered	397	Not realised
DIN EN ISO 3928	30	As-sintered	418	417
DIN EN ISO 3928	0.9	As-sintered	458	447
DIN EN ISO 3928	0.45	As-sintered	432	441
DIN EN ISO 2740	∞	Case-hardened	1102	Not realised
DIN EN ISO 3928	30	Case-hardened	915	947
DIN EN ISO 3928	0.9	Case-hardened	802	781
DIN EN ISO 3928	0.45	Case-hardened	703	725

Table 6 Static tensile test results as a function of the material condition, the notch radius r and the weld line position (1 gate vs 2 gates) [3]

same filling and packing parameters, e.g. the volumetric injection feedstock flow rate, filling pressure, packing pressure profile, filling time and packing time, to ensure similar material properties.

After the injection moulding process, the densities of the right-hand and left-hand gripping ends were measured to guarantee comparable green part densities. After moulding, all specimens were peened with a plastic granulate to remove burrs. Potential residual stresses were eliminated by sintering above the recrystallisation temperature of MIM 8620. Debinding and sintering were carried out in a continuous debinding and sintering walking beam furnace. Catalytic debinding of the specimens was conducted in a low temperature atmosphere of HNO_3 (nitric acid) and N_2 for 390 min. The parts were sintered at 1251°C for around 90 min in a 100% N_2 atmosphere with an atmospheric pressure of 10 mbar. After sintering, the specimens were carburised, case-hardened and tempered. The carburising atmosphere consisted of natural gas, CH_4O (methanol) and N_2 with a carbon potential of 1%. The carburising temperature was around 950°C. The required case hardening depth was d(H = 550 HV 0.1) = 0.3 mm + 0.1 mm, resulting in a required surface hardness of H_0 > 600HV 0.1. After oil quenching, specimens were tempered at 170°C for 2 h in air. A sintered density of 7.4 g/cm³ was achieved.

In the green state, neither the green density nor the dimensions showed any effect induced by the different gate variants. Sintered density was measured on four different specimen geometries (tensile test specimen, un-notched fatigue specimen and notched fatigue specimens with two different notch radii). The differences between the four variants, as well as the differences between the gripping ends, were negligible. Therefore, an averaged sintered density of 7.4 g/cm³ was found. The subsequent case hardening treatment did not affect the sintered density. The macro-hardness was measured on the surface as H = 114 HV 30 for the as-sintered condition and H = 631 HV 30 for the case-hardened condition, respectively (averaged between the four different specimen geometries).

A small nitrogen pick-up of 0.031% was found after sintering in the N_2 atmosphere and the subsequent case hardening treatment. MIM 8620 contains 0.5% Cr, which has a high affinity to nitrogen. The measured oxygen content after sintering and the

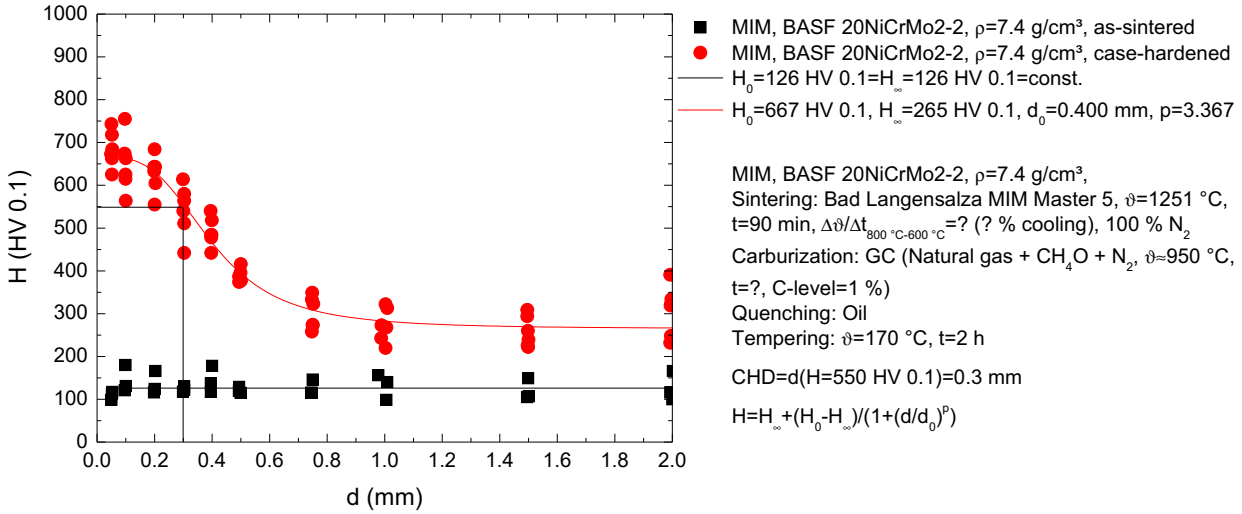

Fig. 9 Micro-hardness profiles for MIM 8620 (20NiCrMo2-2) with a sintered density of 7.4 g/cm³ before (as-sintered condition) and after case hardening (case-hardened condition) [3]

ρ (g/cm³)	R (1)	K_t (1)	k (1)	N_K (1)	σ_A (MPa)	k (1)	N_K (1)	σ_A (MPa)
			1 gate			2 gates		
7.4	-1	1.04	-19.227	3303592	610.78	-14.745	3072990	565.55
7.4	0	1.04	-6.213	172096	362.49	-7.560	309596	333.49
7.4	0.5	1.04	-6.981	198094	195.48	-4.228	128227	194.46
7.4	-1	1.91	-6.520	146430	468.72	-5.643	138222	470.39
7.4	-1	2.47	-5.673	124389	423.18	-5.405	140835	397.07

Table 7 Basquin parameters of the derived bending s-N lines (each s-N line was derived with fifty specimens) as a function of the weld line position (1 gate vs 2 gates) [3]

subsequent case hardening treatment showed typical values < 0.004%. The measured carbon content after sintering was found to be 0.136% (averaged between surface and core regions). Hence, a small decarburisation effect can be assumed. After case hardening, the core carbon content was measured as 0.146%. A sigmoidal carbon profile with an asymptotic plateau in the core region was assumed. The surface roughness parameters after case hardening were Ra = 0.86 µm and Rz = 6.07 µm.

The static mechanical properties were characterised in terms of the stress-strain and the stress-displacement responses. The corresponding ultimate tensile strength values can be defined in the nominal stress system. Table 6 summarises the results. A direct comparison between the two columns shows no effect of the gate variants. From the static tensile tests, it was concluded that weld lines had no negative effect. An interesting observation was the increase in ultimate tensile strength of the as-sintered variants as a function of the notch radius r. The damaging effect from an increasing stress concentration factor K_t is only recognisable for the case-hardened variants. This is related to the plastic constraint effect of ductile materials (notch strengthening) and the higher triaxiality factor due to the stress rearrangement around the notch root. Also, a comparison between the two conditions (as-sintered vs case-hardened) shows the effect from the martensitic transformation and the corresponding carbon content. Fig. 9 shows the micro-hardness profiles of MIM 8620 with a sintered density of 7.4 g/cm³ before (as-sintered condition) and after the case hardening (case-hardened condition). It can be seen from this that a surface hardness of 667 HV 0.1, a core hardness of 265 HV 0.1 and a case hardening depth of d(H = 550 HV 0.1) = 0.3 mm were achieved, in line with the requirements defined earlier.

The promising results from the static tensile tests needed to be confirmed by cyclic tests. Hence, the case-hardened MIM 8620 was cyclically tested with three different loading ratios (R = -1, R = 0 and R = 0.5). The results are summarised in Table 7 in terms of the Basquin parameters of the corresponding bending s-N lines, where k denotes

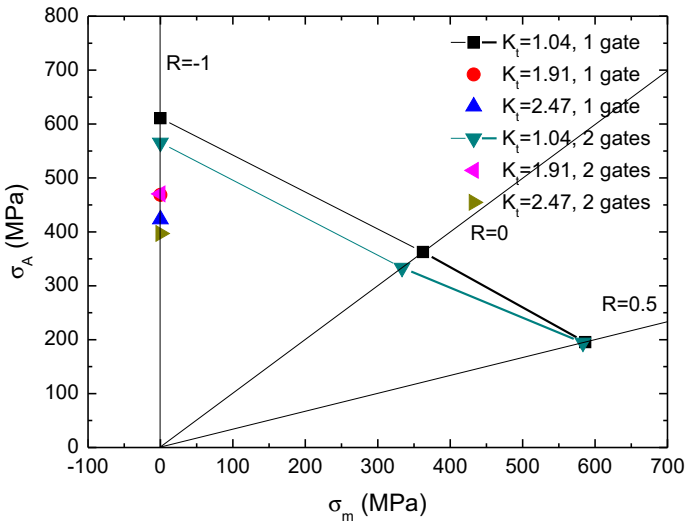

MIM, BASF 20NiCrMo2-2, ρ=7.4 g/cm³,
Sintering: Bad Langensalza MIM Master 5, ϑ=1251 °C, t=90 min, $\Delta\vartheta/\Delta t_{800\,°C\text{-}600\,°C}$=? (? % cooling), 100 % N_2
Carburization: GC (Natural gas + CH_4O + N_2, ϑ≈950 °C, t=?, C-level=1 %)
Quenching: Oil
Tempering: ϑ=170 °C, t=2 h
Testing: Bending loading, nominal stress system

Fig. 10 Haigh damage lines for case-hardened MIM 8620 (20NiCrMo2-2, 1 gate vs 2 gates) material [3]

the slope and N_K the cut-off point. The bending fatigue strength at the knee point was derived for a survival probability of P_s = 50 %.

The three loading ratios R could be used to derive Haigh damage lines in Fig. 10. In general, heat treated steels are known to show extraordinarily high mean stress sensitivities M and this tested material was no exception. From Table 7 and Fig. 10 the mean stress sensitivities M could be quantified as M_2 = 0.69 (1 gate) and M_2 = 0.70 (2 gates) and M_3 = 0.75 (1 gate) and M_3 = 0.56 (2 gates), respectively. In contrast to expectations, the case-hardened MIM 8620 was not perfectly notch sensitive. Due to the high sintered density 7.4 g/cm³ and the high surface hardness of 667 HV 0.1, a high notch sensitivity was expected. The notch factors are $K_f(K_t=1.91)=1.30$ (1 gate), $K_f(K_t=1.91)=1.20$ (2 gates), $K_f(K_t=2.47)=1.44$ (1 gate) and $K_f(K_t=2.47)=1.42$ (2 gates). Obviously, the notch sensitivity and the resulting support factors n_χ are in the same range as for conventional PM steels. The notch sensitivities and the resulting support factors are in the same range as for conventional PM steels.

The effect of the weld lines was investigated five times (different loading ratios and different stress concentration factors). The twin-gated injection moulded fatigue specimens exhibited lower fatigue strength at the knee point. However, the average drop of fatigue strength at the knee point was only 4.3%. This effect was smaller than expected. This observation was based on small injection moulded fatigue specimens, where the temperatures of the feedstock fill fronts could be assumed as high enough to guarantee good welding. Lower feedstock flow temperatures may result in weaker weld lines.

Author

Dr David Whittaker
Tel: +44 1902 338498
whittakerd4@gmail.com

References

[1] Debinding and Sintering Investigations using Optical Dilatometry in Combination with Finite Element Analysis, Holger Friedrich et al. As presented at the Euro PM2019 Congress, Maastricht, the Netherlands, October 13-16, 2019, and published in the proceedings by the European Powder Metallurgy Association (EPMA).

[2] Review of Sintering Behaviour of Different Tool Steels and Low Alloy Steels Made by MIM, Luke Harris et al. As presented at the Euro PM2019 Congress, Maastricht, the Netherlands, October 13-16, 2019, and published in the proceedings by the European Powder Metallurgy Association (EPMA).

[3] Weld Lines and their Effect on the Fatigue Response of Case-Hardened MIM 8620 Steel, Dr.-Ing. Markus Schneider et al. As presented at the Euro PM2019 Congress, Maastricht, the Netherlands, October 13-16, 2019, and published in the proceedings by the European Powder Metallurgy Association (EPMA).

Proceedings

The full proceedings of the Euro PM2019 Congress are available to purchase from the EPMA. Topics covered include:

- Additive Manufacturing
- PM Structural Parts
- Hard Materials & Diamond Tools
- Hot Isostatic Pressing
- New Materials & Applications
- Powder Injection Moulding

www.epma.com

PMCC&AC EXPO

2020 Shenzhen International Powder Metallurgy & Cemented Carbide Exhibition
2020 Shenzhen International Advanced Ceramics Exhibition

July 1-3, 2020

Shenzhen Convention & Exhibition Center, China

INDUSTRY CHAIN EVENTS HELD CONCURRENTLY WITH AN AREA OF 80,000SQM

FOCUS ON GUANGDONG-HONG KONG-MACAO, BLOSSOM THE PEARL RIVER DELTA

WELL-KNOWN ORGANIZATIONS JOINTLY CULTIVATE AND BUILD

BOUNDLESS HIGHTLIGHTS, THE INDUSTRY MUST ATTEND

ORGANIZERS

Wise Exhibition (Guangdong) Co.,Ltd.
Wise Exhibition (HK) Co.,Ltd.

COOPERATION UNITS

※Guangdong Powder Metallurgy Alliance
※Guangdong Institute of Materials and Processing
※National Engineering Research Center of Titanium and Rare Metals Powder Metallurgy
※China Electronics Materials Industry Association Magnetic Materials Branch
※Working Committee of Amorphous materials Application
※China PM Business Website
※China MIM Website China
※Hard Metal Business Website
※Powder Metallurgy Review
※Powder Injection Moulding International

SCOPE

Powder Metallurgy & Cemented Carbide Raw and Auxiliary Materials
Advanced Ceramics Raw Materials
Manufacturing Equipment
Powder Metallurgy & Cemented Carbide Products
Advanced Ceramics Parts/Products
Detection Equipment and Technologies
3D Printing

CONCURRENT EVENTS

1. Powder Metallurgy Industry Technology Development Forum
2. Powder Metallurgy New Product and Technology Promotion Conference
3. 2020 Shenzhen International Cutting Tools and Equipment Exhibition
4. The 18th Shenzhen (China) International Small Motor, Electric Machinery & Magnetic Materials Exhibition
5. 2020 Shenzhen (China) International Coil Winding, Power Supply & Electronic Transformer Exhibition
6. 2020 Shenzhen International Intelligent Manufacturing Fair

FOR PARTICIPATION, PLEASE CONTACT

Wise Exhibition (Guangdong) Co.,Ltd.
The Global Association of the Exhibition Industry (UFI) Chinese Member
Guangdong Fairs Organizer Association Vice Chairman
China Top 10 Outstanding Exhibition Organizer
Tel: +86 2029193563 / 29193588
magmotor@126.com

Scan the QR Codes,follow the WeChat Official Account of PMCC&AC EXPO and add us as friend

www.pmccexpo.com

INOVAR COMMUNICATIONS

DOWNLOAD THE LATEST ISSUE OF METAL AM MAGAZINE FOR FREE

www.metal-am.com

Partner events

Pick up your free print copy of *PIM International* magazine at the following partner conferences, exhibitions and seminars.
For our complete events listing visit www.pim-international.com

2020

Short Course on Powder Handling and Flow for Additive Manufacturing 2020
April 22-24, Bremen, Germany
https://www.ifam.fraunhofer.de/de/Messen_Veranstaltungen/short-course-powder-handling.html

EPHJ Trade Show
June 16-19, Le Grand-Saconnex, Switzerland
https://ephj.ch/en/

WorldPM2020
June 27-July 1, Montréal, Canada
www.worldpm2020.org

PMCC&AC Expo 2020
July 1-3, Shenzhen Shi, China
www.pmccexpo.com

Hannover Messe
July 13-17, Hannover, Germany
www.hannovermesse.de

Powder Handling and Flow for Additive Manufacturing Course
July 15-16, Widnes, United Kingdom
www.gre.ac.uk/engsci/research/groups/wolfson-centre/coupro/sc/am

PM China 2020
August 12-14, Shanghai, China
en.pmexchina.com

PM Life - Additive Manufacturing Module
August 24-28, Dresden, Germany
www.pmlifetraining.com/about/additive-manufacturing

Formnext + PM South China
September 9-11, Shenzhen Shi, China
www.formnext-pm.hk.messefrankfurt.com/shenzhen/en.html

Ceramics Expo 2020
September 22-23, Cleveland, United States
www.ceramicsexpousa.com

Euro PM2020
October 4-7, Lisbon, Portugal
www.europm2020.com

Formnext
November 10-13, Frankfurt, Germany
www.formnext.com

Event listings and media partners

If you would like to see your PIM/MIM/CIM-related event listed in this magazine and on our websites, please contact Nick Williams, email: nick@inovar-communications.com.

We welcome enquiries regarding media partnerships and are always interested to discuss opportunities to cooperate with event organisers and associations worldwide.

advertisers' index

Developing the Powder Metallurgy Future

european powder
metallurgy association

EPMA
european powder metallurgy association

International Congress & Exhibition

4 – 7 October 2020

Lisbon Congress Centre (CCL), Lisbon, Portugal

Over 70% of Exhibition Space Already Reserved

Book now at www.europm2020.com/exhibition

EURO PM2020
CONGRESS & EXHIBITION

www.europm2020.com

EURO PM2020
CONGRESS & EXHIBITION

arburgXworld gives you the tools you need to fully digitalise your company. We can help you to achieve your goal with our Road to Digitalisation. Choose from a wide variety of products and services to improve your production efficiency. Start digitalising now with arburgXworld! "Wir sind da."

www.arburg.com/info/pim/en

ARBURG